
WALL-CLOCK COMPLEXITY FOR ZEROth-ORDER OPTIMIZATION WITH TUNABLE ORACLE FIDELITY

Alexandra Suvorikova^{*,†,1} Igor Pavlov^{*,†,2} Artem Vasin² Georgii Bychkov³
Anastasia Antsiferova³ Darina Dvinskikh⁴ Alexander Gasnikov^{2,5,6}

¹Weierstrass Institute for Applied Analysis and Stochastics, Berlin, Germany

²Moscow Independent Research Institute of Artificial Intelligence, Moscow, Russia

³MSU Institute for Artificial Intelligence, Moscow, Russia

⁴HSE University, Moscow, Russia

⁵Trusted AI Research Center, RAS, Moscow, Russia

⁶Innopolis University, Kazan, Russia

June 1, 2026

ABSTRACT

Zeroth-order (black-box) optimization is applied when gradients are unavailable and objective evaluations rely on expensive simulations. In many such applications, the oracle fidelity is tunable: higher-accuracy queries reduce noise but incur higher computational costs. To capture this trade-off, we study an accuracy-aware wall-clock model where each query with fidelity δ has a cost $c(\delta)$, and we minimize the total time $T_{\text{total}} = \sum_{k=1}^N c(\delta_k)$, subject to a target accuracy constraint. We show how the choice of oracle type, noise model, and optimization scheme induces explicit wall-clock-optimal choices for the algorithmic parameters. For instance, we demonstrate that accelerated methods can be wall-clock inferior to non-accelerated schemes. Furthermore, we characterize the conditions under which a constant fidelity strategy is optimal in the Big-O sense. Our framework provides a unified methodology to translate convergence guarantees into practical fidelity and batching recommendations.

1 Introduction

Black-box optimization (BBO) plays a central role in modern applications, ranging from simulation-based engineering to adversarial machine learning [Kadowaki and Ambai, 2022, Williams and Li, 2023, Liu and Oliveira, 2025]. This setting arises when the objective is defined through a numerical simulation or an algorithmic procedure. Since gradients are unavailable, one usually relies on an oracle that returns approximate values.

A key feature of BBO is that the oracle’s error is controllable. In practice, the oracle’s fidelity δ serves as a tunable parameter, determined by the computational budget allocated to each query. For example, in experimental physics, the oracle fidelity depends on the number of Monte Carlo particle trajectories Shirobokov et al. [2020]; in molecular discovery, the number of internal search restarts impacts the oracle fidelity Hoffman et al. [2022]. Another example is supervised PageRank learning, where estimating the stationary distribution of a parameterized Markov chain by MCMC yields a tunable noisy function-value oracle with cost proportional to δ^{-2} Bogolubsky et al. [2016].

Focusing on Zeroth-Order (ZO) optimization as a primary framework for such problems, we address this limitation by adopting a wall-clock perspective. We explicitly model the dependency between oracle accuracy, iteration count, and total computational time. Specifically, we introduce an accuracy-aware complexity framework in which each oracle query is associated with a cost function $c(\delta)$ that depends on the desired fidelity δ . A similar “tunable oracle” framework has been recently proposed for first-order convex optimization, deriving optimal inexactness schedules to minimize

*Equal contribution.

†Correspondence: suvorikova@wias-berlin.de, 1g0rp4v1@gmail.com.

computational budget Van Dessel and Glineur [2024]. We extend this wall-clock perspective to the zeroth-order setting, where the trade-off governs not only the gradient quality but also the function evaluation itself. **Our contributions are as follows:**

- **A wall-clock framework for tunable-fidelity ZO.** We recast zeroth-order optimization as a joint design problem over the iteration count N and the per-query fidelity schedule $\{\delta_k\}$, under a polynomial cost-fidelity dependence $c(\delta) \propto \delta^{-\gamma}$. We show this is the only regime that produces a non-trivial trade-off.
- **A master lemma turning convergence bounds into wall-clock-optimal designs.** We isolate a structural property—fidelity separability—shared by various methods, and give closed-form optimal schedules in one step (Prop. 1). We also pin down exactly when a uniform schedule is already optimal up to constants.
- **The role of γ depends on the noise model.** Under adversarial noise, γ selects the algorithm (acceleration can hurt once $\gamma \geq 1$) but doesn't tune parameters within it. Under Tsybakov noise, the opposite: γ tunes the parameters, separating standard tuning from overbatching.
- **An intermediate gradient method (IGM).** We propose a new first-order method (Alg. 2) interpolating between GM and FGM, and prove its convergence under inexact gradients with time-varying oracle inexactness (Thm. 1). IGM is what enables the application of our master lemma to the adversarial setting (Prop. 5).
- **End-to-end recipes.** We illustrate and validated empirically the framework.

Paper organization. Sec. 2 introduces the wall-clock model for tunable-fidelity zeroth-order oracles and formulates the fidelity-allocation problem. Sec. 3 explains how standard ZO convergence guarantees can be converted into the fidelity-separable form. Sec. 4 and 5 illustrate the framework under adversarial and Tsybakov noise, respectively. Sec. 6 provides experimental results. Finally, Sec. 7 discusses the main takeaways and limitations. All missing proofs and additional experimental details are deferred to the appendix.

Notations. For an integer $N \geq 1$, we write $[N] := \{1, \dots, N\}$. The Euclidean norm is denoted by $\|\cdot\|$, and $\langle \cdot, \cdot \rangle$ denotes the inner product. We use \mathcal{F}_k for the filtration generated by the algorithm up to iteration k . The terms $O(\cdot)$ and $\tilde{O}(\cdot)$ suppress constant and log factor, respectively.

2 Wall-clock complexity

We consider the problem of minimizing an objective function $\min_{x \in \Omega} f(x)$, where $f : \Omega \rightarrow \mathbb{R}$. We assume that the algorithm accesses f through a noisy black-box oracle: upon receiving a query x , the oracle returns an estimate corrupted by an error ξ ,

$$\hat{f}(x) = f(x) + \xi. \quad (1)$$

We assume the oracle is tunable: it is characterized by a fidelity parameter $\delta > 0$ (representing the inexactness level) which controls the accuracy of the estimation. To formalize the precise dependence of $\xi(x)$ on δ , let \mathcal{F}_k denote the filtration representing the algorithm's history up to step k , and let the current iterate x_k be measurable with respect to \mathcal{F}_k . We consider two widely used models for the oracle inexactness that fit this framework: stochastic and deterministic noise.

Definition 1 (Tsybakov noise). The noise satisfies $\mathbb{E}[\xi^2 \mid \mathcal{F}_k] \leq \delta^2$. If the algorithm queries x_k multiple times, the respective noise realizations are mutually independent conditionally on \mathcal{F}_k .

Definition 2 (Adversarial noise). The noise is determined by a deterministic (but unknown) function of the queried point bounded by the fidelity level, $\xi = \xi(x_k)$ and $|\xi(x_k)| \leq \delta$.

Crucially, we assume a direct trade-off between accuracy and computation: a smaller δ yields less noise but incurs a higher per-query cost $c(\delta)$. Let $\{(x_k, \delta_k)\}_{k \in [N]}$ be a sequence of queries performed by the algorithm. The wall-clock time is

$$T_{\text{total}}(N, \{\delta_k\}_{k \in [N]}) := \sum_{k=1}^N c(\delta_k). \quad (2)$$

Remark 1 (Batching). Let $g(x, h, r, \zeta)$ denote a single gradient estimate constructed from the noisy oracle (1). For a batch size $B \geq 1$, the batched gradient estimate at iteration k is defined as $g_k^{(B)} := \frac{1}{B} \sum_{i=1}^B g(x_k, h_k, r_{k,i}, \zeta_{k,i})$, where, conditionally on x_k , the random variables $\{(r_{k,i}, \zeta_{k,i})\}_{i=1}^B$ are independent and identically distributed.

The averaging reduces variance by $1/B$ but leaves bias unchanged, while wall-clock time scales as $T_{\text{total}} = B \sum_{k=1}^N c(\delta_k)$. Our master analysis treats B as fixed, but case studies (Sec. 4 and 5) optimize $(N, B, \{\delta_k\})$, showing phase transitions between $B = 1$ and $B \gg 1$.

Choice of $c(\delta)$. We assume the computational cost of a single query scales polynomially with the fidelity as $c(\delta) \propto \delta^{-\gamma}$, $\gamma > 0$. Power-law costs naturally fit BBO, as oracle costs scale as a power of accuracy: e.g., a Monte Carlo estimator with M samples achieves $\delta \sim M^{-1/2}$ via the central limit theorem, yielding $c(\delta) \sim \delta^{-2}$. Beyond empirics, the power-law is unique among non-decreasing cost models. Consider three natural regimes: **(i)** $c(\delta) = \Theta(\ln(1/\delta))$, **(ii)** $c(\delta) = \Theta(\delta^{-\gamma})$, and **(iii)** $c(\delta) = e^{\Theta(1/\delta)}$. In (i) improving fidelity is free, so one drives δ as small as possible and T_{total} reduces to N up to log-factors. In (iii) any fidelity gain is expensive, so one uses the coarsest admissible δ and compensates by increasing N . Both regimes collapse the joint design of $(N, \{\delta_k\})$ into a trivial one-parameter problem. Only (ii) produces a trade-off in which the optimal fidelity depends on the problem parameters, and the exponent γ itself drives qualitative phase transitions in the wall-clock-optimal algorithm as shown in Sec. 4 and 5.

Wall-clock optimization problem. To connect T_{total} with the algorithm's choice, we use a generic convergence metric Gap_N . For instance, Gap_N can be $\mathbb{E}[f(x_N) - f(x^*)]$ for convex objectives, or $\frac{1}{N} \sum_{k=1}^N \mathbb{E}[\|\nabla f(x_k)\|^2]$ for non-convex ones. Usually Gap_N is bounded by a deterministic function \mathcal{E} depending on the iteration count N , the fidelities $\{\delta_k\}_k$, and the algorithmic hyperparameters Θ ,

$$\text{Gap}_N \leq \mathcal{E}(N, \{\delta_k\}_{k \in [N]}, \Theta). \quad (3)$$

An example is ZO-GD under the adversarial noise model (Def. 2). If $\delta_k = \delta$, the gap $\text{Gap}_N := f(x_N) - f^*$ is bounded by $\mathcal{E}(N, \delta, \Theta) = \frac{c_1}{N} + c_2 \delta^2$, with constants c_1, c_2 depending on Θ (e.g., step size and Lipschitz constant).

One achieves accuracy $\mathcal{E}(N, \{\delta_k\}_{k \in [N]}, \Theta) \leq \varepsilon$ through various parameter configurations resulting in a different cumulative wall-clock time T_{total} . So, we formulate the following optimization problem,

$$\min_{N, \{\delta_k\}_{k \in [N]}} T_{\text{total}}(N, \{\delta_k\}_{k \in [N]}) \quad \text{subject to} \quad \mathcal{E}(N, \{\delta_k\}_{k \in [N]}, \Theta) \leq \varepsilon.$$

2.1 Optimal Fidelity Allocation

Standard ZO analyses derive error bounds $\mathcal{E}(N, \{\delta_k\}, \Theta)$ assuming uniform fidelity ($\delta_k = \delta$). *Sec. 3 provides a methodology to extend these bounds to time-varying δ_k , revealing a common structural property we term fidelity-separability.*

Definition 3 (Fidelity-separable bound). We say that the error bound $\mathcal{E}(N, \{\delta_k\}_{k \in [N]}, \Theta)$ is *fidelity-separable* if, for any N and Θ , it can be written as

$$\mathcal{E}(N, \{\delta_k\}_{k \in [N]}, \Theta) = \mathcal{E}_0(N, \Theta) + \sum_{k=1}^N \alpha_k(N, \Theta) \delta_k^p,$$

with $\mathcal{E}_0(\cdot)$ and $\alpha_k(\cdot)$ depending on the assumptions on f and the optimization method.

Remark 2. Many algorithms admit the decomposition of Def. 3 either directly or through a finite sum of fidelity-separable terms with different exponents: $\mathcal{E}(\cdot) = \mathcal{E}_0(\cdot) + \sum_{p \in \mathcal{P}} \sum_{k=1}^N \alpha_{k,p} \delta_k^p$. We refer to each $\sum_{k=1}^N \alpha_{k,p} \delta_k^p$ as a *fidelity channel*. In such cases, the wall-clock analysis reduces to determining which channel governs the complexity in the high-precision regime.

The following result provides the closed-form solution for the optimal schedule and the resulting time complexity. Appx. C contains all proofs for this section.

Proposition 1. Fix N and let \mathcal{E} be as in Def. 3. For sufficiently large N such that $\mathcal{E}_0(N, \Theta) \leq \varepsilon - \epsilon$ for some $\epsilon > 0$, the optimal fidelity allocation $\delta_i^*(N)$ and the total wall-clock time $T_{\text{total}}(N)$ are

$$A_N := \sum_{j=1}^N \alpha_j^{\frac{\gamma}{p+\gamma}}(N, \Theta), \quad \delta_i^*(N) = \left(\frac{\epsilon}{A_N} \right)^{\frac{1}{p}} \alpha_i^{-\frac{1}{p+\gamma}}(N, \Theta), \quad T_{\text{total}}(N) = \epsilon^{-\frac{\gamma}{p}} A_N^{\frac{p+\gamma}{p}}. \quad (4)$$

Remark 3. In practice, one may require $c(\delta) = \max\{1, \delta^{-\gamma}\}$ to prevent the per-query cost from vanishing. However, this does not alter the asymptotic scaling of T_{total} (see Lem. 1).

Prop. 1 assumes that δ_k can be reset at every iteration at no extra cost. In practice, changing the fidelity often incurs overhead (re-seeding a Monte Carlo simulator, rebuilding an inner solver, recalibrating a physical oracle), making piecewise-constant or uniform schedules preferable. Cor. 1 bounds the wall-clock penalty of restricting to a uniform schedule; analysis of (6) shows that the penalty is at most constant-order whenever the coefficients $\{\alpha_j\}$ are mildly varying.

Corollary 1. Let $\tilde{A}_N := \sum_{i=1}^N \alpha_i(N, \Theta)$. Under the assumptions of Prop. 1, for a uniform fidelity schedule $\delta_k = \delta$, the optimal level δ^* and the resulting total wall-clock time $T_{\text{total}}^{\text{unif}}$ are

$$\delta^* = \left(\frac{\epsilon}{\tilde{A}_N} \right)^{\frac{1}{p}}, \quad T_{\text{total}}^{\text{unif}}(N) = N \epsilon^{-\frac{\gamma}{p}} \tilde{A}_N^{\frac{\gamma}{p}}.$$

High-precision regime. The large- N assumption is natural in the high-precision regime: as $\epsilon \rightarrow 0$, the constraint $\mathcal{E}_0(N, \Theta) < \epsilon$ with $\mathcal{E}_0(N, \Theta) \asymp N^{-\beta}$ forces $N \gtrsim \epsilon^{-1/\beta} \rightarrow \infty$.

Corollary 2 (Large N). Under Prop. 1, assume $\mathcal{E}_0(N, \Theta) \asymp N^{-\beta}$, $A_N \asymp N^\rho$, with $\beta > 0$ and $\rho > 0$. Suppose that all $\delta_k < 1$. Then

$$N^* \asymp \epsilon^{-1/\beta}, \quad \delta_k^* \asymp \epsilon^{(1+\rho/\beta)/p} \alpha_k(N^*, \Theta)^{-1/(p+\gamma)},$$

For the uniform schedule $\delta_k = \delta$ assume $\tilde{A}_N \asymp N^\sigma$, with $\sigma \in \mathbb{R}$. If $p + \sigma\gamma > 0$,

$$\tilde{N}^* \asymp \epsilon^{-1/\beta}, \quad \delta^* \asymp \epsilon^{(1+\sigma/\beta)/p}. \quad (5)$$

Remark 4. The condition $p + \sigma\gamma > 0$ is automatic for $\sigma \geq 0$, but is restrictive when $\sigma < 0$: then it requires $\gamma < \frac{p}{-\sigma}$. If this fails, (5) does not apply; and the optimum is attained at $\delta^* = 1$.

Reading the exponents. The exponent β governs the deterministic part of the bound and pins down the iteration budget $N^* \asymp \epsilon^{-1/\beta}$, which is identical for both schedules. The exponent σ describes the cumulative growth of the fidelity coefficients $\sum_k \alpha_k$ under the uniform schedule, while ρ captures the same growth under the Lagrangian-optimal allocation in Prop. 1. The wall-clock benefit of time-varying fidelity over a uniform one is therefore controlled by a single scalar gap:

$$R_{\text{opt}}(\epsilon, \gamma) := \frac{T_{\text{total}}(N^*)}{T_{\text{total}}^{\text{unif}}(\tilde{N}^*)} \asymp \epsilon^{\Delta/(\beta p)}, \quad \Delta := p + \sigma\gamma - \rho(p + \gamma). \quad (6)$$

When does a nonuniform schedule help? The term Δ is always non-negative. Indeed, with $q := \frac{\gamma}{p+\gamma} \in (0, 1)$,

Jensen’s inequality applied to $x \mapsto x^q$ gives $A_N \leq N^{1-q} \left(\sum_{j=1}^N \alpha_j \right)^q = N^{1-q} \tilde{A}_N^q$, which, after substituting $A_N \asymp N^\rho$, $\tilde{A}_N \asymp N^\sigma$, yields $\rho(p + \gamma) \leq p + \sigma\gamma$, i.e. $\Delta \geq 0$. Hence the optimal nonuniform schedule is never asymptotically worse than the uniform one. A polynomial speedup ($\Delta > 0$) requires Jensen’s inequality to be strict at the asymptotic level, which demands a sufficiently concentrated coefficient sequence $\{\alpha_j(N, \Theta)\}$. For mildly decaying sequences such as $\alpha_j \asymp j^{-a}$, $a \in (0, 1)$, we get $\rho = 1 - aq$ and $\sigma = 1 - a$, so $\Delta = 0$: in this regime, time-varying fidelity buys at most a constant-factor improvement. Polynomial gains arise when $\{\alpha_j\}$ is heavy-tailed or spike-like. Appx. C.1 provides the formal proof. Sec. A.4 validates the result empirically.

3 From ZO error bounds to fidelity-separable form

To apply Prop. 1 to a zeroth-order method, one must show that its convergence bound \mathcal{E} falls into the fidelity-separable class (Def. 3). We establish this reduction in three steps: we first fix the ingredients of a ZO setup; we then formulate a universal error decomposition shared by a broad family of ZO methods; finally, we illustrate this using the kernel two-point estimator. We begin with characterizing a ZO scenario by three interacting components. **(i) Oracle interface.** The way of constructing the gradient approximation g_k , e.g., one-point, symmetric or forward two-point, ℓ -point, and kernel-smoothed finite differences. **(ii) Noise model.** This work focuses on Tsybakov’s noise (Def. 1) or adversarial (Def. 2). **(iii) Algorithmic template.** The update rule—e.g. (accelerated) GD, SGD—which governs how estimation errors propagate across iterations.

Combinations of (i)–(iii) produce structurally different bounds $\mathcal{E}(\cdot)$. Our goal is to show that these bounds share a common decomposition as in Def. 3. This is routed through the conditional bias $b_k(x)$ and the second moment $V_k(x)$ of a gradient estimate $g_k(x, \cdot)$. Specifically, we assume that there are such functions $b_k(x) \in \mathbb{R}^d$ and $V_k(x) > 0$, that

$$\mathbb{E}[g_k(x, \cdot) \mid \mathcal{F}_k] := \nabla f(x) + b_k(x), \quad \mathbb{E}[\|g_k(x, \cdot)\|^2 \mid \mathcal{F}_k] \leq V_k(x).$$

We next show that the fidelity-separable bound (see Def. (3), Rem. 2) follows from the intermediate error decomposition below,

$$\text{Gap}_N \leq \tilde{\mathcal{E}}_0(N, \Theta) + \sum_{k=1}^N \left[a_k(N, \Theta) \mathbb{E}[\|b_k(x_k)\|] + c_k(N, \Theta) \mathbb{E}[\|b_k(x_k)\|^2] + e_k(N, \Theta) \mathbb{E}[V_k(x_k)] \right], \quad (7)$$

where $\tilde{\mathcal{E}}_0, a_k, c_k, e_k$ depend on the algorithmic hyperparameters Θ and number of steps N .

Proposition 2. *Gradient descent, accelerated gradient descent, SGD schemes satisfy (7). Explicit expressions for (a_k, c_k, e_k) are collected in Tab. 1 in the Appendix.*

Appx. D provides the proof. Crucially, *all fidelity dependence is routed through b_k and V_k , not a_k, c_k, e_k .* It therefore remains to quantify how these two quantities scale with δ_k .

Example: the kernel two-point estimator. We next show how to translate fidelity into concrete bounds on b_k, V_k using the kernel two-point estimator.

Definition 4 (Kernel two-point estimator). Let $h > 0$ be the smoothing radius, $\zeta \sim \text{Unif}(S_2^{d-1})$ a random direction, $r \sim \text{Unif}([-1, 1])$ an independent scalar, and $K: [-1, 1] \rightarrow \mathbb{R}$ a smoothing kernel (Def. 5). Given access to the noisy oracle (1), the estimator at x is

$$g_k(x; h, r, \zeta) := \frac{d}{2h} (\hat{f}(x + hr\zeta) - \hat{f}(x - hr\zeta)) K(r) \zeta. \quad (8)$$

Assumption 1 (Higher-order Smoothness). Fix $\beta \geq 2$ and let $\ell = \lfloor \beta \rfloor$. We assume $f \in \mathcal{F}_\beta(L_\beta)$, meaning f is ℓ -times continuously differentiable and the ℓ -th derivative satisfies the Hölder condition, $\|f^{(\ell)}(x) - f^{(\ell)}(z)\| \leq L_\beta \|x - z\|^{\beta-\ell}$, $\forall x, z \in \mathbb{R}^d$.

Proposition 3 ($\|b_k(x_k)\|$ and $V_k(x_k)$). Let g_k be as in Def. 4. If f satisfy Asm 1, then for any fixed $h > 0$,

$$\|b_k(x_k)\| \lesssim L h^{\beta-1} + \frac{d}{h} \delta_k, \quad V_k(x_k) \lesssim \mathbb{E}[|f(x_k^+) - f(x_k^-)|^2 | \mathcal{F}_{k-1}] + \frac{d^2}{h^2} \delta_k^2. \quad (9)$$

Appx. E contains the proof. Taking expectation and substituting (9) into (7) and collecting powers of δ_k gives a fidelity-separable bound with *two channels* (see Rem. 2). The next sections illustrate the framework. We conclude this section with regularity assumptions required for the subsequent analysis.

Assumption 2 (Regularity of f). For all $x, y \in \mathbb{R}^d$, the differentiable function $f: \mathbb{R}^d \rightarrow \mathbb{R}$ satisfies:

- (i) **L -Smoothness:** $\|\nabla f(x) - \nabla f(y)\| \leq L\|x - y\|$.
- (ii) **μ -Strong Convexity:** $f(y) \geq f(x) + \langle \nabla f(x), y - x \rangle + \frac{\mu}{2} \|y - x\|^2$ (convex if $\mu = 0$).

4 Adversarial noise

This section studies wall-clock complexity under adversarial noise (Def.2). Our main finding is that the cost exponent γ acts as a template selector: it decides whether acceleration is wall-clock-optimal ($\gamma = 1$ phase transition) but does not change the leading-order choices of N, B, δ .

4.1 Wall-clock complexity of gradient methods

Let f satisfy Asm. 2 and let the oracle's answer $\hat{f}(x)$ be corrupted by the adversarial noise (Def. 2). We consider forward finite differences gradient estimation

$$g(x, h) = \frac{1}{h} \sum_{k=1}^d (\hat{f}(x + h e^k) - \hat{f}(x)) e^k, \quad (10)$$

where $\{e^k\}_{k=1}^d$ is an orthonormal basis. Results from [Gasnikov et al., 2023], with $h = 2\sqrt{\delta/L}$, yield $\|b(x)\|_2 \leq 2\sqrt{d\delta L}$. First, consider the case $\delta_k = \delta$. If f is strongly convex (Asm. 2, $\mu > 0$),

$$f(x_N) - f^* \lesssim \mathcal{E}(N, \delta, \Theta) := LR^2 \exp\left(-\left(\frac{\mu}{L}\right)^{\frac{1}{p}} N\right) + \left(\frac{L}{\mu}\right)^{\frac{2p-1}{p}} d\delta, \quad (11)$$

with $\Theta = (L, p)$. Using gradient methods with intermediate convergence; see Devolder et al. [2013]. The parameter $p \in [1, 2]$ controls the rate of convergence: $p = 1$ recovers GM, and $p = 2$ recovers fast GM (FGM) [Vasin et al., 2023].

Proposition 4 (Uniform schedule δ). Consider gradient estimate (10). Let f satisfy Asm. 2. The wall-clock time complexity required to achieve $\mathcal{E}(N, \delta, \Theta) \leq \varepsilon$ is

$$T_{\text{total}} = \begin{cases} \tilde{O}\left(\left(\frac{L}{\mu}\right)^{\frac{1}{p}(1-\gamma)+2\gamma} \left(\frac{\varepsilon}{d}\right)^{-\gamma}\right), & \text{if } \mu > 0, \\ O\left(\left(\frac{\varepsilon}{9d}\right)^{-\gamma} \left(\frac{3LR^2}{\varepsilon}\right)^{\gamma+\frac{1}{p}}\right), & \text{if } \mu = 0. \end{cases} \quad (12)$$

Appx. F provides proof. Per (12), the optimal p for strongly convex problems ($\mu > 0$) depends on γ : $p = 2$ (FGM) is best for $\gamma < 1$, and $p = 1$ (GM) for $\gamma > 1$. Thus, accelerated methods may actually be wall-clock slower if $\gamma > 1$; Sec. A.2) provides experiments. In the convex regime ($\mu = 0$, $LR^2/\varepsilon > 1$), however, $p = 2$ is optimal across all γ .

To analyse $\{\delta_k\}_k$ selected using Prop. 1, we introduce an intermediate gradient method (IGM) (Alg. 2) and prove its convergence (Thm. 1),

$$f(x^N) - f^* \leq \left(1 - \frac{1}{16} \left(\frac{\mu}{L}\right)^{\frac{1}{p}}\right)^N LR^2 + 6d \left(\frac{\mu}{L}\right)^{2\frac{1-p}{p}} \sum_{k=0}^{N-1} \left(1 - \frac{1}{16} \left(\frac{\mu}{L}\right)^{\frac{1}{p}}\right)^{N-k-1} \delta_k.$$

Thus we can obtain the following result.

Proposition 5 (Time-varying δ_k). *Under assumptions of Prop. 4, if $\mu > 0$,*

$$T_{\text{total}}^{\text{IGM}} = \begin{cases} \tilde{O}\left(\left(\frac{\varepsilon}{12d}\right)^{-\gamma} \left(\frac{L}{\mu}\right)^{\frac{1-\gamma}{p}+2\gamma}\right), & \text{if } \gamma \approx 0, \\ O\left((1 + \gamma^{-1}) \left(\frac{\varepsilon}{12d}\right)^{-\gamma} \left(\frac{L}{\mu}\right)^{\frac{1-\gamma}{p}+2\gamma}\right) & \text{if } \gamma \not\approx 0, \end{cases}$$

The case $\gamma \approx 0$ corresponds constant time for any δ precision calculation, thus it makes sense chose $\delta_k = \delta$. Such case refers to Proposition 4. Further, if $\mu = 0$,

$$T_{\text{total}}^{\text{IGM}} = \begin{cases} \tilde{O}\left(\left(\frac{\varepsilon}{24d}\right)^{-\gamma} \left(\frac{2LR^2}{\varepsilon}\right)^{\frac{1-\gamma}{p}+2\gamma}\right), & \text{if } \gamma \approx 0, \\ O\left((1 + \gamma^{-1}) \left(\frac{\varepsilon}{24d}\right)^{-\gamma} \left(\frac{2LR^2}{\varepsilon}\right)^{\frac{1-\gamma}{p}+2\gamma}\right) & \text{if } \gamma \not\approx 0. \end{cases}$$

4.2 Accelerated ZO-SGD with adversarial noise

Set $f(x) := \mathbb{E}_\zeta[f(x, \zeta)]$, where ζ is a r.v. with an unknown distribution. Let the oracle output be corrupted by deterministic adversarial noise, $\hat{f}(x, \zeta) := f(x, \zeta) + \xi(x)$ and $|\xi(x)| \leq \delta$. Let $f(x, \cdot)$ satisfy Assm. 1 uniformly in ζ with some $\beta \geq 2$, so that the same holds for $f(x) = \mathbb{E}_\zeta[f(x, \zeta)]$. Assume there exists $\sigma_* > 0$ such that $\mathbb{E}_\zeta \|\nabla f(x^*, \zeta) - \nabla f(x^*)\|^2 \leq \sigma_*^2$, $x^* := \arg \min_x f(x)$.

We use the accelerated zero-order SGD by Lobanov and Gasnikov [2023]. To estimate the gradient, we employ a two-point scheme (see Def. 4) and adopt batching (see Rem. 1). Let B be the batch size. For the sake of transparency, we assume a constant smoothing parameter $h_t \equiv h$. Setting $Q := BN$, we use Thm. 3.1 by Bychkov et al. [2024], and write

$$\begin{aligned} \text{Gap}_N := \mathbb{E}f(x_N) - f^* &\lesssim \mathcal{E}(N, B, \delta, \Theta) := \frac{LR^2}{N^2} + \frac{LR^2}{Q} + \frac{R}{\sqrt{Q}} \left(\sqrt{d\kappa\sigma_*} + \sqrt{d\kappa Lh} + \sqrt{\kappa \frac{d\delta}{h}} \right) \\ &\quad + \underbrace{R \left(\kappa_\beta Lh^{\beta-1} + \frac{d\delta}{h} \right)}_{(I)} + \underbrace{N \left(\kappa_\beta^2 Lh^{2(\beta-1)} + \frac{d^2\delta^2}{Lh^2} \right)}_{(II)}, \end{aligned}$$

with κ, κ_β defined in (20), and $\Theta := (d, \sigma_*, L, R, h)$. Note that for a fixed δ , (I) and (II) are balanced by choosing $h^*(\delta) = \left(\frac{d\delta}{\kappa_\beta L}\right)^{1/\beta}$ (see Appx. G).

Proposition 6. *Let $Q := BN$, $p = \frac{\beta-1}{\beta}$, and $c(\Delta) = \Delta^{-\gamma}$. Define $a_1 := (\kappa_\beta L)^{1/\beta} d^{(\beta-1)/\beta}$, $a_2 := \kappa_\beta^{2/\beta} L^{2/\beta-1} d^{2(\beta-1)/\beta}$. In the large- N , large- Q regime, the optimal design satisfies*

$$N^* \asymp \frac{LR^2}{\varepsilon}, \quad Q^* \asymp \frac{R^2 \kappa d \sigma_*}{\varepsilon^2}, \quad B^* = \frac{Q^*}{N^*} \asymp \frac{\kappa d \sigma_*}{L\varepsilon}.$$

The optimal fidelity is $\delta^* \asymp \frac{\varepsilon^{\frac{\beta-1}{\beta}}}{d\kappa_\beta^{\frac{1}{\beta-1}} L^{\frac{1}{\beta-1}} R^{\frac{\beta}{\beta-1}}}$ and $h^* = h^*(\delta^*)$. Consequently,

$$T_{\text{total}}^* \asymp \frac{\kappa \sigma_* d^{1+\gamma} \kappa_\beta^{\frac{\gamma}{\beta-1}} L^{\frac{\gamma}{\beta-1}} R^{2+\frac{\gamma\beta}{\beta-1}}}{\varepsilon^{2+\frac{\gamma\beta}{\beta-1}}}$$

Take-away message. After balancing h , the adversarial model reduces to two fidelity channels, $Ra_1\delta^p$ and $Na_2\delta^{2p}$. In the large- N regime the second channel is active, which determines δ^* . The total number of oracle calls is instead dictated by σ_* , $Q^* = BN^* \asymp \frac{R^2\kappa d\sigma_*}{\varepsilon^2}$, and $B^* \asymp \frac{\kappa d\sigma_*}{L\varepsilon}$. Thus the batching regime is controlled by comparing B^* with N^* : if $B^* \leq N^*$, then $\kappa d\sigma_* \lesssim L^2R^2$. Hence, small σ_* leads to moderate batching, while large σ_* leads to overbatching.

In this adversarial large- N regime, γ affects the final wall-clock cost through $(\delta^*)^{-\gamma}$, but it does not change the leading-order choices of N^* , B^* , δ^* . *The next section shows that under another noise regime, the oracle-cost exponent γ can also change the optimal tuning parameters.*

5 Tsybakov's noise

This section considers batched setting (see Rem. 1). So, the objective is $T_{\text{total}}(N, \delta) = BN\delta^{-\gamma}$. In contrast to Sec. 4, under Tsybakov noise (Def. 1) the cost exponent γ acts as a parameter tuner controlling batching, with threshold $\gamma = 2$.

5.1 Strongly convex case: the batched baseline

Let f satisfy Asm. 2 with $\mu > 0$, Asm. 1 with $\beta \geq 2$, and assume $\|f^{(2)}(x) - f^{(2)}(z)\| \leq L$ for all x, z . We use the batched ℓ_2 -randomized estimator of Akhavan et al. [2024]. Using Cor. 19 by [Akhavan et al., 2024], we derive the following bound for the batched case (see Appx. I for detail),

$$\text{Gap}_N := \mathbb{E}[f(\hat{x}_N) - f^*] \lesssim \underbrace{\frac{dL^2R^2}{\mu N}}_{\varepsilon_0(N, \Theta)} + \underbrace{\frac{L_\beta^{2/\beta}}{\mu} \left(\frac{d^2\delta^2}{BN}\right)^{\frac{\beta-1}{\beta}}}_{\text{(I)}} + \underbrace{\frac{d^{1+2/\beta}L^2}{\mu N^{1+1/\beta}} \left(\frac{\delta^2}{BL_\beta^2}\right)^{1/\beta}}_{\text{(II)}}, \quad (13)$$

where $\Theta = R$ and L_β comes from Asm. 1. Rem. 2 applies to 13 with two channels. In the high-precision regime, (I) is an active channel; see Appx. I.

Proposition 7 (Optimal batched design under strongly convex Tsybakov noise). *Let the assumptions of Sec. 5.1 hold, and let $\mathcal{E}(N, B, \delta)$ be given by (13).*

If $0 < \gamma < 2$, then batching is not beneficial at the leading order: $B^ = 1$, and*

$$N^* \asymp \frac{dL^2R^2}{\mu\varepsilon} \frac{2\beta - 2 + \gamma}{(\beta - 1)(2 - \gamma)}, \quad \delta^* \asymp d^{-1/2}LR\mu^{\frac{1}{2(\beta-1)}}L_\beta^{-\frac{1}{\beta-1}}\varepsilon^{\frac{1}{2(\beta-1)}}C_\beta(\gamma),$$

where $C_\beta(\gamma) := \left(\frac{\gamma\beta}{2\beta-2+\gamma}\right)^{\frac{\beta}{2(\beta-1)}} \left(\frac{2\beta-2+\gamma}{(\beta-1)(2-\gamma)}\right)^{1/2}$. Consequently,

$$T_{\text{total}}^* \asymp d^{\frac{2+\gamma}{2}}L^{2-\gamma}R^{2-\gamma}L_\beta^{\frac{\gamma}{\beta-1}}\mu^{-\frac{2\beta-2+\gamma}{2(\beta-1)}}\varepsilon^{-\frac{2\beta-2+\gamma}{2(\beta-1)}}C_\beta(\gamma)$$

If $\gamma \geq 2$, the optimum is attained at the boundary $\delta^ = 1$, and*

$$T_{\text{total}}^* \asymp d^2L_\beta^{2/(\beta-1)}\mu^{-\beta/(\beta-1)}\varepsilon^{-\beta/(\beta-1)}.$$

The same total-work order can be achieved either sequentially with $B = 1$, or with a larger batch size and fewer sequential steps.

Take-away message. The Tsybakov model couples the iteration budget, fidelity and batch size through the main noise channel $(BN)^{-(\beta-1)/\beta}\delta^{2(\beta-1)/\beta}$. For $0 < \gamma < 2$, reducing δ is cheaper than batching, hence $B^* \asymp 1$. For $\gamma \geq 2$, reducing δ is too expensive and the optimum moves to $\delta^* = 1$. In this regime, batching does not improve the leading total oracle work, but it can trade parallelism for smaller sequential depth.

5.2 Tsybakov noise, accelerated convex case: batching as a new tuning parameter

We use the accelerated ZO-SGD scheme [Lobanov et al., 2024] with the batched two-point estimator (Rem. 1). The convergence bound is

$$\begin{aligned} \mathcal{E}(N, B, \delta, h, \Theta) &\lesssim \frac{LR^2}{N^2} \max \left\{ 1, \left(\frac{\kappa d}{B}\right)^2 \right\} + N \min \left\{ \frac{B}{\kappa}, \frac{\kappa d^2}{B} \right\} \left(\frac{Lh^2}{d} + \frac{\delta^2}{Lh^2} \right) \\ &\quad + \tilde{R}\kappa_\beta L_\beta h^{\beta-1} + \frac{N(\kappa_\beta L_\beta h^{\beta-1})^2}{L}. \end{aligned}$$

with κ_β, L_β defined in Def. 4 and $\Theta = (\kappa, R, \tilde{R})$.

Proposition 8 (Optimal design under accelerated Tsybakov noise). *Assume $\tilde{R} = O(R)$, and fix some suitable $h > 0$. In the small-batch regime $B \leq 4\kappa d$, set $Q := BN$. Then we get*

$$Q^* \asymp \kappa d R \sqrt{L} \varepsilon^{-1/2} \left(\frac{2+3\gamma}{2+\gamma} \right)^{1/2}, \quad \delta^* \asymp h L^{1/4} (dR)^{-1/2} \varepsilon^{3/4} G(\gamma), \quad (14)$$

with $G(\gamma) := \frac{(2\gamma)^{1/2}(2+\gamma)^{1/4}}{(2+3\gamma)^{3/4}}$. Let C_γ be a constant depending only on γ . We get,

$$T^* \asymp \kappa d^{\frac{2+\gamma}{2}} R^{\frac{2+\gamma}{2}} L^{\frac{2-\gamma}{4}} \varepsilon^{-\frac{2+3\gamma}{4}} h^{-\gamma} C_\gamma.$$

In the large-batch regime $B > 4\kappa d$, the active constraints imply $\delta^2 \asymp \frac{\varepsilon B L h^2}{N \kappa d^2}$, $T^*(B, h) \propto B^{1-\gamma/2}$. Hence $\gamma = 2$ is the batching threshold. For $0 < \gamma \leq 2$, overbatching is not beneficial at leading order. For $\gamma > 2$, the optimum increases B until $\delta^* = 1$, yielding

$$N^* \asymp R L^{\frac{1}{2}} \varepsilon^{-\frac{1}{2}}, \quad B^* \asymp \kappa d^2 R L^{-\frac{1}{2}} \varepsilon^{-\frac{3}{2}} h^{-2}, \quad T^* \asymp \kappa d^2 R^2 \varepsilon^{-2} h^{-2}.$$

Appx. H provides the proof.

Choice of h . Prop. 8 should be read conditionally on an admissible smoothing radius h . This parameter is not arbitrary: in the small-batch regime, the optimal choice is $h_{\text{sm}}^*(B) = \min\{H_1, H_2, H_3(B)\}$, with $H_1 \asymp \varepsilon^{3/4}$, $H_2 \asymp \varepsilon^{1/(\beta-1)}$, and $H_3(B) \asymp (\frac{B\varepsilon^{3/2}}{d})^{1/(2\beta-2)}$; Appx. H provides the details. Therefore the small-batch wall-clock bound should be

$$T_{\text{sm}}^*(B) \asymp \frac{\kappa d^{\frac{2+\gamma}{2}} R^{\frac{2+\gamma}{2}} L^{\frac{2-\gamma}{4}} C_\gamma}{\varepsilon^{\frac{2+3\gamma}{4}} (h_{\text{sm}}^*(B))^\gamma}$$

In the overbatching regime $\gamma > 2$, the optimal smoothing radius is again the largest admissible one, $h_{\text{lg}}^* = \min\{K_1, K_2, K_3\}$, where $K_1 \asymp d^{\frac{1}{4}}$, $K_2 \asymp \varepsilon^{\frac{1}{\beta-1}}$, and $K_3 \asymp \varepsilon^{\frac{3}{2(2\beta-2)}}$; Appx. H provides the detail. The optimized overbatching complexity is $T_{\text{overbatch}}^* \asymp \kappa d^2 R^2 \varepsilon^{-2} (h_{\text{lg}}^*)^{-2}$.

Take-away message. This case has the same logic as Sec. 5.1, but now batching and smoothing provide additional tuning parameters. In the small-batch regime (14), the optimal solution is $Q^* \asymp d R \sqrt{L} \varepsilon^{-1/2}$, $\delta^* \asymp h^* G(\gamma) L^{1/4} (dR)^{-1/2} \varepsilon^{3/4}$, and h^* is the largest smoothing radius allowed by the constraints. Thus, as in Sec. 5.1, the fidelity is not chosen from ε alone: its prefactor depends on the oracle-cost exponent γ , and it is also coupled to the smoothing choice h^* . Notably, in this regime, batching does not improve the leading active trade-off between Q and δ , because everything depends on $Q = BN$. However, batching can indirectly help if the smoothing constraint, $h^* = H_3(B)$, is active.

The difference appears when B is optimized. In the large-batch regime, the wall-clock cost scales as $T(B) \propto B^{1-\gamma/2}$. Therefore $\gamma = 2$ governs batching. For $0 < \gamma \leq 2$, increasing B does not improve the leading active trade-off, so one may take $B^* = 1$ unless a larger batch is needed to relax the admissible smoothing radius. For $\gamma > 2$, fidelity is too expensive; instead of decreasing δ , the method increases the batch size until $\delta^* = 1$. Thus, in this setting, the expensive-fidelity regime is handled by overbatching rather than by increasing N .

5.3 Regularization and comparison

We compare two convex Tsybakov designs. REGULARIZED ZO-SGD applies the strongly convex batched baseline of Sec. 5.1 to $f_\mu(x) = f(x) + \frac{\mu}{2} \|x - x_0\|^2$, with $\mu \asymp \varepsilon/R^2$. ACCELERATED ZO-SGD is the accelerated convex method of Sec. 5.2. Let T_{reg} and T_{acc} denote their wall-clock complexities. Details are deferred to Appx. I.1.

Prop. 7 gives, for REGULARIZED ZO-SGD,

$$T_{\text{reg}} \asymp \begin{cases} \frac{d^{1+\frac{\gamma}{2}} L^{2-\gamma} L_\beta^{\frac{\gamma}{\beta-1}} R^{4-\gamma+\frac{\gamma}{\beta-1}}}{\varepsilon^{2+\frac{\gamma}{\beta-1}}}, & 0 < \gamma < 2, \\ \frac{d^2 L_\beta^{\frac{2}{\beta-1}} R^{\frac{2\beta}{\beta-1}}}{\varepsilon^{2+\frac{2}{\beta-1}}}, & \gamma \geq 2. \end{cases}$$

For ACCELERATED ZO-SGD, Sec. 5.2 gives

$$T_{\text{acc}} \asymp \begin{cases} \frac{d^{1+\frac{\gamma}{2}}}{\varepsilon^{\frac{1}{2}+\frac{3\gamma}{4}+\gamma s}}, & s := \max\left\{\frac{3}{4}, \frac{1}{\beta-1}\right\}, \quad 0 < \gamma < 2, \\ \frac{d^2}{\varepsilon^{2+\frac{2}{\beta-1}}}, & \gamma \geq 2. \end{cases}$$

Thus, for $0 < \gamma < 2$, ACCELERATED ZO-SGD has the better ε -scaling when $\beta \leq 7/3$, or when $\beta > 7/3$ and $\gamma < \gamma_{\text{crit}}(\beta) := \frac{3(\beta-1)}{3\beta-5}$. For $\beta > 7/3$ and $\gamma_{\text{crit}}(\beta) < \gamma < 2$, REGULARIZED ZO-SGD is better. For $\gamma \geq 2$, both methods satisfy $T_{\text{reg}} \asymp T_{\text{acc}} \asymp d^2 \varepsilon^{-2-\frac{2}{\beta-1}}$, but ACCELERATED ZO-SGD has smaller depth, $N_{\text{acc}} \asymp R\sqrt{L} \varepsilon^{-1/2}$, $N_{\text{reg}} \asymp dL^2 R^4 \varepsilon^{-2}$.

6 End-to-end recipe: supervised PageRank with an MCMC oracle

PageRank [Page et al., 1999] is a method for ranking the nodes of a graph by importance—originally the pages of the web, ordered by how likely a user randomly following links is to land on each one. Formally, it scores each node by its mass under the stationary distribution of a random walk that, at each step, follows an outgoing edge with probability $1 - \alpha$ and with probability α restarts from a fixed distribution; a node is ranked highly when many important nodes link to it. PageRank [Bogolubsky et al., 2016] instead makes the walk *tunable*: the probability of following a given edge, and of restarting at a given node, become functions of node and edge features—properties of a page, the strength of a link—combined through a weight vector ϕ . These weights are fitted on training queries for which the desired ordering of nodes is known, so that the stationary distribution of the tuned walk reproduces those orderings and generalizes to unseen graphs.

The training set is organized into queries: each query $q \in Q$ is a separate ranking instance. Given a directed graph $\Gamma_q = (V_q, E_q)$ for each query $q \in Q$, a seed set $U_q \subset V_q$, node features $V_i^q \in \mathbb{R}^{m_1}$, edge features $E_{ij}^q \in \mathbb{R}^{m_2}$, and a restart probability $\alpha \in (0, 1)$, the parameter $\phi = (\phi_1, \phi_2) \in \mathbb{R}^m$ (where $m = m_1 + m_2$) induces a restart distribution $\pi_q^0(\phi)$ supported on U_q and a transition matrix $P_q(\phi)$ defined by

$$[\pi_q^0(\phi)]_i = \frac{\langle \phi_1, V_i^q \rangle}{\sum_{l \in U_q} \langle \phi_1, V_l^q \rangle}, \quad [P_q(\phi)]_{ij} = \frac{\langle \phi_2, E_{ij}^q \rangle}{\sum_{l: i \rightarrow l \in E_q} \langle \phi_2, E_{il}^q \rangle},$$

for $i \in U_q$ and $i \rightarrow j \in E_q$, respectively. The stationary distribution $\pi_q(\phi) \in \mathbb{R}^{p_q}$ satisfies $\pi = \alpha \pi_q^0(\phi) + (1 - \alpha) P_q(\phi)^\top \pi$. The loss is

$$f(\phi) = \frac{1}{|Q|} \sum_{q=1}^{|Q|} \|(A_q \pi_q(\phi))_+\|_2^2, \quad (15)$$

where $A_q \in \mathbb{R}^{r_q \times p_q}$ encodes the labelled-pair comparisons. The feasible set is the Euclidean ball $\Phi = \{\phi \in \mathbb{R}^m : \|\phi - \hat{\phi}\|_2 \leq R\}$, which is chosen to lie entirely within \mathbb{R}_+^m . The optimization problem is:

$$\min_{\phi \in \Phi} f(\phi).$$

We operate under the local convexity assumption introduced by Bogolubsky et al. [2016, Theorem 2], which states that Φ can be chosen as a sufficiently small neighborhood of a local minimizer ϕ^* over which f is convex.

6.1 The MCMC zero-order oracle

Rather than computing $\pi_q(\phi)$ by power iteration, we estimate it by independent samples from the random-surfer representation of PageRank. One sample is generated by drawing

$$v_0 \sim \pi_q^0(\phi), \quad K \sim \text{Geom}(\alpha) - 1,$$

and then applying K transitions according to $P_q(\phi)$. The returned state v_K has distribution

$$\alpha \sum_{t \geq 0} (1 - \alpha)^t (P_q(\phi)^\top)^t \pi_q^0(\phi) = \pi_q(\phi),$$

which is exactly the solution of $\pi_q(\phi) = \alpha \pi_q^0(\phi) + (1 - \alpha) P_q(\phi)^\top \pi_q(\phi)$. Thus the sampler is the geometric-stopping random-surfer sampler for the PageRank stationary distribution. The resulting empirical histogram $\hat{\pi}_q$ satisfies, by the Central Limit Theorem,

$$\mathbb{E} [\hat{\pi}_q | \phi] = \pi_q(\phi), \quad \mathbb{E} [\|\hat{\pi}_q - \pi_q(\phi)\|_2^2 | \phi] \leq \frac{C}{M}, \quad (16)$$

Algorithm 1 Accelerated ZO-SGD for supervised-PageRank learning with a tunable zeroth-order oracle.

Require: initial point $\phi_0 \in \Phi$; iterations N ; batch size B ; step size η ; smoothing radius h ; fidelity δ ; kernel K ; momentum cap $\bar{\beta} \in [0, 1)$.

- 1: Set $\phi_{-1} \leftarrow \phi_0$; $t_0 \leftarrow 1$.
- 2: **for** $k = 0, 1, \dots, N - 1$ **do**
- 3: $t_{k+1} \leftarrow \frac{1}{2}(1 + \sqrt{1 + 4t_k^2})$, $\beta_k \leftarrow \min(\bar{\beta}, (t_k - 1)/t_{k+1})$.
- 4: $y_k \leftarrow \text{Proj}_{\Phi}(\phi_k + \beta_k(\phi_k - \phi_{k-1}))$.
- 5: **for** $i = 1, \dots, B$ **do**
- 6: Sample $r_{k,i} \sim \text{Unif}([-1, 1])$, $u_{k,i} \sim \text{Unif}(\mathbb{S}^{m-1})$.
- 7: Query the tunable zeroth-order oracle at $\phi_{k,i}^+ = y_k + hr_{k,i}u_{k,i}$ and $\phi_{k,i}^- = y_k - hr_{k,i}u_{k,i}$, obtaining $\hat{f}(\phi_{k,i}^+; \delta)$ and $\hat{f}(\phi_{k,i}^-; \delta)$.
- 8: Form the two-point kernel estimate

$$g_{k,i} = \frac{m}{2h} \left(\hat{f}(\phi_{k,i}^+; \delta) - \hat{f}(\phi_{k,i}^-; \delta) \right) K(r_{k,i})u_{k,i}.$$

- 9: **end for**
 - 10: $\bar{g}_k \leftarrow \frac{1}{B} \sum_{i=1}^B g_{k,i}$; $\phi_{k+1} \leftarrow \text{Proj}_{\Phi}(y_k - \eta \bar{g}_k)$.
 - 11: **end for**
 - 12: **return** ϕ_N .
-

for an explicitly computable constant C independent of M . Plugging into (15) and using the Lipschitz-continuity of $u \mapsto (Au)_+$, the plug-in loss estimator satisfies a mean-square oracle guarantee

$$\mathbb{E} \left[(\hat{f}(\phi; \delta) - f(\phi))^2 \middle| \phi \right] \leq \delta^2, \quad M = \left\lceil \frac{C'}{\delta^2} \right\rceil.$$

Thus, up to the calibration constant C' , the MCMC sample budget required for a level δ scales as $M(\delta) \asymp \delta^{-2}$. This gives the oracle-cost exponent

$$c(\delta) \asymp \delta^{-2} \implies \gamma = 2.$$

The constant C' is at most a polynomial in the supremum of the loss on Φ and the spectral gap; in our experiments, we calibrate it once. Independent calls at the same ϕ produce independent noises, matching Def. 1.

6.2 Instantiating the accelerated ZO-SGD of Sec. 5.2

We solve the problem with the accelerated ZO-SGD scheme of Sec. 5.2 (labelled ‘‘Method B’’ in the figures below), instantiated on the Euclidean ball $\Phi = \{\phi : \|\phi - \hat{\phi}\| \leq R\}$ (see Alg. 1). The main experiments use a calibrated Tsybakov proxy oracle,

$$\hat{f}(\phi; \delta) = f(\phi) + \xi, \quad \xi \sim \mathcal{N}(0, \delta^2),$$

with the cost $c(\delta) = \delta^{-\gamma}$. This model isolates the optimization effect predicted by Sec. 5.2 while matching the variance–cost scaling of the MCMC PageRank sampler, for which $\gamma = 2$.

Bias and variance ($\beta = 2$). We fix the smoothness level $\beta = 2$ (Asm. 1). Since the proxy oracle is centered, its noise contributes to the second moment but not to the conditional bias of the two-point estimator. Prop. 3 therefore gives

$$\|b_k(\phi_k)\| \lesssim Lh, \quad V_k(\phi_k) \lesssim G^2 + \frac{m^2 \delta_k^2}{h^2}. \quad (17)$$

With batching, the stochastic contribution scales as

$$V_k^{(B)}(\phi_k) \lesssim G^2 + \frac{m^2 \delta_k^2}{Bh^2}.$$

The actual plug-in MCMC oracle of Sec. 6.1 is used to motivate the cost exponent $\gamma = 2$; its finite-sample bias is included in the mean-square oracle guarantee.

6.3 Wall-clock-optimal design

We now specialize the accelerated Tsybakov design of Prop. 8 to $\gamma = 2$; in its notation the ambient dimension is $d = m = m_1 + m_2$. Throughout, $\tilde{O}(\cdot)$ hides logarithmic factors.

Small-batch regime ($0 < \gamma < 2$). With $Q = BN$, Prop. 8 gives $B^* = 1$ and

$$Q^* \asymp \kappa m R \sqrt{L} \varepsilon^{-1/2} \left(\frac{2+3\gamma}{2+\gamma} \right)^{1/2}, \quad \delta^* \asymp h L^{1/4} (mR)^{-1/2} \varepsilon^{3/4} G(\gamma), \quad G(\gamma) = \frac{(2\gamma)^{1/2} (2+\gamma)^{1/4}}{(2+3\gamma)^{3/4}}, \quad (18)$$

with wall-clock cost $T^* \asymp \kappa m^{1+\gamma/2} R^{1+\gamma/2} L^{1/2-\gamma/4} \varepsilon^{-1/2-3\gamma/4} h^{-\gamma} C_\gamma$.

Boundary regime ($\gamma > 2$): **over-batching**. Here $T^*(B, h) \propto B^{1-\gamma/2}$ is decreasing in B while the interior fidelity satisfies $\delta^*(B, h) < 1$; the optimum raises B until $\delta^* = 1$, calling the oracle at the cheapest fidelity and absorbing its variance through batching:

$$N^* \asymp R \sqrt{L} \varepsilon^{-1/2}, \quad B^* \asymp \kappa m^2 R L^{-1/2} \varepsilon^{-3/2} h^{-2}, \quad T^* \asymp \kappa m^2 R^2 \varepsilon^{-2} h^{-2}. \quad (19)$$

If $\gamma = 2$. Substituting $\gamma = 2$ into either (18) or (19) gives the same leading scaling $T^* \asymp \varepsilon^{-2} h^{-2}$ for our fixed-size instance. Equivalently, $T^*(B, h) \propto B^{1-\gamma/2} \equiv B^0$ is flat in B : the same leading wall-clock order can be achieved either with smaller batches and larger sequential depth, or by distributing the work across larger batches at a constant-level fidelity. The MCMC-motivated cost model $\gamma = 2$ thus lies at the batching threshold predicted by Sec. 5.2.

Remark 5 (Why the cheapest fidelity is optimal). Under the Tsybakov proxy, the oracle variance scales as δ^2 , while the per-call cost scales as δ^{-2} . Hence $\delta^2 c(\delta)$ is constant in δ . Once the smoothing bias is kept subdominant, paying for higher fidelity does not improve the variance–cost trade-off; the surplus budget is better spent on increasing B or N .

Remark 6 (Connection to the Bogolubsky et al. [2016] bound). Bogolubsky et al. [2016, Thm. 2] obtain a $\tilde{O}(\varepsilon^{-1})$ arithmetic complexity for their gradient-free method. This rate relies on their lower-level PageRank solver: by Lemma 1 of Bogolubsky et al. [2016], an accuracy δ for the function value is obtained with an inner cost logarithmic in $1/\delta$. Thus their result belongs to the log-cost oracle regime discussed in Sec. 2.

Our setting addresses a different lower-level implementation: a sampling-based PageRank oracle for which achieving mean-square accuracy δ^2 requires $M(\delta) \asymp \delta^{-2}$ samples. In this polynomial-cost regime, simply combining an outer zeroth-order method with a high-accuracy inner oracle can be suboptimal, because the inner sampling cost becomes a leading term. The wall-clock design above instead optimizes the iteration count, fidelity, and batch size jointly; for the variance-dominated Tsybakov model at $\gamma = 2$, this yields the scaling $\tilde{O}(\varepsilon^{-2} h^{-2})$.

6.4 Numerical validation

We implement Alg. 1 in NumPy on a synthetic supervised-PageRank instance built in the spirit of Bogolubsky et al. [2016]. We take $|Q| = 4$ queries with $p_q = 20$ nodes each, $m_1 = m_2 = 4$ ($m = 8$), random directed graphs of expected out-degree 3, positive node/edge features, $\alpha = 0.15$, and a label set $\{1, \dots, 5\}$ defining the pair-comparison matrices A_q . The feasible ball is

$$\Phi = \{\phi : \|\phi - \mathbf{1}\| \leq 0.45\} \subset \mathbb{R}_{++}^m,$$

the kernel is $K(r) = 3r$, and $\bar{\beta} = 0.95$. The optimum $f^* \approx 7.282$ (initial gap ≈ 0.217) is precomputed by deterministic projected gradient descent on the exact loss. We report the wall-clock cost at which the running mean

$$\bar{f}_k = \frac{1}{T} \sum_{j=k-T+1}^k f(\phi_j)$$

over $T = 20$ iterates first drops below ε . We additionally include a sanity check for the actual MCMC sampler to confirm its δ^{-2} sample-budget scaling.

Experiment 1 (convergence). Using the Tsybakov proxy oracle, we run $N = 2000$ iterations at $\delta = 0.05$, $h = 0.1$, $B = 1$, and $\eta = 3 \cdot 10^{-4}$. The method reaches residual $\sim 10^{-3}$ in $\sim 10^3$ iterations and $\sim 10^6$ cost units, with the characteristic FISTA staircase (Fig. 1).

Experiment 2 (the optimal fidelity δ^*). Sweeping δ on a log-grid from $5 \cdot 10^{-3}$ to 1 at target $\varepsilon = 0.05$ (Fig. 2) reproduces the structure of Sec. 6.3: **(i)** for small δ the cost falls as $T_{\text{total}} \propto \delta^{-2}$ (the cost of the calls, iterations bounded); **(ii)** the optimal δ^* for $B = 1$ sits just below the divergence threshold ($\delta \approx 0.24$), beyond which noise overwhelms descent; **(iii)** raising B to 4 pushes that threshold right ($B = 4$ still converges at $\delta = 0.38$), the overbatching trade-off of (19).

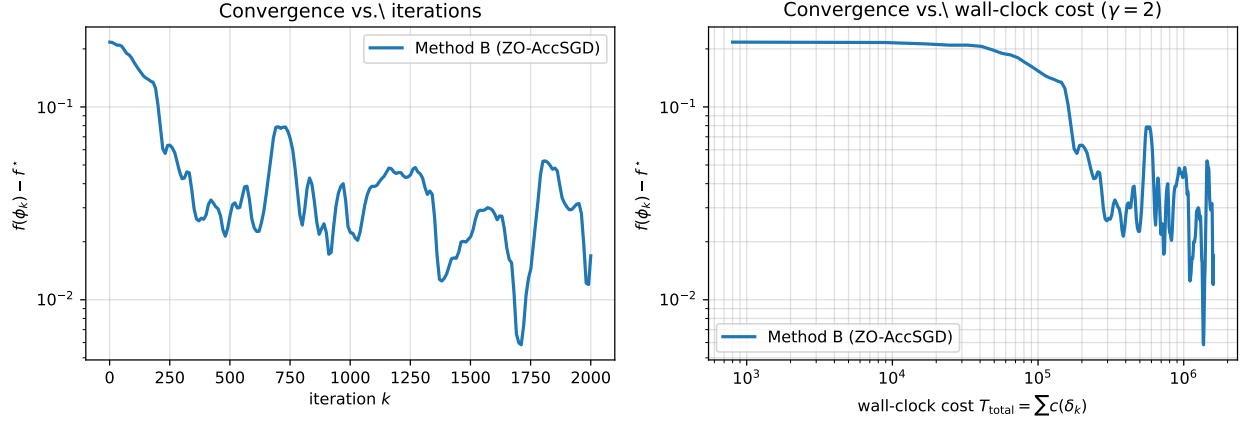


Figure 1: Convergence of the accelerated ZO-SGD on the synthetic supervised-PageRank instance. Left: trailing-mean residual vs. iteration k . Right: same vs. wall-clock cost $T_{\text{total}} = \sum c(\delta_k)$ at $\gamma = 2$.

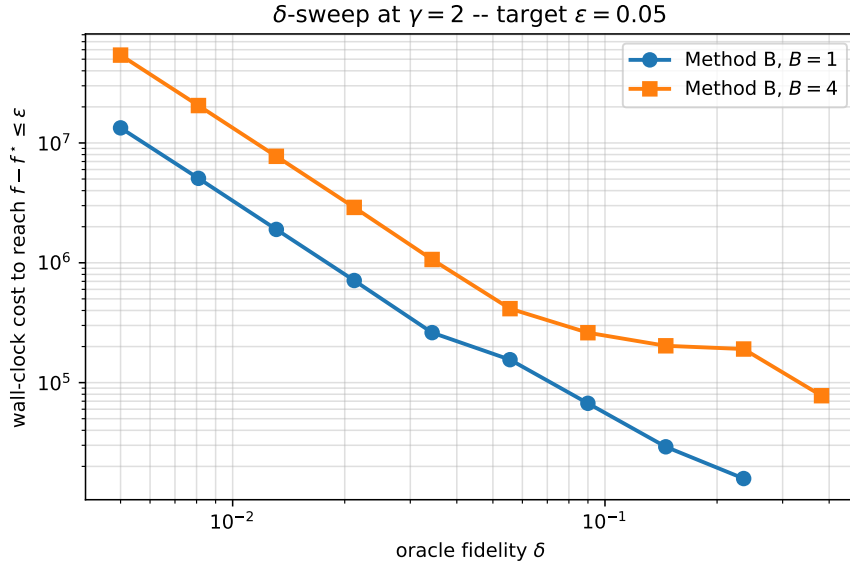


Figure 2: Wall-clock cost vs. fidelity δ at $\gamma = 2$, $\varepsilon = 0.05$. At small δ the cost scales as δ^{-2} ; the optimum sits just below the divergence threshold, matching the boundary behaviour of (19). Larger B shifts the threshold right.

Experiment 3 (flat batching at $\gamma = 2$). Fixing $\delta \in \{0.02, 0.1, 0.5\}$ and sweeping $B \in \{1, \dots, 32\}$ (with the step size scaled by $\eta_B \propto 1/(\delta/\sqrt{B})$) yields Fig. 3: at $\delta = 0.02$ batching is wasteful (cost grows linearly in B); at $\delta = 0.5$ the unbatched method does not converge at all, and the cost is essentially flat across $B \in \{2, 4, 8, 16\}$ — the empirical signature of $T^*(B) \propto B^{1-\gamma/2} = B^0$ at $\gamma = 2$.

Experiment 4 (phase transition in γ). Replacing $c(\delta) = \delta^{-2}$ by $c(\delta) = \delta^{-\gamma}$ for $\gamma \in \{0.5, 1, 1.5, 2, 2.5, 3\}$ (noise distribution unchanged) and jointly optimizing over (B, δ) gives Fig. 4: at $\gamma = 0.5$ the optimum is interior ($\delta^* \approx 0.03$, $B^* = 1$), and as γ grows it migrates to the boundary ($\delta^* = 1$, $B^* = 4$). The migration occurs slightly below the asymptotic threshold $\gamma_{\text{crit}} = 2$: this is expected, since the threshold is a small- ε , large- N statement while our instance is mid-precision ($\varepsilon = 0.05$ against an initial gap of 0.22). The qualitative prediction — δ^* jumping to the boundary and B^* above 1 as γ rises — is robustly borne out.

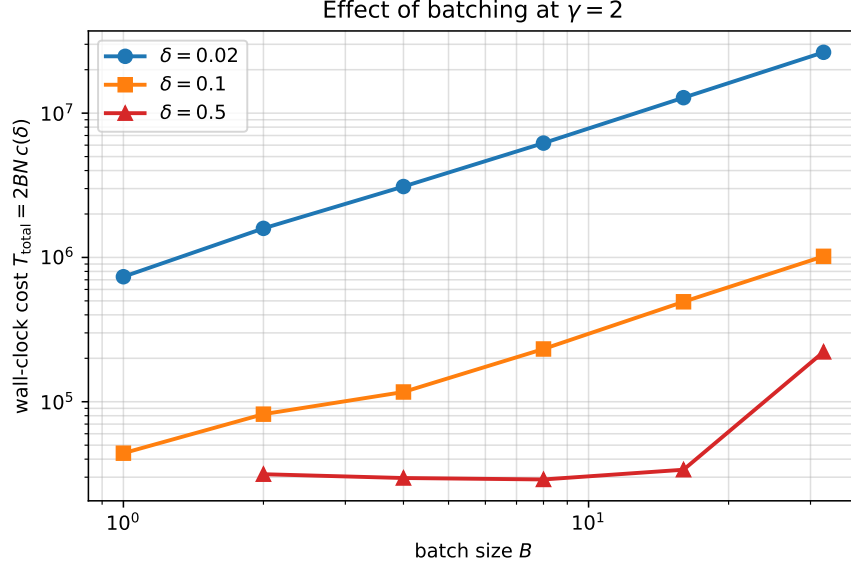


Figure 3: Effect of batch size B at three fidelities, $\gamma = 2$. At $\delta = 0.02$ cost grows linearly in B . At $\delta = 0.5$ (boundary), $B = 1$ does not converge (no marker), and cost is flat-to-helpful for $B \in \{2, 4, 8, 16\}$ — overbatching at the predicted boundary.

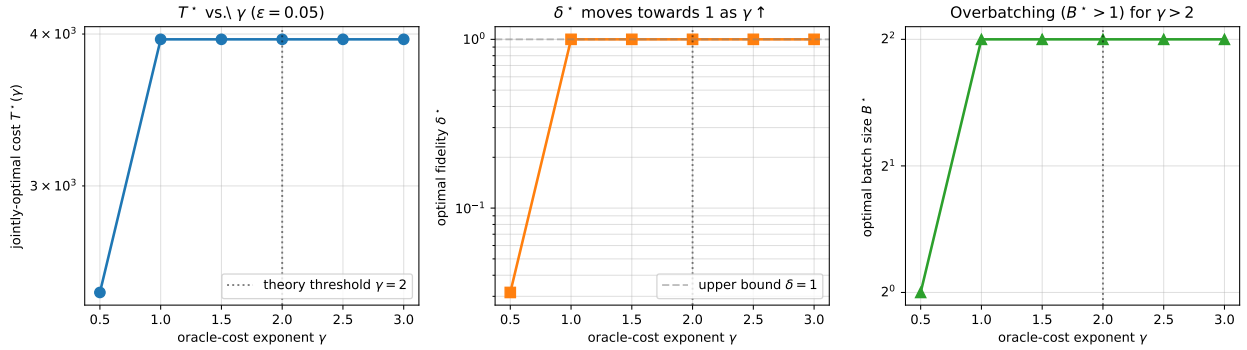


Figure 4: Phase transition in γ . Left: jointly optimized cost $T^*(\gamma)$. Centre: δ^* migrates from ≈ 0.03 at $\gamma = 0.5$ to 1 as γ crosses the threshold. Right: B^* jumps from 1 to 4 at the same transition (overbatching).

7 Discussion and limitations

Discussion. Our framework reveals that the oracle-cost exponent γ behaves differently depending on the noise model. Under adversarial noise, it acts as a template selector: a phase transition at $\gamma = 1$ makes non-accelerated GM wall-clock optimal over FGM, while optimal N , B , δ remain γ -independent. Under Tsybakov noise, γ is a parameter tuner, setting a batching threshold ($\gamma = 2$) that induces overbatching. Neither template dominates universally (Sec. 5.3); the choice depends on β and γ via $\gamma_{\text{crit}}(\beta) = \frac{3(\beta-1)}{3\beta-5}$. Finally, the gap $\Delta = p + \sigma\gamma - \rho(p + \gamma)$ in (6) precisely diagnoses when adaptive fidelity yields polynomial (rather than constant) wall-clock gains, matching empirical observations.

Limitations. (i) We assume a polynomial oracle cost $c(\delta) \propto \delta^{-\gamma}$. While this drives the non-trivial trade-offs, real oracles may have fixed overheads or regime-dependent exponents. (ii) We assume zero switching costs for fidelity (Prop. 1); explicit switching penalties remain unmodeled. (iii) Our closed-form bounds target the high-precision limit ($\varepsilon \rightarrow 0$); moderate ε requires boundary analysis. (iv) Fidelity-separability is proven for first-order templates (GD, FGM, MD, SGD; Prop. 2) under both noise models; extending this to trust-region, surrogate, or second-order ZO methods is left open. (v) Optimal schedules require known problem constants (L, μ, σ_*) . Future research. Practical

applications motivate extending our framework from absolute noise δ to composite noise models (supported empirically in Appx. A.1).

Future work will explore composite adversarial noise, $|\hat{f}(x) - f(x)| \leq \beta(f(x) - f^*)^q + \delta$ [Vasin et al., 2025], and Tsybakov noise under a strong growth condition, $\mathbb{E}(\hat{f}(x) - f(x))^2 \leq \rho(f(x) - f^*)^q + \delta^2$ [Vaswani et al., 2019]. Developing adaptive estimation for unknown problem constants is another key next step.

References

- Tadashi Kadowaki and Mitsuru Ambai. Lossy compression of matrices by black box optimisation of mixed integer nonlinear programming. *Scientific Reports*, 12(1):15482, 2022.
- Phoenix Neale Williams and Ke Li. Black-box sparse adversarial attack via multi-objective optimisation. In *Proceedings of the IEEE/CVF Conference on Computer Vision and Pattern Recognition*, pages 12291–12301, 2023.
- Yu Liu and Fabricio Oliveira. Simulator-based surrogate optimisation employing adaptive uncertainty-aware sampling. *Computers & Chemical Engineering*, page 109243, 2025.
- Sergey Shirobokov, Vladislav Belavin, Michael Kagan, Andrei Ustyuzhanin, and Atilim Gunes Baydin. Black-box optimization with local generative surrogates. *Advances in neural information processing systems*, 33:14650–14662, 2020.
- Samuel C Hoffman, Vijil Chenthamarakshan, Kahini Wadhawan, Pin-Yu Chen, and Payel Das. Optimizing molecules using efficient queries from property evaluations. *Nature Machine Intelligence*, 4(1):21–31, 2022.
- Lev Bogolubsky, Pavel Dvurechenskii, Alexander Gasnikov, Gleb Gusev, Yurii Nesterov, Andrei M Raigorodskii, Aleksey Tikhonov, and Maksim Zhukovskii. Learning supervised pagerank with gradient-based and gradient-free optimization methods. *Advances in neural information processing systems*, 29, 2016.
- Guillaume Van Dessel and François Glineur. Optimal inexactness schedules for tunable oracle-based methods. *Optimization Methods and Software*, 39(3):664–698, 2024.
- Alexander Gasnikov, Darina Dvinskikh, Pavel Dvurechensky, Eduard Gorbunov, Aleksandr Beznosikov, and Alexander Lobanov. Randomized gradient-free methods in convex optimization. In *Encyclopedia of Optimization*, pages 1–15. Springer, 2023.
- Olivier Devolder, François Glineur, Yurii Nesterov, et al. Intermediate gradient methods for smooth convex problems with inexact oracle. Technical report, Technical report, CORE-2013017, 2013.
- Artem Vasin, Alexander Gasnikov, Pavel Dvurechensky, and Vladimir Spokoiny. Accelerated gradient methods with absolute and relative noise in the gradient. *Optimization Methods and Software*, 38(6):1180–1229, 2023.
- Aleksandr Lobanov and Alexander Gasnikov. Accelerated zero-order sgd method for solving the black box optimization problem under “overparametrization” condition. In *International Conference on Optimization and Applications*, pages 72–83. Springer, 2023.
- Georgii Bychkov, Darina Dvinskikh, Anastasia Antsiferova, Alexander Gasnikov, and Aleksandr Lobanov. Accelerated zero-order sgd under high-order smoothness and overparameterized regime. *arXiv preprint arXiv:2411.13999*, 2024.
- Arya Akhavan, Evgenii Chzhen, Massimiliano Pontil, and Alexandre B Tsybakov. Gradient-free optimization of highly smooth functions: improved analysis and a new algorithm. *Journal of Machine Learning Research*, 25(370):1–50, 2024.
- Aleksandr Lobanov, Nail Bashirov, and Alexander Gasnikov. The “black-box” optimization problem: Zero-order accelerated stochastic method via kernel approximation. *Journal of Optimization Theory and Applications*, 203(3): 2451–2486, 2024.
- Lawrence Page, Sergey Brin, Rajeev Motwani, and Terry Winograd. The pagerank citation ranking: Bring order to the web. In *Proc. of the 7th International World Wide Web Conf.–1998*, 1999.
- Artem Vasin, Valery Krivchenko, Dmitry Kovalev, Fedyor Stonyakin, Nazarii Tupitsa, Pavel Dvurechensky, Mohammad Alkousa, Nikita Kornilov, and Alexander Gasnikov. On solving minimization and min-max problems by first-order methods with relative error in gradients. *arXiv preprint arXiv:2503.06628*, 2025.
- Sharan Vaswani, Francis Bach, and Mark Schmidt. Fast and faster convergence of sgd for over-parameterized models and an accelerated perceptron. In *The 22nd international conference on artificial intelligence and statistics*, pages 1195–1204. PMLR, 2019.
- Diederik P Kingma and Jimmy Ba. Adam: A method for stochastic optimization. *arXiv preprint arXiv:1412.6980*, 2014.

Li Deng. The mnist database of handwritten digit images for machine learning research [best of the web]. *IEEE signal processing magazine*, 29(6):141–142, 2012.

Kaiming He, Xiangyu Zhang, Shaoqing Ren, and Jian Sun. Deep residual learning for image recognition. In *Proceedings of the IEEE conference on computer vision and pattern recognition*, pages 770–778, 2016.

Alex Krizhevsky, Geoffrey Hinton, et al. Learning multiple layers of features from tiny images. 2009.

Pavel Dvurechensky and Alexander Gasnikov. Stochastic intermediate gradient method for convex problems with stochastic inexact oracle. *Journal of Optimization Theory and Applications*, 171(1):121–145, 2016.

Fedor Stonyakin, Alexander Tyurin, Alexander Gasnikov, Pavel Dvurechensky, Artem Agafonov, Darina Dvinskikh, Mohammad Alkousa, Dmitry Pasechnyuk, Sergei Artamonov, and Victorya Piskunova. Inexact relative smoothness and strong convexity for optimization and variational inequalities by inexact model. *arXiv preprint arXiv:2001.09013*, 2020.

Fedor Stonyakin, Alexander Tyurin, Alexander Gasnikov, Pavel Dvurechensky, Artem Agafonov, Darina Dvinskikh, Mohammad Alkousa, Dmitry Pasechnyuk, Sergei Artamonov, and Victorya Piskunova. Inexact model: A framework for optimization and variational inequalities. *Optimization Methods and Software*, 36(6):1155–1201, 2021.

Yurii Nesterov. *Lectures on convex optimization*, volume 137. Springer, 2018.

A Experiments

A.1 Estimating γ for deep learning problems

Hardware details: Experiments were performed on Intel(R) Core(TM) i9-12900H: 14 cores, 32 GB RAM, NVIDIA RTX 3080 Ti Mobile GPU 16 GiB.

Experiments details: For most experiments below was used Adam [Kingma and Ba, 2014] with learning rate = 0.001.

We provide experiments for various deep learning problems. We will estimate the error as the calculation accuracy decreases, thus, at each iteration we will calculate loss using different floating point numbers – $f_{FP16}(x^k)$ and $f_{FP64}f(x^k)$. Our goal is to estimate the γ parameter in model $c(\delta) = \delta^{-\gamma}$, assuming that $f_{FP64}(x^k)$ real function value. Thus

$$\delta_k = |f_{FP64}(x^k) - f_{FP16}(x^k)|, \quad \delta^* = \max_{0 \leq k \leq N-1} \delta_k, \quad \gamma_k = -\log_{\delta^*}(T_k^{FP16}),$$

where T_k^{FP16} is the calculation time of loss using FP16.

In this experiments, the network is not trained via ZO methods, however, at each point of the trajectory, additional steps of the forward pass are performed. We will plot training curves - loss on train dataset, accuracy on test part and δ_k, T_k, γ_k . Firstly we consider simple custom convolutional neural network and MNIST [Deng, 2012] dataset.

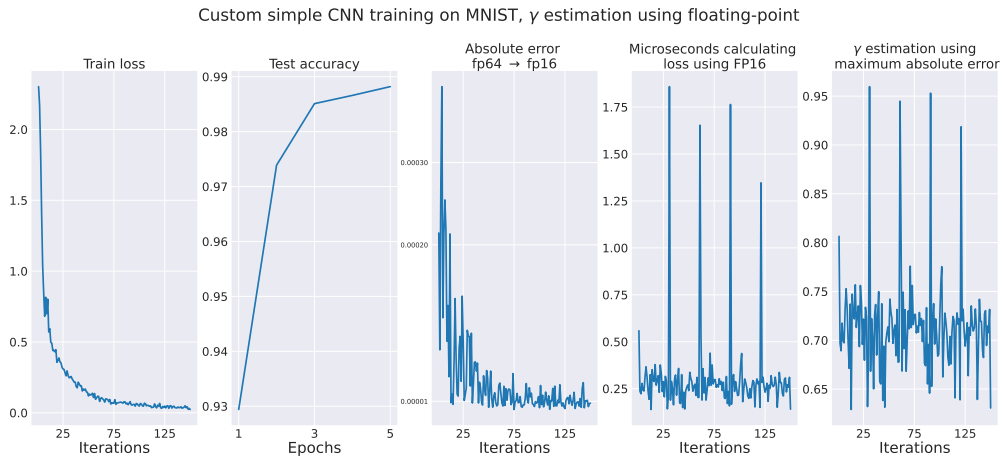


Figure 5: Simple custom CNN, MNIST, batch size – 2048

On the Figure 5 established, that $0.6 \leq \gamma \leq 1$. Note that the graph shows that the error decreases as the loss decreases, thus it is motivates to consider relative error $|\hat{f}(x) - f(x)| \leq \beta(f(x) - f^*)^q$. The following experiment uses the same idea for ResNet-18 [He et al., 2016] and CIFAR-10 [Krizhevsky et al., 2009].

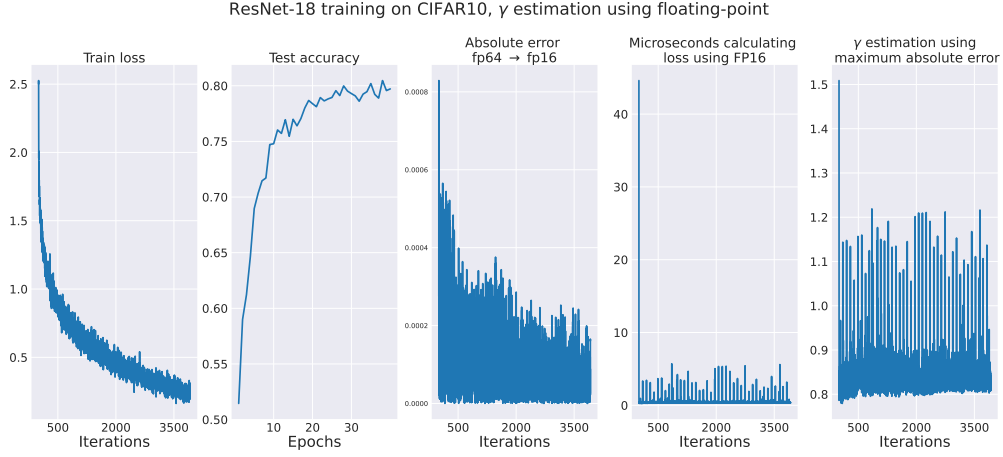


Figure 6: ResNet-18, CIFAR10, batch size – 512

Figure 6 demonstrates, that $0.7 \leq \gamma \leq 1.6$.

A.2 Comparison of GM vs. FGM

We compare GM and FGM on three strongly convex problems: (i) ridge regression on the UCI Superconductivity dataset with 81 features ¹, (ii) a synthetic quadratic objective, (iii) regularized logistic regression on a binarized version of the digits dataset ². In all cases, the ... demonstrates similar behaviour. So, below present only (i), and the rest is in Appx. A.3.

In (i), we considered $f(w) = \frac{1}{2n} \|Xw - Y\|_2^2 + \frac{\lambda}{2} \|w\|_2^2$. We set the target accuracy $\varepsilon = 10^{-8}$, and use the search of δ over 300 logarithmically spaced points between 10^{-15} and 10^{-2} . Fig. 7 presents the result; the empirical phase transition occurs around $\gamma \approx 0.9$, supporting the claim of Prop. 4

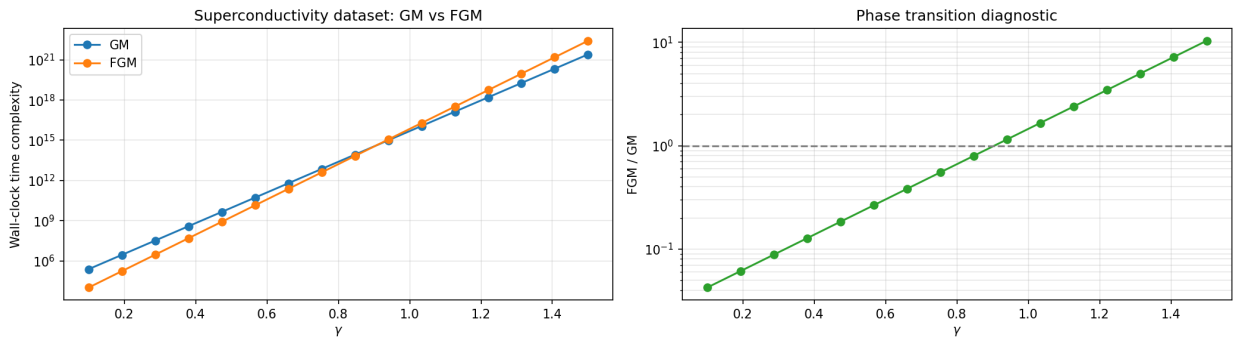


Figure 7: Comparison of the wall-clock time of GM and FGM on ridge regression over the UCI Superconductivity dataset. Left: optimal wall-clock time after tuning δ . Right: the corresponding phase transition as a function of γ

¹<https://archive.ics.uci.edu/dataset/464/superconductivity+data>

²https://scikit-learn.org/1.5/auto_examples/datasets/plot_digits_last_image.html

A.3 Additional details for the GM vs. FGM experiments

We compared standard gradient descent (GM) and the fast gradient method (FGM, implemented as STM in the code) on three problems: a synthetic quadratic objective, ridge regression, and regularized logistic regression. The performance criterion was the wall-clock time required to reach a prescribed target accuracy ε .

In all experiments, the parameter γ was varied over 10 uniformly spaced values between 0.1 and 1.5. For each value of γ , we selected a single fixed noise level δ used throughout the whole run. The value of δ was chosen by grid search over 300 logarithmically spaced points between 10^{-15} and 10^{-2} , with the search truncated at the corresponding theoretical threshold: $\delta \leq \mu\varepsilon/(Ld)$ for GM and $\delta \leq \mu^{3/2}\varepsilon/(L^{3/2}d)$ for FGM. For every candidate δ , we ran the method and recorded the time needed to reach accuracy ε ; the best such wall-clock time was reported.

For the synthetic quadratic experiment, the objective was $f(x) = \frac{1}{2}x^\top Qx$, where Q is diagonal with eigenvalues ranging from $\mu = 1$ to $L = 10$, and the dimension is $d = 20$. We used coordinate-wise forward finite differences, with gradient estimate $\nabla f(x)_i = (\hat{f}(x + he_i) - \hat{f}(x))/h$, where $h = 2\sqrt{\delta/L}$ was chosen according to the theory. The target accuracy was $\varepsilon = 10^{-6}$. The noisy oracle used a deterministic adversarial perturbation with sign given by $\text{sign}(\sin(\sum_i x_i))$. The results are shown in Figure 8.

For ridge regression, we considered $f(w) = \frac{1}{2n}\|Xw - Y\|_2^2 + \frac{\lambda}{2}\|w\|_2^2$ on the UCI Superconductivity dataset with 81 features.³ The target accuracy was $\varepsilon = 10^{-8}$, and the search over δ used the same logarithmic grid as above. The results are shown in Figure 7; the empirical phase transition occurs around $\gamma \approx 0.9$.

For regularized logistic regression, we used $f(x) = \frac{1}{n}\sum_{i=1}^n \log(1 + \exp(-y_i a_i^\top x)) + \frac{\lambda}{2}\|x\|^2$ on the `digits` dataset from `scikit-learn`, converted into a binary classification problem by grouping digits 0–4 into one class and digits 5–9 into the other.⁴ The target accuracy was $\varepsilon = 10^{-4}$, and δ was tuned over the same grid. The results are shown in Figure 9; in this case, the phase transition appears around $\gamma \approx 0.6$.

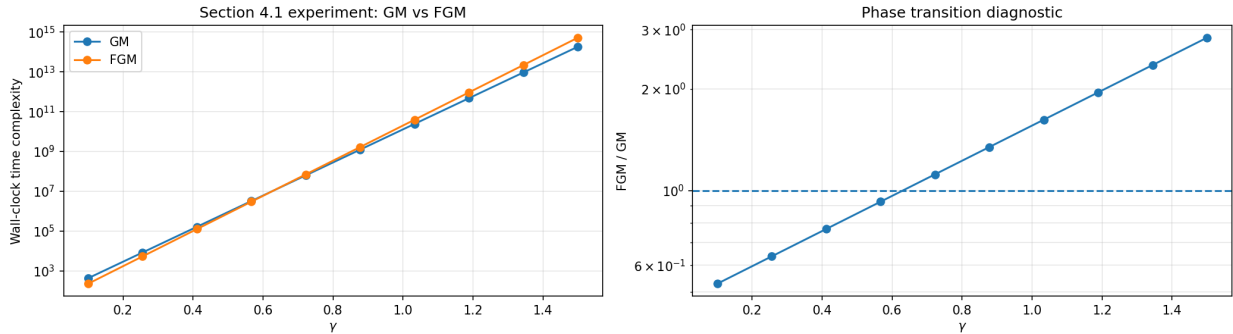


Figure 8: Comparison of GM and FGM on the quadratic objective.

³<https://archive.ics.uci.edu/dataset/464/superconductivity+data>

⁴https://scikit-learn.org/1.5/auto_examples/datasets/plot_digits_last_image.html

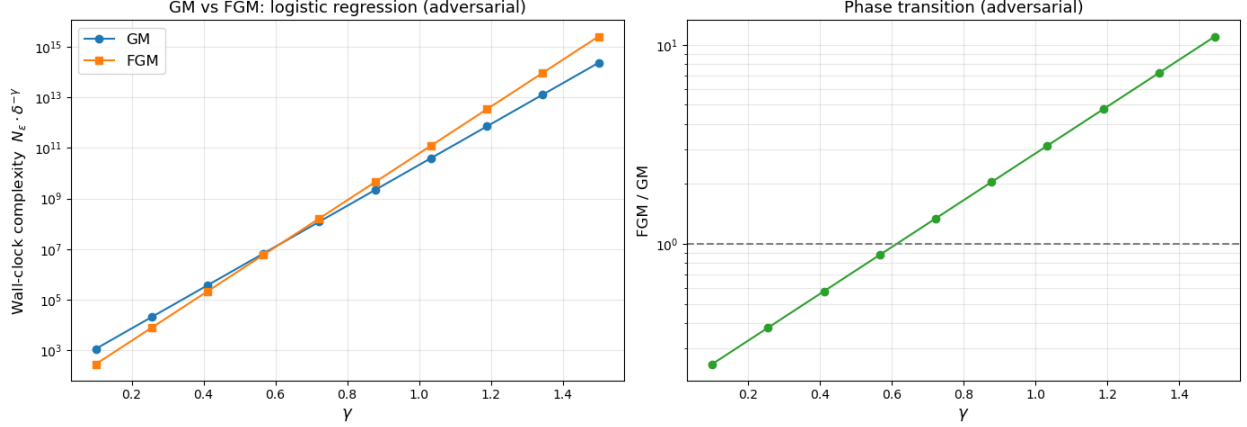


Figure 9: Comparison of the wall-clock time of GM and FGM on regularized logistic regression.

A.4 Comparison of fidelity allocation strategies

This section illustrates the results from Sec. 2.1. We consider FGM on $f(x) = \frac{\mu}{2}x_1^2 + \frac{L}{2}x_2^2$, under assumption of oracle with adversarial noise (Assumption 2). We compare two schedules: $\delta_k = \delta_0$ and $\delta_k = \delta_{k-1} \left(1 + \frac{\mu}{4L} + \sqrt{\frac{\mu}{2L}}\right)^{-\frac{1}{p+\gamma}}$ (motivated by Lemma 1). Fig. 10 shows that the adaptive schedule consistently outperforms the fixed-noise baseline. Specifically, the optimal δ_0 is larger for the adaptive strategy, and this strategy achieves lower wall-clock time across the range of target accuracies we tested. However it’s important to note that the difference is not so significant which is consistent with the theory (Prop. 9). Full details of the noise model and the tuning procedure are given in Appx. A.5.

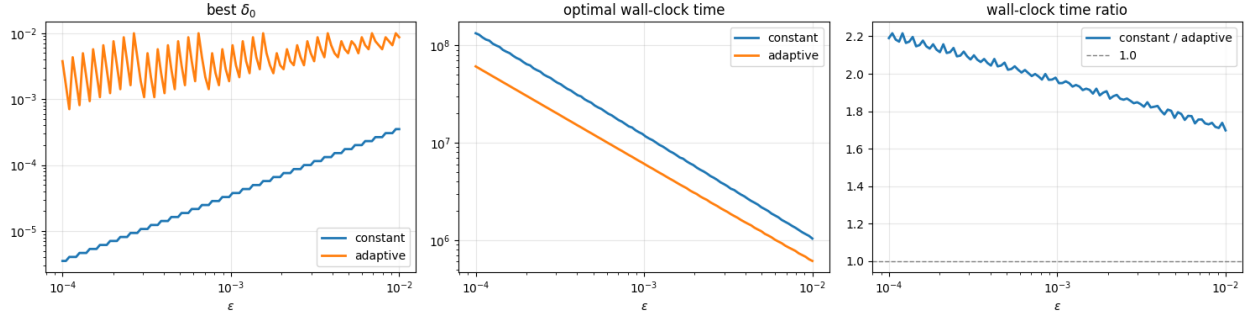


Figure 10: Comparison of fidelity allocation strategies on each iteration

A.5 Additional details for the scheduling experiments

In the second group of experiments, we considered the two-dimensional quadratic objective $f(x) = \frac{\mu}{2}x_1^2 + \frac{L}{2}x_2^2$. The gradient was approximated using central finite differences:

$$\tilde{\nabla} f(x) = \left(\frac{\hat{f}(x + he_1) - \hat{f}(x - he_1)}{2h}, \frac{\hat{f}(x + he_2) - \hat{f}(x - he_2)}{2h} \right).$$

The noise model was greedy and adversarial. At every iteration, the next point x_{k+1} depends on four noisy oracle values, corresponding to the points $x + he_1$, $x - he_1$, $x + he_2$, and $x - he_2$. Since each noisy value can vary independently within the interval $[f(\cdot) - \delta, f(\cdot) + \delta]$, the adversary has four degrees of freedom and chooses the perturbation that maximizes $f(x_{k+1})$ at the next iterate.

Because x_{k+1} is obtained from the finite-difference estimate through an affine transformation, the resulting objective is a convex continuous function of these four perturbations. Therefore, its maximum over the box $[-\delta, \delta]^4$ is attained at a vertex, so it is sufficient to enumerate all 16 vertices and choose the worst one.

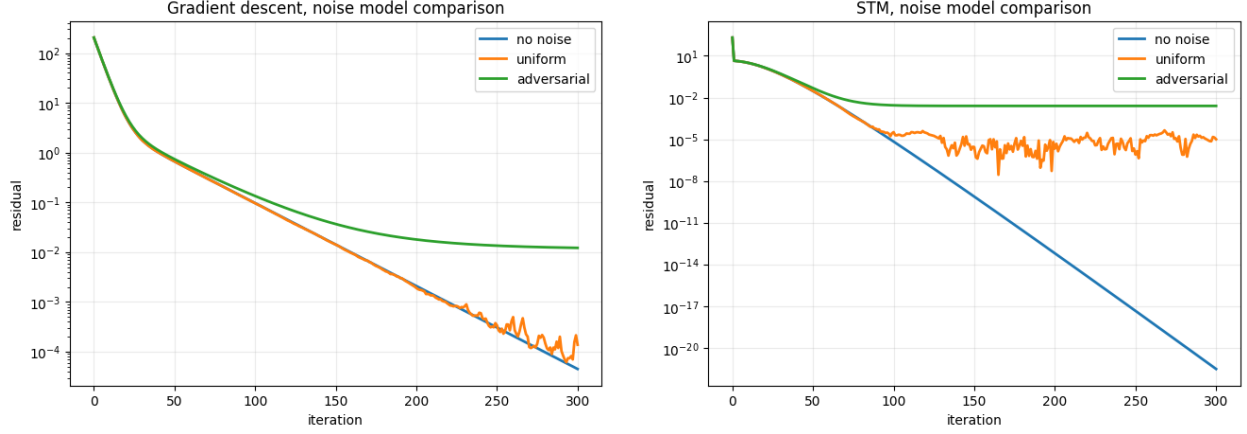


Figure 11: Comparison of convergence in function residual under different noise models.

Figure 11 compares the convergence behavior of GM and FGM under this worst-case noise model, under uniformly random noise from $[-\delta, \delta]$, and in the noiseless setting.

For this noise model, we considered the following strategies for choosing δ_k at each step of FGM: $\delta_k = \delta_0$, and

$$\delta_k = \delta_{k-1} \left(1 + \frac{\mu}{4L} + \sqrt{\frac{\mu}{2L}} \right)^{-\frac{1}{1+\gamma}},$$

with δ_0 selected over a logarithmic grid from 10^{-8} to 10^{-2} .

We now introduce an adaptive strategy motivated by the master lemma. Recall that the convergence rate of the accelerated method (FGM) [Vasin et al., 2023] with a noisy gradient, where the gradient is approximated using one of the schemes

$$\tilde{\nabla} f(x)_i = \frac{\hat{f}(x + he_i) - \hat{f}(x)}{h} \quad \text{or} \quad \tilde{\nabla} f(x)_i = \frac{\hat{f}(x + he_i) - \hat{f}(x - he_i)}{2h},$$

for N iterations with varying noise levels, has the form

$$f(x) - f(x^*) \lesssim LR^2 \exp\left(-\frac{1}{2}\sqrt{\frac{\mu}{2L}}N\right) + \sum_{i=0}^N \frac{dL}{\mu} \left(1 + \frac{\mu}{4L} + \sqrt{\frac{\mu}{2L}} \right)^{i-N} \delta_i.$$

According to the master lemma,

$$\delta_i^*(N) = \left(\frac{\epsilon}{A_N} \right) \alpha_i^{-\frac{1}{1+\gamma}}, \quad A_N := \sum_{j=1}^N \alpha_j^{\frac{\gamma}{1+\gamma}}.$$

Therefore, in the accelerated setting,

$$\frac{\delta_{i+1}^*(N)}{\delta_i^*(N)} = \left(\frac{\alpha_i}{\alpha_{i+1}} \right)^{\frac{1}{1+\gamma}} = \left(\frac{1}{1 + \frac{\mu}{4L} + \sqrt{\frac{\mu}{2L}}} \right)^{\frac{1}{1+\gamma}}.$$

This relation motivates the adaptive strategy

$$\delta_k = \delta_{k-1} \left(1 + \frac{\mu}{4L} + \sqrt{\frac{\mu}{2L}} \right)^{-\frac{1}{1+\gamma}}.$$

As before, we tune δ_0 over the same logarithmic grid. Figure 10 shows three plots. The left panel illustrates how the optimal initial noise depends on the target accuracy. As expected, when δ decreases across iterations, larger values of the initial noise level δ_0 become preferable. The middle panel shows that the adaptive strategy outperforms the strategy with fixed δ at every iteration. Finally, the right panel reports the ratio between the runtime of the strategy $\delta_k = \delta_0$ and that of the adaptive strategy. At the same time, this plot indicates that the gain from adaptivity remains rather modest, which is consistent with the theory:

Proposition 9 (Logarithmic gain for geometrically decaying coefficients). *Fix N and assume that the fidelity-separable channel has coefficients*

$$\alpha_k(N, \Theta) = Cq^{N-k}, \quad k = 1, \dots, N,$$

where $C > 0$ and

$$q = \frac{1}{1 + \frac{\mu}{4L} + \sqrt{\frac{\mu}{2L}}} \in (0, 1).$$

Let

$$T_{\text{total}}^{\text{var}}(N)$$

denote the optimal wall-clock time under the time-varying fidelity schedule of Prop. 1, and let

$$T_{\text{total}}^{\text{unif}}(N)$$

denote the optimal wall-clock time under the uniform restriction $\delta_1 = \dots = \delta_N$. If

$$N \asymp \sqrt{\frac{L}{\mu}} \log\left(\frac{LR^2}{\varepsilon}\right),$$

then, in the high-precision regime,

$$\frac{T_{\text{total}}^{\text{unif}}(N)}{T_{\text{total}}^{\text{var}}(N)} = O\left(\log\left(\frac{LR^2}{\varepsilon}\right)\right).$$

Equivalently, the time-varying fidelity schedule improves the best uniform schedule by at most a logarithmic factor for this geometric coefficient profile.

Proof. For fixed N , Prop. 1 gives

$$T_{\text{total}}^{\text{var}}(N) = \epsilon^{-\gamma/p} \left(\sum_{k=1}^N \alpha_k^{\frac{\gamma}{p+\gamma}} \right)^{\frac{p+\gamma}{p}},$$

where $\epsilon = \varepsilon - \mathcal{E}_0(N, \Theta)$ is the accuracy budget allocated to the fidelity channel. By Cor. 1, the best uniform schedule satisfies

$$T_{\text{total}}^{\text{unif}}(N) = N\epsilon^{-\gamma/p} \left(\sum_{k=1}^N \alpha_k \right)^{\gamma/p}.$$

Hence the common factor $\epsilon^{-\gamma/p}$ cancels in the ratio. Put

$$s := \frac{\gamma}{p+\gamma} \in (0, 1).$$

Since $\alpha_k = Cq^{N-k}$, the constant C also cancels, and after changing indices $r = N - k$ we obtain

$$\frac{T_{\text{total}}^{\text{unif}}(N)}{T_{\text{total}}^{\text{var}}(N)} = N \frac{\left(\sum_{r=0}^{N-1} q^r \right)^{\gamma/p}}{\left(\sum_{r=0}^{N-1} q^{sr} \right)^{(p+\gamma)/p}}.$$

Using the geometric-sum identities,

$$\sum_{r=0}^{N-1} q^r = \frac{1 - q^N}{1 - q}, \quad \sum_{r=0}^{N-1} q^{sr} = \frac{1 - q^{sN}}{1 - q^s},$$

we get

$$\frac{T_{\text{total}}^{\text{unif}}(N)}{T_{\text{total}}^{\text{var}}(N)} = N \frac{(1 - q^N)^{\gamma/p} (1 - q^s)^{(p+\gamma)/p}}{(1 - q)^{\gamma/p} (1 - q^{sN})^{(p+\gamma)/p}}.$$

For the chosen value of q ,

$$1 - q = \frac{\frac{\mu}{4L} + \sqrt{\frac{\mu}{2L}}}{1 + \frac{\mu}{4L} + \sqrt{\frac{\mu}{2L}}} = \Theta\left(\sqrt{\frac{\mu}{L}}\right)$$

as $L/\mu \rightarrow \infty$. Moreover, since $s \in (0, 1)$ is fixed,

$$1 - q^s = \Theta(1 - q) = \Theta\left(\sqrt{\frac{\mu}{L}}\right).$$

Finally,

$$N \asymp \sqrt{\frac{L}{\mu}} \log\left(\frac{LR^2}{\varepsilon}\right)$$

implies that $N(1-q) \asymp \log(LR^2/\varepsilon)$, so in the high-precision regime q^{sN} is bounded away from 1 and $(1-q^N)^{\gamma/p} \leq 1$. Therefore,

$$\frac{T_{\text{total}}^{\text{unif}}(N)}{T_{\text{total}}^{\text{var}}(N)} = O\left(N \frac{(1-q)^{(p+\gamma)/p}}{(1-q)^{\gamma/p}}\right) = O(N(1-q)).$$

Substituting $1-q = \Theta(\sqrt{\mu/L})$ yields

$$\frac{T_{\text{total}}^{\text{unif}}(N)}{T_{\text{total}}^{\text{var}}(N)} = O\left(\log\left(\frac{LR^2}{\varepsilon}\right)\right),$$

as claimed. \square

B Some definitions

Definition 5 (Smoothing kernel). We assume that a kernel function $K : [-1, 1] \rightarrow \mathbb{R}$ is such that for a fixed $\beta \geq 2$: $\int_{-1}^1 K(r) dr = 0$, $\int_{-1}^1 rK(r) dr = 1$, and $\int_{-1}^1 |r|^\beta |K(r)| dr < \infty$. Additionally, if $\beta > 2$, we require $\int_{-1}^1 r^j K(r) dr = 0$ for all $j = 2, \dots, \lfloor \beta \rfloor$. Further, we set

$$\kappa_\beta = \int |u|^\beta |K(u)| du, \quad \kappa = \int |K(u)|^2 du. \quad (20)$$

C Proofs from Sec. 2.1

Proof of Master Lemma 1. Since $\Phi(N, \Theta)$ does not depend on $\delta_1, \dots, \delta_N$, our goal is to minimize $\sum \delta_i^{-\gamma}$ subject to $\sum \alpha_i \delta_i^p = \varepsilon$. The Lagrangian is

$$\mathcal{L} = \sum_{i=1}^N \delta_i^{-\gamma} + \lambda \left(\sum_{i=1}^N \alpha_i \delta_i^p - \varepsilon \right).$$

The stationarity condition $\frac{\partial \mathcal{L}}{\partial \delta_i} = 0$:

$$-\gamma \delta_i^{-\gamma-1} + \lambda p \alpha_i \delta_i^{p-1} = 0 \implies \delta_i = \left(\frac{\gamma}{\lambda \alpha_i p} \right)^{\frac{1}{p+\gamma}}. \quad (21)$$

Substituting the equation for δ_i into the λ -constraint, and then substituting δ_i^* into the objective function, yields (4). \square

Lemma 1. Let $c(\delta) := \max\{\delta^{-\gamma}, 1\}$ for some $\gamma > 0$ and $\delta > 0$. Fix N and assume that the bound $\mathcal{E}(N, \{\delta_k\}_{k \in [N]}, \Theta)$ admits a decomposition

$$\mathcal{E}(N, \{\delta_k\}_{k \in [N]}, \Theta) = \Phi(N, \Theta) + \sum_{k=1}^N \alpha_k \delta_k^p$$

with α_k being depend on the choice of gradient estimator, noise model and optimization algorithm. Let $\mathcal{E}(N, \{\delta_k\}_{k \in [N]}, \Theta) \lesssim \varepsilon$. Denote

$$K(N, m) := \left(\frac{\varepsilon - \sum_{i=m+1}^N \alpha_i}{\sum_{i=1}^m \alpha_i^{-\frac{\gamma}{p+\gamma}}} \right)^{\frac{1}{p}}.$$

Then we get the following solution

$$\delta_k(N) = \begin{cases} K(N, m^*) \alpha_k^{-\frac{1}{p+\gamma}}, & \text{if } k \leq m^* \\ 1, & \text{if } k > m^*, \end{cases}$$

where m^* is the smallest m satisfying

$$K(N, m) \alpha_m^{-\frac{1}{p+\gamma}} < 1 \quad \text{and} \quad K(m) \alpha_{m+1}^{-\frac{1}{p+\gamma}} \geq 1.$$

Proof. The Lagrangian is

$$\mathcal{L} = \sum_{i=1}^N \delta_i^{-\gamma} + \lambda_0 \left(\sum_{i=1}^N \alpha_i \delta_i^p - \varepsilon \right) + \sum_{i=1}^N \lambda_i (\delta_i - 1) - \sum_{i=1}^N \tilde{\lambda}_i \delta_i.$$

If $0 < \delta_i < 1$, (21) holds. Let

$$K := \left(\frac{\gamma}{\lambda_0 p} \right)^{\frac{1}{p+\gamma}}.$$

If $\delta_i = 1$, then $\tilde{\lambda}_i = 0$ and

$$-\gamma + \lambda_0 \alpha_i p + \lambda_i = 0 \Rightarrow \lambda_i = \gamma - \lambda_0 \alpha_i p \geq 0 \Rightarrow \lambda_0 \alpha_i p \leq \gamma.$$

Next, let us rearrange δ_i in increasing order, and let m be s.t. $\delta_m \in (0, 1)$ and $\delta_{m+1} = 1$ (m is not known so far). Thus,

$$K^p \sum_{i=1}^m \alpha_i^{1-\frac{p}{p+\gamma}} + \sum_{i=m+1}^N \alpha_i \leq \varepsilon \Rightarrow K(m) := \left(\frac{\varepsilon - \sum_{i=m+1}^N \alpha_i}{\sum_{i=1}^m \alpha_i^{-\frac{\gamma}{p+\gamma}}} \right)^{\frac{1}{p}}$$

Finally, using the explicit form of α_i , we have to find the smallest m , s.t.

$$K(m) \alpha_m^{-\frac{1}{p+\gamma}} < 1 \quad \text{and} \quad K(m) \alpha_{m+1}^{-\frac{1}{p+\gamma}} \geq 1.$$

□

Corollary 3 (Large N full version). *Under Prop. 1, assume that, as $N \rightarrow \infty$,*

$$\mathcal{E}_0(N, \Theta) \asymp N^{-\beta}, \quad A_N(\gamma) := \sum_{j=1}^N \alpha_j(N, \Theta)^{\gamma/(p+\gamma)} \asymp (\gamma) N^\rho,$$

with $\beta > 0$ and $\rho > 0$. Let

$$D_\gamma := \rho(p + \gamma) + \beta\gamma.$$

Then the continuous interior optimizer is

$$N^* = \left(\frac{C_0 D_\gamma}{\rho(p + \gamma) \varepsilon} \right)^{1/\beta},$$

and

$$\delta_k^* = \left(\frac{\beta\gamma\varepsilon}{D_\gamma C_A(\gamma)(N^*)^\rho} \right)^{1/p} \alpha_k(N^*, \Theta)^{-1/(p+\gamma)}.$$

For the uniform schedule $\delta_k \equiv \delta$, assume that

$$\tilde{A}_N := \sum_{j=1}^N \alpha_j(N, \Theta) \sim \tilde{C}_A N^\sigma,$$

where $\sigma \in \mathbb{R}$ and $p + \sigma\gamma > 0$. Let

$$\tilde{D}_\gamma := p + \sigma\gamma + \beta\gamma.$$

Then the continuous interior optimizer under the uniform restriction is

$$\tilde{N}^* = \left(\frac{C_0 \tilde{D}_\gamma}{(p + \sigma\gamma) \varepsilon} \right)^{1/\beta}, \quad \delta^* = \left(\frac{\beta\gamma\varepsilon}{\tilde{D}_\gamma \tilde{C}_A (\tilde{N}^*)^\sigma} \right)^{1/p}.$$

For integer horizons, the displayed values are continuous relaxations; the integer optimizer is obtained by minimizing the same one-dimensional objective over feasible $N \in \mathbb{N}$, which does not affect the leading ε -scaling.

Proof. We first consider the nonuniform case. For a fixed feasible horizon N , define

$$\eta_N := \varepsilon - \mathcal{E}_0(N, \Theta) = \varepsilon - C_0 N^{-\beta}.$$

By Prop. 1, the fixed- N optimal fidelity allocation is

$$\delta_k^*(N) = \left(\frac{\eta_N}{A_N(\gamma)} \right)^{1/p} \alpha_k(N, \Theta)^{-1/(p+\gamma)},$$

and the corresponding wall-clock cost is

$$T^*(N) \asymp \eta_N^{-\gamma/p} A_N(\gamma)^{(p+\gamma)/p}.$$

Using $A_N(\gamma) \sim C_A(\gamma)N^\rho$, the continuous relaxation is

$$T^*(N) \asymp (\varepsilon - C_0 N^{-\beta})^{-\gamma/p} (C_A(\gamma)N^\rho)^{(p+\gamma)/p}.$$

Equivalently,

$$\log T^*(N) = -\frac{\gamma}{p} \log(\varepsilon - C_0 N^{-\beta}) + \frac{\rho(p+\gamma)}{p} \log N + \text{const.}$$

The first-order condition gives

$$\frac{\rho(p+\gamma)}{pN} = \frac{\gamma \beta C_0 N^{-\beta-1}}{p \varepsilon - C_0 N^{-\beta}}.$$

Hence

$$\rho(p+\gamma)(\varepsilon - C_0 N^{-\beta}) = \beta \gamma C_0 N^{-\beta}.$$

Therefore

$$C_0 N^{-\beta} = \frac{\rho(p+\gamma)}{\rho(p+\gamma) + \beta \gamma} \varepsilon = \frac{\rho(p+\gamma)}{D_\gamma} \varepsilon,$$

which yields

$$N^* = \left(\frac{C_0 D_\gamma}{\rho(p+\gamma)\varepsilon} \right)^{1/\beta}.$$

At this horizon,

$$\eta_{N^*} = \varepsilon - C_0 (N^*)^{-\beta} = \frac{\beta \gamma}{D_\gamma} \varepsilon.$$

Substituting this and

$$A_{N^*}(\gamma) \asymp C_A(\gamma)(N^*)^\rho$$

into the fixed- N allocation formula gives

$$\delta_k^* = \left(\frac{\beta \gamma \varepsilon}{D_\gamma C_A(\gamma)(N^*)^\rho} \right)^{1/p} \alpha_k(N^*, \Theta)^{-1/(p+\gamma)}.$$

In particular,

$$N^* \asymp \varepsilon^{-1/\beta}, \quad \delta_k^* \asymp \varepsilon^{(1+\rho/\beta)/p} \alpha_k(N^*, \Theta)^{-1/(p+\gamma)}.$$

We now consider the uniform restriction $\delta_k \equiv \delta$. For fixed N , the error constraint becomes

$$\mathcal{E}_0(N, \Theta) + \tilde{A}_N \delta^p \leq \varepsilon.$$

Thus the largest admissible uniform fidelity level is

$$\delta^*(N) = \left(\frac{\varepsilon - C_0 N^{-\beta}}{\tilde{A}_N} \right)^{1/p}.$$

The fixed- N wall-clock cost is therefore

$$T_{\text{unif}}^*(N) \asymp N(\delta^*(N))^{-\gamma} = N \left(\frac{\tilde{A}_N}{\varepsilon - C_0 N^{-\beta}} \right)^{\gamma/p}.$$

Using $\tilde{A}_N \sim \tilde{C}_A N^\sigma$, we get

$$T_{\text{unif}}^*(N) \asymp N \left(\frac{\tilde{C}_A N^\sigma}{\varepsilon - C_0 N^{-\beta}} \right)^{\gamma/p}.$$

Equivalently,

$$\log T_{\text{unif}}^*(N) = \left(1 + \frac{\sigma\gamma}{p} \right) \log N - \frac{\gamma}{p} \log(\varepsilon - C_0 N^{-\beta}) + \text{const.}$$

The condition $p + \sigma\gamma > 0$ ensures that the continuous objective grows for sufficiently large N , so the interior critical point gives the interior minimizer. Differentiating gives

$$1 + \frac{\sigma\gamma}{p} = \frac{\beta\gamma}{p} \frac{C_0 N^{-\beta}}{\varepsilon - C_0 N^{-\beta}}.$$

Hence

$$C_0 N^{-\beta} = \frac{p + \sigma\gamma}{p + \sigma\gamma + \beta\gamma} \varepsilon = \frac{p + \sigma\gamma}{\tilde{D}_\gamma} \varepsilon.$$

Therefore

$$\tilde{N}^* = \left(\frac{C_0 \tilde{D}_\gamma}{(p + \sigma\gamma)\varepsilon} \right)^{1/\beta},$$

and

$$\varepsilon - C_0 (\tilde{N}^*)^{-\beta} = \frac{\beta\gamma}{\tilde{D}_\gamma} \varepsilon.$$

Substituting into the fixed- N formula for $\delta^*(N)$ yields

$$\delta^* = \left(\frac{\beta\gamma \varepsilon}{\tilde{D}_\gamma \tilde{C}_A (\tilde{N}^*)^\sigma} \right)^{1/p}.$$

Consequently,

$$\tilde{N}^* \asymp \varepsilon^{-1/\beta}, \quad \delta^* \asymp \varepsilon^{(1+\sigma/\beta)/p}.$$

The argument above covers the interior optimum only. If the resulting fidelity level violates an admissible upper bound, e.g. $\delta^* > 1$, then the optimizer lies on the boundary of the fidelity set and the displayed interior formulas do not apply. \square

C.1 Optimized nonuniform-to-uniform cost ratio.

For the nonuniform allocation, Prop. 1 gives, for fixed N ,

$$T_{\text{total}}(N) \asymp (\varepsilon - C_0 N^{-\beta})^{-\gamma/p} (C_A(\gamma) N^\rho)^{(p+\gamma)/p}.$$

At the continuous optimum,

$$N^* = \left(\frac{C_0 D_\gamma}{\rho(p + \gamma)\varepsilon} \right)^{1/\beta}, \quad \varepsilon - C_0 (N^*)^{-\beta} = \frac{\beta\gamma}{D_\gamma} \varepsilon,$$

where $D_\gamma = \rho(p + \gamma) + \beta\gamma$. Hence

$$T_{\text{total}}(N^*) \asymp C_A(\gamma)^{(p+\gamma)/p} \left(\frac{\beta\gamma}{D_\gamma} \right)^{-\gamma/p} \left(\frac{C_0 D_\gamma}{\rho(p + \gamma)} \right)^{\frac{\rho(p+\gamma)}{\beta p}} \varepsilon^{-D_\gamma/(\beta p)}.$$

For the uniform allocation,

$$T_{\text{total}}^{\text{unif}}(N) \asymp N \left(\frac{\tilde{C}_A N^\sigma}{\varepsilon - C_0 N^{-\beta}} \right)^{\gamma/p}.$$

At the continuous optimum,

$$\tilde{N}^* = \left(\frac{C_0 \tilde{D}_\gamma}{(p + \sigma\gamma)\varepsilon} \right)^{1/\beta}, \quad \varepsilon - C_0 (\tilde{N}^*)^{-\beta} = \frac{\beta\gamma}{\tilde{D}_\gamma} \varepsilon,$$

where $\tilde{D}_\gamma = p + \sigma\gamma + \beta\gamma$. Therefore

$$T_{\text{total}}^{\text{unif}}(\tilde{N}^*) \asymp \tilde{C}_A^{\gamma/p} \left(\frac{\beta\gamma}{\tilde{D}_\gamma} \right)^{-\gamma/p} \left(\frac{C_0 \tilde{D}_\gamma}{p + \sigma\gamma} \right)^{\frac{p+\sigma\gamma}{\beta p}} \varepsilon^{-\tilde{D}_\gamma/(\beta p)}.$$

Dividing the two estimates yields

$$R_{\text{opt}}(\varepsilon, \gamma) := \frac{T_{\text{total}}(N^*)}{T_{\text{total}}^{\text{unif}}(\tilde{N}^*)} \asymp K_\gamma \varepsilon^{(\tilde{D}_\gamma - D_\gamma)/(\beta p)}.$$

Since

$$\tilde{D}_\gamma - D_\gamma = p + \sigma\gamma - \rho(p + \gamma),$$

we obtain

$$R_{\text{opt}}(\varepsilon, \gamma) \asymp K_\gamma \varepsilon^{\frac{p+\sigma\gamma-\rho(p+\gamma)}{\beta p}}.$$

Thus $R_{\text{opt}}(\varepsilon, \gamma) \rightarrow 0$ as $\varepsilon \rightarrow 0$ whenever

$$\rho(p + \gamma) < p + \sigma\gamma.$$

D Proof of Prop. 2

The idea of the proof is as follows.

Proof sketch The estimate g_k enters the per-step inequality only through the inner product $\langle g_k, v_k \rangle$ with an \mathcal{F}_{k-1} -measurable vector v_k (e.g. $v_k = x_k - x^*$ for GD) and through the squared norm $\|g_k\|^2$. Taking the conditional expectation gives $\mathbb{E}[\langle g_k, v_k \rangle \mid \mathcal{F}_{k-1}] = \langle \nabla f(x_k), v_k \rangle + \langle b_k(x_k), v_k \rangle$; Cauchy–Schwarz on the bias term produces $\|b_k\| \cdot \|v_k\|$, while $\mathbb{E}[\|g_k\|^2 \mid \mathcal{F}_{k-1}] \leq V_k$ handles the squared-norm term. A Young-type inequality applied to any cross term involving $\|b_k\| \cdot \|v_k\|$ yields the quadratic contribution $\|b_k\|^2$. Telescoping across iterations gives the three sums in (7).

Table 1 provides specific examples of error decomposition (7). Namely, a_k multiplies the linear bias term, c_k multiplies the squared bias term, and e_k multiplies the second-moment term of the stochastic gradient estimator. These coefficients depend only on the underlying first-order method and not on the particular zeroth-order oracle.

This separation is useful because the oracle-specific estimates enter only through bounds on the conditional bias b_k and second moment V_k . In particular, mirror descent accumulates the bias linearly through the regret inequality, nonconvex SGD converts the bias-gradient cross term into a squared-bias contribution, strongly convex SGD propagates the errors through the contraction weights, and accelerated SGD amplifies them according to the acceleration weights.

Table 1: Coefficients a_k, c_k, e_k in the error decomposition (7). A dash “—” indicates the term is absent.

Method	Gap _N	a_k	c_k	e_k	Ref.
Mirror Descent (cvx)	$\mathbb{E}[f(\bar{x}_N)] - f^*$	$\frac{\alpha_k D_K}{S_N}$	—	$\frac{\alpha_k^2}{2S_N}$	Prop. 10
SGD (nonconvex)	$\mathbb{E}[\frac{1}{S_N} \sum_k \alpha_k \ \nabla f(x_k)\ ^2]$	—	$\frac{\alpha_k}{S_N}$	$\frac{L\alpha_k^2}{S_N}$	Prop. 11
SGD (μ -str. cvx)	$f(x_N) - f^*$	—	$\frac{L\rho_N \alpha_k}{\mu\rho_{k+1}}$	$\frac{L\rho_N \alpha_k^2}{\rho_{k+1}}$	Prop. 12
Accelerated SGD (cvx)	$f(x_N^{ag}) - f^*$	$\frac{\gamma_k R}{\beta_N \gamma_N}$	$\frac{\gamma_k^2}{\beta_N \gamma_N}$	$\frac{\gamma_k^2}{\beta_N \gamma_N}$	Prop. 13

Notation. $S_N := \sum_{t=0}^{N-1} \alpha_t$; $\rho_{k+1} := \prod_{s=0}^k (1 - \alpha_s \mu)$; $D_K := \sup_{x \in K} \|x - x^*\|$; $R := \|x_0 - x^*\|$; $\beta_N \gamma_N$ is the normalization of the accelerated scheme; B is the batch size. All equalities hold up to universal constants.

Proposition 10 (Mirror descent with biased stochastic gradients). *Let $K \subset \mathbb{R}^d$ be convex and compact, and let $x^* \in K$ be a minimizer of a convex function f . Consider mirror descent*

$$x_{k+1} = \arg \min_{x \in K} \{ \alpha_k \langle \hat{g}_k, x \rangle + D_\psi(x, x_k) \},$$

where ψ is 1-strongly convex with respect to a norm $\|\cdot\|$ and D_ψ is the associated Bregman divergence. Suppose

$$\mathbb{E}[\hat{g}_k \mid \mathcal{F}_k] = \nabla f(x_k) + b_k(x_k), \quad \mathbb{E}[\|\hat{g}_k\|_*^2 \mid \mathcal{F}_k] \leq V_k(x_k).$$

Let $D_K := \sup_{x \in K} \|x - x^*\|$ and $S_N := \sum_{k=0}^{N-1} \alpha_k$. Then the averaged point $\bar{x}_N := S_N^{-1} \sum_{k=0}^{N-1} \alpha_k x_k$ satisfies

$$\mathbb{E}[f(\bar{x}_N) - f^*] \leq \frac{D_\psi(x^*, x_0)}{S_N} + \sum_{k=0}^{N-1} \left[\frac{\alpha_k D_K}{S_N} \mathbb{E}\|b_k(x_k)\| + \frac{\alpha_k^2}{2S_N} \mathbb{E}V_k(x_k) \right].$$

Thus, in (7),

$$a_k = \frac{\alpha_k D_K}{S_N}, \quad c_k = 0, \quad e_k = \frac{\alpha_k^2}{2S_N}.$$

Proof. The standard mirror-descent three-point inequality gives, for every $x \in K$,

$$\alpha_k \langle \hat{g}_k, x_k - x \rangle \leq D_\psi(x, x_k) - D_\psi(x, x_{k+1}) + \frac{\alpha_k^2}{2} \|\hat{g}_k\|_*^2.$$

Taking $x = x^*$ and conditional expectation with respect to \mathcal{F}_k ,

$$\alpha_k \langle \nabla f(x_k), x_k - x^* \rangle \leq \mathbb{E}[D_\psi(x^*, x_k) - D_\psi(x^*, x_{k+1}) \mid \mathcal{F}_k] + \frac{\alpha_k^2}{2} V_k(x_k) + \alpha_k \langle b_k(x_k), x^* - x_k \rangle.$$

By convexity, $f(x_k) - f^* \leq \langle \nabla f(x_k), x_k - x^* \rangle$, and by Cauchy–Schwarz,

$$\langle b_k(x_k), x^* - x_k \rangle \leq D_K \|b_k(x_k)\|.$$

Summing over k , taking total expectation, and using convexity once more, $f(\bar{x}_N) \leq S_N^{-1} \sum_k \alpha_k f(x_k)$, yields the claim. \square

Proposition 11 (Nonconvex SGD with biased stochastic gradients). *Let f be L -smooth and consider the SGD recursion*

$$x_{k+1} = x_k - \alpha_k \hat{g}_k,$$

where

$$\mathbb{E}[\hat{g}_k \mid \mathcal{F}_k] = \nabla f(x_k) + b_k(x_k), \quad \mathbb{E}[\|\hat{g}_k\|^2 \mid \mathcal{F}_k] \leq V_k(x_k).$$

Let $S_N := \sum_{k=0}^{N-1} \alpha_k$. Then

$$\frac{1}{S_N} \sum_{k=0}^{N-1} \alpha_k \mathbb{E} \|\nabla f(x_k)\|^2 \lesssim \frac{f(x_0) - f_{\text{inf}}}{S_N} + \sum_{k=0}^{N-1} \left[\frac{\alpha_k}{S_N} \mathbb{E} \|b_k(x_k)\|^2 + \frac{L\alpha_k^2}{S_N} \mathbb{E}V_k(x_k) \right].$$

Thus, in (7),

$$a_k = 0, \quad c_k = \frac{\alpha_k}{S_N}, \quad e_k = \frac{L\alpha_k^2}{S_N},$$

up to universal constants.

Proof. By L -smoothness,

$$f(x_{k+1}) \leq f(x_k) - \alpha_k \langle \nabla f(x_k), \hat{g}_k \rangle + \frac{L\alpha_k^2}{2} \|\hat{g}_k\|^2.$$

Taking conditional expectation gives

$$\mathbb{E}[f(x_{k+1}) \mid \mathcal{F}_k] \leq f(x_k) - \alpha_k \|\nabla f(x_k)\|^2 - \alpha_k \langle \nabla f(x_k), b_k(x_k) \rangle + \frac{L\alpha_k^2}{2} V_k(x_k).$$

Using Young's inequality,

$$-\langle \nabla f(x_k), b_k(x_k) \rangle \leq \frac{1}{2} \|\nabla f(x_k)\|^2 + \frac{1}{2} \|b_k(x_k)\|^2,$$

we obtain

$$\frac{\alpha_k}{2} \|\nabla f(x_k)\|^2 \leq f(x_k) - \mathbb{E}[f(x_{k+1}) \mid \mathcal{F}_k] + \frac{\alpha_k}{2} \|b_k(x_k)\|^2 + \frac{L\alpha_k^2}{2} V_k(x_k).$$

Summing and dividing by S_N gives the stated bound, after absorbing absolute constants. \square

Proposition 12 (Strongly convex SGD with biased stochastic gradients). *Let f be μ -strongly convex and L -smooth, and let $x^* = \arg \min_x f(x)$. Consider*

$$x_{k+1} = x_k - \alpha_k \hat{g}_k, \quad 0 < \alpha_k \leq \frac{1}{L},$$

where

$$\mathbb{E}[\hat{g}_k \mid \mathcal{F}_k] = \nabla f(x_k) + b_k(x_k), \quad \mathbb{E}[\|\hat{g}_k\|^2 \mid \mathcal{F}_k] \leq V_k(x_k).$$

Define

$$\rho_0 := 1, \quad \rho_{k+1} := \prod_{s=0}^k (1 - \mu\alpha_s).$$

Then

$$\mathbb{E}\|x_N - x^*\|^2 \lesssim \rho_N \|x_0 - x^*\|^2 + \rho_N \sum_{k=0}^{N-1} \left[\frac{\alpha_k}{\mu\rho_{k+1}} \mathbb{E}\|b_k(x_k)\|^2 + \frac{\alpha_k^2}{\rho_{k+1}} \mathbb{E}V_k(x_k) \right].$$

Consequently,

$$\mathbb{E}[f(x_N) - f^*] \lesssim L\rho_N \|x_0 - x^*\|^2 + \sum_{k=0}^{N-1} \left[\frac{L\rho_N\alpha_k}{\mu\rho_{k+1}} \mathbb{E}\|b_k(x_k)\|^2 + \frac{L\rho_N\alpha_k^2}{\rho_{k+1}} \mathbb{E}V_k(x_k) \right].$$

Thus, in the decomposition (7), the corresponding coefficients are

$$a_k = 0, \quad c_k = \frac{L\rho_N\alpha_k}{\mu\rho_{k+1}}, \quad e_k = \frac{L\rho_N\alpha_k^2}{\rho_{k+1}},$$

up to universal constants.

Proof. Using the update rule,

$$\|x_{k+1} - x^*\|^2 = \|x_k - x^*\|^2 - 2\alpha_k \langle \hat{g}_k, x_k - x^* \rangle + \alpha_k^2 \|\hat{g}_k\|^2.$$

Taking conditional expectation gives

$$\mathbb{E}[\|x_{k+1} - x^*\|^2 \mid \mathcal{F}_k] \leq \|x_k - x^*\|^2 - 2\alpha_k \langle \nabla f(x_k), x_k - x^* \rangle - 2\alpha_k \langle b_k(x_k), x_k - x^* \rangle + \alpha_k^2 V_k(x_k).$$

Since f is μ -strongly convex and x^* is its minimizer,

$$\langle \nabla f(x_k), x_k - x^* \rangle \geq \mu \|x_k - x^*\|^2.$$

For the bias term, Young's inequality gives

$$2\alpha_k |\langle b_k(x_k), x_k - x^* \rangle| \leq \mu\alpha_k \|x_k - x^*\|^2 + \frac{\alpha_k}{\mu} \|b_k(x_k)\|^2.$$

Therefore,

$$\mathbb{E}[\|x_{k+1} - x^*\|^2 \mid \mathcal{F}_k] \leq (1 - \mu\alpha_k) \|x_k - x^*\|^2 + \frac{\alpha_k}{\mu} \|b_k(x_k)\|^2 + \alpha_k^2 V_k(x_k).$$

Taking total expectation and unrolling the recursion yields

$$\mathbb{E}\|x_N - x^*\|^2 \leq \rho_N \|x_0 - x^*\|^2 + \rho_N \sum_{k=0}^{N-1} \left[\frac{\alpha_k}{\mu\rho_{k+1}} \mathbb{E}\|b_k(x_k)\|^2 + \frac{\alpha_k^2}{\rho_{k+1}} \mathbb{E}V_k(x_k) \right].$$

Finally, by L -smoothness and $\nabla f(x^*) = 0$,

$$f(x_N) - f^* \leq \frac{L}{2} \|x_N - x^*\|^2.$$

Multiplying the previous display by $L/2$ and absorbing universal constants gives the claimed bound. \square

Proposition 13 (Accelerated SGD with biased stochastic gradients). *Consider the accelerated stochastic scheme used in the ZO-AccSGD analysis, with weights (β_k, γ_k) . Let the estimator g_k satisfy*

$$\mathbb{E}[g_k \mid \mathcal{F}_k] = \nabla f(y_k) + b_k(y_k), \quad \mathbb{E}[\|g_k\|^2 \mid \mathcal{F}_k] \leq V_k(y_k).$$

Assume that in the accelerated Lyapunov recursion the gradient error enters as

$$\beta_N \gamma_N (f(x_N^{ag}) - f^*) \leq R_0 + \sum_{k=0}^{N-1} [\gamma_k \langle g_k - \nabla f(y_k), x^* - z_k \rangle + \gamma_k^2 \|g_k - \nabla f(y_k)\|^2],$$

where R_0 is independent of the oracle fidelity. If $\|z_k - x^*\| \leq R$ along the trajectory, then

$$\mathbb{E}[f(x_N^{ag}) - f^*] \leq \tilde{E}_0(N, \Theta) + \sum_{k=0}^{N-1} \left[\frac{\gamma_k R}{\beta_N \gamma_N} \mathbb{E}\|b_k(y_k)\| + \frac{\gamma_k^2}{\beta_N \gamma_N} \mathbb{E}\|b_k(y_k)\|^2 + \frac{\gamma_k^2}{\beta_N \gamma_N} \mathbb{E}V_k(y_k) \right].$$

Thus, in the decomposition (7), the corresponding coefficients are

$$a_k = \frac{\gamma_k R}{\beta_N \gamma_N}, \quad c_k = \frac{\gamma_k^2}{\beta_N \gamma_N}, \quad e_k = \frac{\gamma_k^2}{\beta_N \gamma_N}.$$

Proof. Let

$$\varepsilon_k := g_k - \mathbb{E}[g_k \mid \mathcal{F}_k].$$

Then

$$\mathbb{E}[\varepsilon_k \mid \mathcal{F}_k] = 0, \quad g_k - \nabla f(y_k) = b_k(y_k) + \varepsilon_k.$$

For the linear term in the accelerated recursion, taking conditional expectation gives

$$\mathbb{E}[\langle g_k - \nabla f(y_k), x^* - z_k \rangle \mid \mathcal{F}_k] = \langle b_k(y_k), x^* - z_k \rangle.$$

Hence, by Cauchy–Schwarz and the assumption $\|z_k - x^*\| \leq R$,

$$\mathbb{E}[\langle g_k - \nabla f(y_k), x^* - z_k \rangle \mid \mathcal{F}_k] \leq R \|b_k(y_k)\|.$$

For the quadratic term, we first note that

$$\begin{aligned} \mathbb{E}[\|g_k - \nabla f(y_k)\|^2 \mid \mathcal{F}_k] &= \mathbb{E}[\|b_k(y_k) + \varepsilon_k\|^2 \mid \mathcal{F}_k] \\ &= \|b_k(y_k)\|^2 + \mathbb{E}[\|\varepsilon_k\|^2 \mid \mathcal{F}_k], \end{aligned}$$

because $\mathbb{E}[\varepsilon_k \mid \mathcal{F}_k] = 0$. Moreover,

$$\begin{aligned} \mathbb{E}[\|\varepsilon_k\|^2 \mid \mathcal{F}_k] &= \mathbb{E}[\|g_k - \mathbb{E}[g_k \mid \mathcal{F}_k]\|^2 \mid \mathcal{F}_k] \\ &= \mathbb{E}[\|g_k\|^2 \mid \mathcal{F}_k] - \|\mathbb{E}[g_k \mid \mathcal{F}_k]\|^2 \\ &\leq \mathbb{E}[\|g_k\|^2 \mid \mathcal{F}_k] \leq V_k(y_k). \end{aligned}$$

Therefore,

$$\mathbb{E}[\|g_k - \nabla f(y_k)\|^2 \mid \mathcal{F}_k] \leq \|b_k(y_k)\|^2 + V_k(y_k).$$

Taking conditional expectation in the accelerated Lyapunov recursion and using the two bounds above yields

$$\beta_N \gamma_N \mathbb{E}[f(x_N^{ag}) - f^*] \leq \tilde{R}_0 + \sum_{k=0}^{N-1} [\gamma_k R \mathbb{E}\|b_k(y_k)\| + \gamma_k^2 \mathbb{E}\|b_k(y_k)\|^2 + \gamma_k^2 \mathbb{E}V_k(y_k)],$$

where \tilde{R}_0 is independent of the oracle fidelity. Dividing by $\beta_N \gamma_N$ and absorbing $\tilde{R}_0/(\beta_N \gamma_N)$ into $\tilde{E}_0(N, \Theta)$ gives the claim. \square

E Proof of Prop. 3

As an example, we consider a two-point oracle.

Lemma 2. *Let $\hat{f}(x) = f(x) + \xi_t(x)$ and consider the two-point estimator (Def. 4) with bandwidth h_t and batch size B . Let $x_t^\pm = x_{t,i} \pm h_t r_{t,i} \zeta_{t,i}$ and set*

$$\xi_{t,i}^+ := \xi_t^+(x_{t,i}^+), \quad \xi_{t,i}^- := \xi_t^-(x_{t,i}^-), \quad \Delta_{t,i} := \xi_{t,i}^+ - \xi_{t,i}^-. \quad (22)$$

Then

$$\|b_t\|_* \lesssim \kappa_\beta L_\beta h_t^{\beta-1} + \frac{d}{h_t} \mathbb{E}^{1/2}[\Delta_{t,1}^2 | \mathcal{F}_t], \quad V_t \lesssim \frac{1}{B} \mathbb{E}[\|g_{t,1}\|_*^2 | \mathcal{F}_t] + \frac{d^2}{B h_t^2} \mathbb{E}[\Delta_{t,1}^2 | \mathcal{F}_t],$$

where

$$g_{t,1} := \frac{d}{2h_t} \left(f(x_{t,1}^+) - f(x_{t,1}^-) \right) K(r_1) \zeta_1.$$

Proof. We use (22) and write

$$\hat{g}(x_t, h_t, r_i, \zeta_i) := \underbrace{\frac{d}{2h_t} \left(f(x_{t,i}^+) - f(x_{t,i}^-) \right) K(r_i) \zeta_i}_{g_{i,t} :=} + \frac{d}{2h_t} K(r_i) \zeta_i \Delta_{t,i}.$$

Then, if we use batching with the batch size B , we get

$$\hat{\mathbf{g}}(x_t) := \frac{1}{B} \sum_{i=1}^B \hat{g}(x_t, h_t, r_i, \zeta_i).$$

Next, we note that

$$\mathbb{E}[\hat{\mathbf{g}}(x_t) | \mathcal{F}_t] - \nabla f(x_t) = \mathbb{E}[g_{1,t} | \mathcal{F}_t] - \nabla f(x_t) + \frac{d}{2h_t} \mathbb{E}[K(r) \zeta \Delta_{1,t} | \mathcal{F}_t].$$

Using the result from Bychkov et al. [2024], to control the first term in the r.h.s., and applying Cauchy–Schwarz inequality to the second term, we get

$$\|\mathbb{E}[\hat{\mathbf{g}}(x_t) | \mathcal{F}_t] - \nabla f(x_t)\| \lesssim \kappa_\beta L_\beta h_t^{\beta-1} + \frac{d}{h_t} \mathbb{E}[\Delta_{1,t}^2 | \mathcal{F}_t].$$

Thus,

$$b_t := \kappa_\beta L_\beta h_t^{\beta-1} + \frac{d}{h_t} \mathbb{E}^{1/2}[\Delta_{1,t}^2 | \mathcal{F}_t].$$

Similarly we get

$$V_t := \frac{2}{B} \mathbb{E}[\|g_{t,1}\|_*^2 | \mathcal{F}_t] + \frac{d^2}{B h_t^2} \mathbb{E}[\Delta_{t,1}^2 | \mathcal{F}_t].$$

□

Under either noise model (Definitions 1 and 2), $\mathbb{E}[\Delta_k^2 | \mathcal{F}_{k-1}] \lesssim \delta_k^2$, so we get

$$\|b_k(x_k)\| \lesssim \kappa_\beta L h^{\beta-1} + \frac{d}{h} \delta_k, \quad V_k(x_k) \lesssim G^2 + \frac{d^2}{h^2} \delta_k^2, \quad (23)$$

where G^2 bounds $\mathbb{E}[|f(x_k^+) - f(x_k^-)|^2 | \mathcal{F}_{k-1}]$ (for instance, via Lipschitz continuity of f).

F Wall-clock complexity for adversarial noise missing proofs and remarks

Let x_N be an estimate obtained after N steps and let the corresponding approximation error be $\mathcal{E}(N, \delta, \Theta)$. Dvurechensky and Gasnikov [2016] and Devolder et al. [2013] ensure that if f is strongly convex (Asm. 2, $\mu > 0$), the bound is

$$f(x_N) - f^* \lesssim \mathcal{E}(N, \delta, \Theta) := LR^2 \exp\left(-\left(\frac{\mu}{L}\right)^{\frac{1}{p}} N\right) + \left(\frac{L}{\mu}\right)^{\frac{2p-1}{p}} d\delta,$$

where $R := \|x_0 - x^*\|$. Applying Corollary 1 for convergence above (case) one can obtain result provided in Proposition 4 (case $\mu > 0$).

Remark 7. Analysis of (12) demonstrates that if $\gamma < 1$, the wall-clock time complexity is optimal (minimal) for $p = 2$. This corresponds to FGM. If $\gamma \geq 1$, the optimal wall-clock time complexity is achieved at $p = 1$. This corresponds to GM. Thus, the upper bound on the wall-clock time complexity is tighter for GM; so, accelerated methods can be wall-clock inferior to non-accelerated schemes.

Furthermore, if f is convex (i.e., Assumption 2 with $\mu = 0$ holds), convergence can be expressed as:

$$f(x_N) - f^* \lesssim \mathcal{E}(N, \delta, \Theta) := \frac{LR^2}{N^p} + \sqrt{d\delta}L\tilde{R}_N + N^{p-1}d\delta, \quad (24)$$

where $\tilde{R}_N = \max_{k \leq N-1} \|x^k - x^*\|_2$ is a parameter depending on the convergence trajectory of the chosen algorithm.

Using stopping criteria similar to those proposed in Vasin et al. [2023] or setting $\tilde{R}_N = O(R)$ and Corollary 1 the second part of result of the Proposition 4 can be obtained.

Proof of Proposition 4 (case $\mu = 0$)

Proof. Convergence bound (24) can be expressed as:

$$\frac{LR^2}{N^p} + 2 \max\{\sqrt{d\delta}LR, N^{p-1}d\delta\}.$$

Then we can apply Corollary 1 to both components of error accumulation. Estimating iterations amount:

$$\frac{LR^2}{N^p} \leq \frac{\varepsilon}{3} \Rightarrow N = O\left(\left(\frac{3LR^2}{\varepsilon}\right)^{1/p}\right).$$

1. Applying Corollary 1 to component $\sqrt{d\delta}LR$:

$$\begin{aligned} T_{\text{total}}^{(1)} &\leq N \left(\frac{2\varepsilon}{3}\right)^{-2\gamma} (2\sqrt{d}LR)^{2\gamma} \leq \left(\frac{3LR^2}{\varepsilon}\right)^{1/p} \left(\frac{9}{4\varepsilon^2}\right)^\gamma (4dLR^2)^\gamma \\ &= \left(\frac{3LR^2}{\varepsilon}\right)^{1/p} \left(\frac{9dLR^2}{\varepsilon^2}\right)^\gamma = O\left(\left(\frac{\varepsilon}{9d}\right)^{-\gamma} \left(\frac{LR^2}{\varepsilon}\right)^{\gamma+\frac{1}{p}}\right). \end{aligned}$$

2. Applying Corollary 1 to component $N^{p-1}d\delta$:

$$\begin{aligned} T_{\text{total}}^{(2)} &\leq N \left(\frac{2\varepsilon}{3}\right)^{-\gamma} (N^{p-1}d)^\gamma \leq \left(\frac{3LR^2}{\varepsilon}\right)^{1/p} \left(\frac{3}{2\varepsilon}\right)^\gamma \left(\left(\frac{3LR^2}{\varepsilon}\right)^{\gamma(p-1)/p}\right) d^\gamma \\ &= O\left(\left(\frac{2\varepsilon}{3d}\right)^{-\gamma} \left(\frac{3LR^2}{\varepsilon}\right)^{\gamma+\frac{1-\gamma}{p}}\right). \end{aligned}$$

Then we can use maximum of $T_{\text{total}}^{(1)}$ and $T_{\text{total}}^{(2)}$ for total estimation of wall clock time for $\mathcal{E}(N, \delta, \Theta) \leq \varepsilon$ solution. Note, that we can assume, that $\varepsilon \leq LR^2$, since L -smoothness (Assumptions 2) implies $f(x) - f^* \leq \frac{1}{2}LR^2$. Thus we can estimate T_{total} :

$$\begin{aligned} T_{\text{total}} &= O\left(\max\left\{T_{\text{total}}^{(1)}, T_{\text{total}}^{(2)}\right\}\right) \\ &= O\left(\max\left\{\left(\frac{\varepsilon}{9d}\right)^{-\gamma} \left(\frac{LR^2}{\varepsilon}\right)^{\gamma+\frac{1}{p}}, \left(\frac{2\varepsilon}{3d}\right)^{-\gamma} \left(\frac{3LR^2}{\varepsilon}\right)^{\gamma+\frac{1-\gamma}{p}}\right\}\right) \\ &= O\left(\left(\frac{\varepsilon}{9d}\right)^{-\gamma} \cdot \max\left\{\left(\frac{LR^2}{\varepsilon}\right)^{\gamma+\frac{1}{p}}, \left(\frac{3LR^2}{\varepsilon}\right)^{\gamma+\frac{1-\gamma}{p}}\right\}\right) \\ &= O\left(\left(\frac{\varepsilon}{9d}\right)^{-\gamma} \left(\frac{3LR^2}{\varepsilon}\right)^{\gamma+\frac{1}{p}}\right) \end{aligned}$$

□

Algorithm 2 IGM (Intermediate Gradient Method).

Require: Starting point x^0 , number of steps N , L – smoothness parameter, μ – strong convexity parameter, ν – intermediate parameter.

- 1: **Set** $u^0 = x^0$.
 - 2: **Set** $h = \frac{1}{4L}$.
 - 3: **Set** $s = \left(1 + \frac{1}{4} \left(\frac{\mu}{2L}\right)^\nu\right)$.
 - 4: **Set** $m = \left(1 - \frac{1}{4} \left(\frac{\mu}{2L}\right)^\nu\right)$.
 - 5: **Set** $q = \frac{\mu}{16L}$.
 - 6: **Set** $\omega = \frac{(m-s) + \sqrt{(s-m)^2 + 4mq}}{(m-s) + \sqrt{(s-m)^2 + 4mq}}$.
 - 7: **for** $k = 0 \dots N - 1$ **do**
 - 8: $y^k = \frac{\omega u^k + x^k}{1 + \omega}$.
 - 9: $u^{k+1} = (1 - \omega)u^k + \omega y^k - \frac{2\omega}{\mu} \tilde{\nabla} f(y^k)$.
 - 10: $x^{k+1} = y^k - h \tilde{\nabla} f(y^k)$.
 - 11: **end for**
 - 12: **return Output:** x^N .
-

Remark 8. The convex case result of Proposition 4 indicates that for any $\gamma > 0$ the optimal choice of method is FGM (i.e., $p = 2$). Note that full gradient approximation requires d queries to the oracle [Gasnikov et al., 2023]. Consequently, under sequential queries, the bounds (12) scale by a factor of d . However, the wall-clock time complexity remains invariant under parallel oracle queries.

In papers Stonyakin et al. [2020, 2021] were obtained results for fast gradient method and $(\{\delta_k\}_{k=0}^{N-1}, L, \mu)$ inexact models described at Devolder et al. [2013]. To study wall-clock complexity for time-varying δ_k we introduce the following intermediate gradient method.

We will establish convergence of Algorithm 2 with inexact gradient $\tilde{\nabla} f$, satisfying:

$$(\forall x \in \mathbb{R}^d) \quad \tilde{\nabla} f(x) = \nabla f(x) + \zeta_a(x), \quad \|\zeta_a(x)\|_2 \leq \Delta. \quad (25)$$

Following [Nesterov, 2018, p. 83], let us introduce a parameterized set of functions Ψ , its element defined for $c \in \mathbb{R}$, $\kappa \in \mathbb{R}^{++}$, and $u \in \mathbb{R}^n$, as follows

$$\psi(x|c, \kappa, u) = c + \frac{\kappa}{2} \|x - u\|_2^2, \quad \forall x \in \mathbb{R}^n. \quad (26)$$

According to Nesterov [2018], we can mention to the following useful properties of the class Ψ .

Lemma 3. *Let $\psi_1, \psi_2 \in \Psi$. Then $\forall \eta_1, \eta_2, c_1, c_2 \in \mathbb{R}, \forall \kappa_1, \kappa_2 \in \mathbb{R}^{++}$, and $\forall u, v \in \mathbb{R}^n$, we have*

$$\eta_1 \psi_1(x|c_1, \kappa_1, u) + \eta_2 \psi_2(x|c_2, \kappa_2, v) = \psi_3(x|c_3, \kappa_3, w),$$

where

$$c_3 = \eta_1 c_1 + \eta_2 c_2 + \frac{\eta_1 \eta_2 \kappa_1 \kappa_2}{2(\eta_1 \kappa_1 + \eta_2 \kappa_2)} \|u - v\|_2^2,$$

$$\kappa_3 = \eta_1 \kappa_1 + \eta_2 \kappa_2, \quad w = \frac{\eta_1 \kappa_1 u + \eta_2 \kappa_2 v}{\eta_1 \kappa_1 + \eta_2 \kappa_2}.$$

Lemma 4. *Let $0 < \lambda < 1$, $A > 0$, $\psi_0, \psi \in \Psi$, $z \in \mathbb{R}^n$ such that*

$$f(z) \leq \min_{x \in \mathbb{R}^n} \psi(x) + A,$$

and

$$\psi(x) \leq \lambda \psi_0(x) + (1 - \lambda) f(x), \quad \forall x \in \mathbb{R}^n.$$

Then

$$f(z) - f^* \leq \lambda(\psi_0(x^*) - f^*) + A.$$

Proof.

$$\begin{aligned} f(z) - f^* &\leq \min_{x \in \mathbb{R}^n} \psi(x) + A - f^* \\ &\leq \psi(x^*) - f^* + A \leq \lambda \psi_0(x^*) + (1 - \lambda) f(x^*) - f^* + A \\ &= \lambda(\psi_0(x^*) - f^*) + A. \end{aligned}$$

□

Lemma 5. Let $\tilde{\nabla}f$ satisfies error condition (25), $0 < \mu \leq L$, then:

$$\begin{aligned} \forall \nu \geq 0 \quad \|\tilde{\nabla}f(x)\|_2^2 &\geq \left(1 - \frac{1}{4} \left(\frac{\mu}{2L}\right)^\nu\right) \|\nabla f(x)\|_2^2 - \left(4 \left(\frac{2L}{\mu}\right)^\nu - 1\right) \Delta^2, \\ \|\tilde{\nabla}f(x)\|_2^2 &\leq \left(1 + \frac{1}{4} \left(\frac{\mu}{2L}\right)^\nu\right) \|\nabla f(x)\|_2^2 + \left(1 + 4 \left(\frac{2L}{\mu}\right)^\nu\right) \Delta^2. \end{aligned}$$

Proof.

$$\begin{aligned} \|\tilde{\nabla}f(x)\|_2^2 &= \|\nabla f(x) + \zeta_a(x)\|_2^2 = \|\nabla f(x)\|_2^2 + 2\langle \nabla f(x), \zeta_a(x) \rangle + \|\zeta_a(x)\|_2^2 \\ &\stackrel{\text{Fenchel ineq.}}{\leq} \left(1 + \frac{1}{\lambda}\right) \|\nabla f(x)\|_2^2 + (1 + \lambda) \|\zeta_a(x)\|_2^2 \\ &\stackrel{\lambda=4(2L/\mu)^\nu}{\leq} \left(1 + \frac{1}{4} \left(\frac{\mu}{2L}\right)^\nu\right) \|\nabla f(x)\|_2^2 + \left(1 + 4 \left(\frac{2L}{\mu}\right)^\nu\right) \Delta^2. \end{aligned}$$

Similarly for the lower bound. □

Lemma 6. Let $\tilde{\nabla}f$ satisfies error condition (25), $0 < \mu \leq L, 0 < \nu$, then:

$$\begin{aligned} \left\|x - z + \frac{2}{\mu} \tilde{\nabla}f(z)\right\|_2^2 &\leq \langle \nabla f(z), x - z \rangle + \frac{\mu}{2} \|x - z\|_2^2 \\ &\quad + \frac{1}{\mu} \left(1 + \frac{1}{4} \left(\frac{\mu}{2L}\right)^\nu\right) \|\nabla f(z)\|_2^2 \\ &\quad + \frac{1}{\mu} \left(4 \left(\frac{2L}{\mu}\right)^\nu + 2\right) \Delta^2, \\ \left\|x - z + \frac{2}{\mu} \tilde{\nabla}f(z)\right\|_2^2 &\geq \langle \nabla f(z), x - z \rangle \\ &\quad + \frac{1}{\mu} \left(1 - \frac{1}{4} \left(\frac{\mu}{2L}\right)^\nu\right) \|\nabla f(z)\|_2^2 \\ &\quad - \frac{4}{\mu} \left(\frac{2L}{\mu}\right)^\nu \Delta^2. \end{aligned}$$

Proof. We will find bounds for each term of sum:

$$\left\|x - z + \frac{2}{\mu} \tilde{\nabla}f(z)\right\|_2^2 = \frac{\mu}{4} \|x - z\|_2^2 + \langle \tilde{\nabla}f(z), x - z \rangle + \frac{1}{\mu} \|\tilde{\nabla}f(z)\|_2^2.$$

Linear form:

$$\langle \tilde{\nabla}f(z), x - z \rangle \leq \langle \nabla f(z), x - z \rangle + \frac{1}{\mu} \Delta^2 + \frac{\mu}{4} \|x - z\|_2^2.$$

$$\langle \tilde{\nabla}f(z), x - z \rangle \geq \langle \nabla f(z), x - z \rangle - \frac{1}{\mu} \Delta^2 - \frac{\mu}{4} \|x - z\|_2^2.$$

Quadratic term:

$$\|\tilde{\nabla}f(z)\|_2^2 \stackrel{\text{Lemma 5}}{\leq} \left(1 + \frac{1}{4} \left(\frac{\mu}{2L}\right)^\nu\right) \|\nabla f(z)\|_2^2 + \left(4 \left(\frac{2L}{\mu}\right)^\nu + 1\right) \Delta^2.$$

$$\|\tilde{\nabla}f(z)\|_2^2 \stackrel{\text{Lemma 5}}{\geq} \left(1 - \frac{1}{4} \left(\frac{\mu}{2L}\right)^\nu\right) \|\nabla f(z)\|_2^2 - \left(4 \left(\frac{2L}{\mu}\right)^\nu - 1\right) \Delta^2.$$

Then we can sum up estimations above:

$$\begin{aligned}
\frac{\mu}{4} \left\| x - z + \frac{2}{\mu} \tilde{\nabla} f(z) \right\|_2^2 &\leq \langle \nabla f(z), x - z \rangle + \frac{\mu}{2} \|x - z\|_2^2 \\
&+ \frac{1}{\mu} \left(1 + \frac{1}{4} \left(\frac{\mu}{2L} \right)^\nu \right) \|\nabla f(z)\|_2^2 \\
&+ \frac{1}{\mu} \left(4 \left(\frac{2L}{\mu} \right)^\nu + 1 \right) \Delta^2 + \frac{\Delta^2}{\mu} \\
&\leq \langle \nabla f(z), x - z \rangle + \frac{\mu}{2} \|x - z\|_2^2 \\
&+ \frac{1}{\mu} \left(1 + \frac{1}{4} \left(\frac{\mu}{2L} \right)^\nu \right) \|\nabla f(z)\|_2^2 \\
&+ \frac{1}{\mu} \left(4 \left(\frac{2L}{\mu} \right)^\nu + 2 \right) \Delta^2. \\
\frac{\mu}{4} \left\| x - z + \frac{2}{\mu} \tilde{\nabla} f(z) \right\|_2^2 &\geq \langle \nabla f(z), x - z \rangle \\
&+ \frac{1}{\mu} \left(1 - \frac{1}{4} \left(\frac{\mu}{2L} \right)^\nu \right) \|\nabla f(z)\|_2^2 \\
&- \frac{4}{\mu} \left(\frac{2L}{\mu} \right)^\nu \Delta^2.
\end{aligned}$$

□

Lemma 7. *Let f satisfies (2) function and $\tilde{\nabla} f$ satisfies (25). Then for any $z \in \mathbb{R}^n$ and $\nu > 0$, there is $\phi_{z,\nu} \in \Psi$, such that:*

$$\begin{aligned}
\phi_{z,\nu}(x) &= c_\phi + \frac{\kappa_\phi}{2} \|x - u_\phi\|_2^2 \leq f(x), \quad \forall x \in \mathbb{R}^n. \\
c_\phi &:= f(z) - \frac{1}{\mu} \left(1 + \frac{1}{4} \left(\frac{\mu}{2L} \right)^\nu \right) \|\nabla f(z)\|_2^2 - \frac{1}{\mu} \left(4 \left(\frac{2L}{\mu} \right)^\nu + 2 \right) \Delta^2, \\
\kappa_\phi &:= \mu/2, \\
u_\phi &:= z - \frac{2}{\mu} \tilde{\nabla} f(z).
\end{aligned}$$

Proof. Proof follows directly from Lemma 6 and strong convexity Def. (2). □

Now, for Algorithm 2, we have $u^0 = x^0, x^0 \in \mathbb{R}^d$. Let u^k be defined in Algorithm 2 and ω defined in Algorithm 2. Let us define the following sequences:

$$\lambda_0 = 1, \quad c_0 = f(x^0), \quad \lambda_{k+1} = (1 - \omega)\lambda_k, \quad \forall k \geq 0, \quad (27)$$

$$\psi_k(x|c_k, \mu/2, u^k) = c_k + \frac{\mu}{4} \|x - u^k\|_2^2, \quad \forall k \geq 0 \quad (28)$$

Also $\phi_{y^k,\nu}$ is the function that is obtained from Lemma 7. We define, recursively

$$\psi_{k+1}(x|c_{k+1}, \mu/2, u^{k+1}) := (1 - \omega)\psi_k(x|c_k, \mu/2, u^k) + \omega\phi_{y^k,\nu}(x), \quad \forall k \geq 0. \quad (29)$$

Error accumulation sequence also required to be defined:

$$E_0 = 0, \quad E_{k+1} = (1 - \omega)E_k + 3 \left(\frac{\mu}{L} \right)^{1-2\nu} \frac{\Delta_k^2}{\mu}, \quad \|\tilde{\nabla} f(y^k) - \nabla f(y^k)\|_2 \leq \Delta_k. \quad (30)$$

The following Lemma motivates the definition of function $\phi_{y^k,\nu}$.

Lemma 8. *Let $\{\lambda_k\}_{k \geq 0}$ be a sequence defined in (27) and $\{\psi_k\}_{k \geq 0}$ be the corresponding functions (29). Then*

$$\psi_k(x) \leq \lambda_k \psi_0(x) + (1 - \lambda_k) f(x), \quad \forall k \geq 0 \text{ and } \forall x \in \mathbb{R}^n.$$

Proof. By the principle of induction. For $k = 0$, the inequality is obvious. Assume that inequality takes place for k . From (29), and Lemma 7, we get

$$\begin{aligned}\psi_{k+1}(x) &= (1 - \omega)\psi_k(x) + \omega\phi_{y^k, \nu}(x) \\ &\leq (1 - \omega)((1 - \lambda_k)f(x) + \lambda_k\psi_0(x)) + \omega f(x) \\ &= \lambda_{k+1}\psi_0(x) + (1 - \lambda_{k+1})f(x).\end{aligned}$$

□

Lemma 9. Let variables s, m defined at Algorithm 2, ω is the largest root of the quadratic equation

$$m\omega^2 + (s - m)\omega - q = 0, \quad (31)$$

where $q = \frac{\mu}{16L}$, $0 \leq \nu \leq 1/2$. Then:

$$\frac{1}{8} \left(\frac{\mu}{2L} \right)^{1-\nu} \leq \omega \leq \frac{1}{4} \left(\frac{\mu}{2L} \right)^{1-\nu}.$$

Proof. By solving the equation (31) and choosing the largest root we get

$$\omega = \frac{(m - s) + \sqrt{(s - m)^2 + 4mq}}{2m}. \quad (32)$$

Let us assume that $\omega > \frac{1}{4} \left(\frac{\mu}{2L} \right)^{1-\nu}$. Then

$$\begin{aligned}m\omega^2 + (s - m)\omega - q &> \left(1 - \frac{1}{4} \left(\frac{\mu}{2L} \right)^\nu\right) \frac{1}{16} \left(\frac{\mu}{2L} \right)^{2(1-\nu)} \\ &+ \frac{1}{2} \left(\frac{\mu}{2L} \right)^\nu \cdot \frac{1}{4} \left(\frac{\mu}{2L} \right)^{1-\nu} - \frac{1}{16} \frac{\mu}{L} > 0.\end{aligned}$$

which is contradiction with (31). Hence $\omega \leq \left(\frac{\mu}{2L} \right)^{1-\nu}$.

One can note, that $m < 1$ (from definition). So we can prove lower bound for ω . Let us prove by contradiction. To that end, we assume $\omega < \frac{1}{8} \left(\frac{\mu}{L} \right)^{1-\nu}$. Then:

$$\begin{aligned}m\omega^2 + (s - m)\omega - q &< \frac{1}{64} \left(\frac{\mu}{2L} \right)^{2(1-\nu)} + \frac{1}{2} \left(\frac{\mu}{2L} \right)^\nu \cdot \frac{1}{8} \left(\frac{\mu}{2L} \right)^{1-\nu} - \frac{\mu}{16L} \\ &\stackrel{0 \leq \nu \leq 1/2}{\leq} \frac{1}{128} \frac{\mu}{L} + \frac{1}{32} \frac{\mu}{L} - \frac{1}{16} \frac{\mu}{L} < 0.\end{aligned}$$

Thus, we come to a contradiction because ω is a root of the equation $m\omega^2 + (s - m)\omega - q = 0$.

□

Lemma 10. Let f satisfies (2), $\tilde{\nabla} f$ satisfies noise condition (25),

$$f(x^{k+1}) \leq f(y^k) - \frac{1}{16L} \|\nabla f(y^k)\|_2^2 + \frac{3}{16L} \Delta_k^2.$$

Where:

$$h = \frac{1}{4L}. \quad (33)$$

Proof. Using smoothness of function f we get:

$$f(x^{k+1}) \leq f(y^k) + \langle \nabla f(y^k), x^{k+1} - y^k \rangle + \frac{L}{2} \|x^{k+1} - y^k\|_2^2.$$

Let us estimate terms. Linear form:

$$\begin{aligned}
\langle \nabla f(y^k), x^{k+1} - y^k \rangle &= -h \langle \nabla f(y^k), \tilde{\nabla} f(y^k) \rangle \\
&= -h \left(\|\nabla f(y^k)\|_2^2 + \langle \nabla f(y^k), \zeta_a(y^k) \rangle \right) \\
&\stackrel{\text{Fenchel ineq.}}{\leq} -h \left(\|\nabla f(y^k)\|_2^2 - \frac{\lambda}{2} \|\nabla f(y^k)\|_2^2 - \frac{1}{2\lambda} \Delta_k^2 \right) \\
&\stackrel{\lambda=1}{\leq} -h \left(\frac{1}{2} \|\nabla f(y^k)\|_2^2 - \frac{1}{2} \Delta_k^2 \right).
\end{aligned}$$

Quadratic term:

$$\|x^{k+1} - y^k\|_2^2 = h^2 \|\tilde{\nabla} f(y^k)\|_2^2 \leq 2h^2 (\|\nabla f(y^k)\|_2^2 + \Delta_k^2).$$

Combining this inequalities:

$$\begin{aligned}
f(x^{k+1}) &\leq f(y^k) - h \left(\frac{1}{2} \|\nabla f(y^k)\|_2^2 - \frac{1}{2} \Delta_k^2 \right) \\
&+ Lh^2 (\|\nabla f(y^k)\|_2^2 + \Delta_k^2) \\
&= f(y^k) + h \|\nabla f(y^k)\|_2^2 \left(Lh - \frac{1}{2} \right) \\
&+ h \Delta_k^2 \left(\frac{1}{2} + hL \right) \\
&\stackrel{h \text{ definition}}{=} f(y^k) - \frac{1}{16L} \|\nabla f(y^k)\|_2^2 + \frac{3}{16L} \Delta_k^2.
\end{aligned}$$

□

Lemma 11. *Let f satisfies (2), $\tilde{\nabla} f$ satisfies (25), $\{x^k\}_{k \geq 0}$ be a sequence of points generated by Algorithm 2, and $c_k \forall k \geq 0$ be a minimal value of the function ψ_k corresponding to Algorithm 2, $0 \leq \nu \leq 1/2$. Then $c_k \geq f(x^k) - E_k \forall k \geq 0$, where E_k defined at (30).*

Proof. We will use the principle of mathematical induction to prove the statement of this lemma. For $k = 0$, it is obvious that $c_0 \geq f(x^0)$. Now, let us assume that $c_k \geq f(x^k) - E_k$, and prove the statement for $k + 1$. For this, from Lemma 3, Def. (29) and definition of ϕ_{y^k} from Lemma 7 we have

$$c_{k+1} = (1 - \omega)c_k \tag{34}$$

$$+ \omega \left(f(y^k) - \frac{s}{\mu} \|\nabla f(y^k)\|_2^2 - \frac{1}{\mu} \left(4 \left(\frac{2L}{\mu} \right)^\nu + 2 \right) \Delta_k^2 \right) \tag{35}$$

$$+ \frac{\omega(1 - \omega)\mu}{4} \left\| y^k - u^k - \frac{2}{\mu} \tilde{\nabla} f(y^k) \right\|_2^2. \tag{36}$$

From Lemma 6 we can estimate last term:

$$\begin{aligned}
\frac{\omega(1 - \omega)\mu}{4} \left\| y^k - u^k - \frac{2}{\mu} \tilde{\nabla} f(y^k) \right\|_2^2 &\geq \omega(1 - \omega) \langle \nabla f(y^k), u^k - y^k \rangle \\
&+ \frac{m\omega(1 - \omega)}{\mu} \|\nabla f(y^k)\|_2^2 \\
&- \frac{4\omega(1 - \omega)}{\mu} \left(\frac{2L}{\mu} \right)^\nu \Delta_k^2.
\end{aligned}$$

Combining the inequalities above and grouping the corresponding terms:

$$\begin{aligned}
c_{k+1} &\geq (1 - \omega)c_k + \omega f(y^k) + \omega(1 - \omega) \langle \nabla f(y^k), u^k - y^k \rangle \\
&- \frac{1}{\mu} (\omega s - \omega(1 - \omega)m) \|\nabla f(y^k)\|_2^2 \\
&\stackrel{(i)}{-} \frac{\omega}{\mu} \left(8 \left(\frac{2L}{\mu} \right)^\nu + 4 \right) \Delta_k^2,
\end{aligned}$$

(i) can be obtained from $0 \leq \omega < 1$ (Lemma 32):

$$\omega \left(4 \left(\frac{2L}{\mu} \right)^\nu + 2 \right) + 4\omega(1-\omega) \left(\frac{2L}{\mu} \right)^\nu \leq \omega \left(8 \left(\frac{2L}{\mu} \right)^\nu + 2 \right).$$

From convexity of function f and induction hypothesis:

$$\begin{aligned} (1-\omega)c_k &\geq (1-\omega)(f(x^k) - E_k) \\ &\geq (1-\omega)(f(y^k) + \langle \nabla f(y^k), x^k - y^k \rangle) - (1-\omega)\xi_k, \end{aligned}$$

then, using definition y^k we can eliminate the linear form:

$$\langle \nabla f(y^k), \omega(1-\omega)(x^k - y^k) + (1-\omega)(x^k - y^k) \rangle = 0$$

and continue c_{k+1} estimation:

$$\begin{aligned} c_{k+1} &\geq f(y^k) - (1-\omega)E_k \\ &\quad - \frac{1}{\mu}(\omega s - \omega(1-\omega)m) \|\nabla f(y^k)\|_2^2 \\ &\quad - \frac{2\omega}{\mu} \left(4 \left(\frac{2L}{\mu} \right)^\nu + 1 \right) \Delta_k^2, \end{aligned}$$

From ω definition one can simplify the coefficient of the gradient norm:

$$\begin{aligned} c_{k+1} &\geq f(y^k) - (1-\omega)E_k - \frac{q}{\mu} \|\nabla f(y^k)\|_2^2 - \frac{2\omega}{\mu} \left(4 \left(\frac{2L}{\mu} \right)^\nu + 1 \right) \Delta_k^2 \\ &\geq f(y^k) - (1-\omega)E_k - \frac{1}{16L} \|\nabla f(y^k)\|_2^2 - \frac{2\omega}{\mu} \left(4 \left(\frac{2L}{\mu} \right)^\nu + 1 \right) \Delta_k^2. \\ &\stackrel{\text{Lemma 9}}{\geq} f(y^k) - (1-\omega)E_k - \frac{1}{16L} \|\nabla f(y^k)\|_2^2 - \left(\frac{\mu}{2L} \right)^{1-2\nu} \frac{5\Delta_k^2}{2\mu}. \end{aligned}$$

Since $x^{k+1} = y^k - h\tilde{\nabla}f(y^k)$, where h selected consistently with the Lemma 10 we can obtain:

$$\begin{aligned} c_{k+1} &\geq f(x^{k+1}) - (1-\omega)E_k - \frac{3}{16L} \Delta_k^2 - \left(\frac{\mu}{2L} \right)^{1-2\nu} \frac{5\Delta_k^2}{2\mu} \\ &= f(x^{k+1}) - (1-\omega)E_k - \frac{\mu}{L} \cdot \frac{3\Delta_k^2}{16\mu} - \left(\frac{\mu}{2L} \right)^{1-2\nu} \frac{5\Delta_k^2}{2\mu} \\ &\geq f(x^{k+1}) - (1-\omega)E_k - 3 \left(\frac{\mu}{L} \right)^{1-2\nu} \frac{\Delta_k^2}{\mu} \\ &\stackrel{E_k \text{ definition}}{=} f(x^{k+1}) - E_{k+1}. \end{aligned}$$

□

Finally we able to prove convergence of Algorithm 2.

Theorem 1. *Let f be an L -smooth and μ -strongly convex function (Assumption 2), $\tilde{\nabla}f$ satisfies error condition (25). Then Algorithm 2 generates x^N , s.t.*

$$\begin{aligned} f(x^N) - f^* &\leq \left(1 - \frac{1}{8} \left(\frac{\mu}{2L} \right)^{1-\nu} \right)^N \left(f(x^0) - f^* + \frac{\mu}{4} R^2 \right) \\ &\quad + 3 \left(\frac{\mu}{L} \right)^{1-2\nu} \sum_{k=0}^{N-1} \left(1 - \frac{1}{8} \left(\frac{\mu}{2L} \right)^{1-\nu} \right)^{N-k-1} \frac{\Delta_k^2}{\mu} \\ &\leq \left(1 - \frac{1}{16} \left(\frac{\mu}{L} \right)^{1-\nu} \right)^N LR^2 \\ &\quad + 3 \left(\frac{\mu}{L} \right)^{1-2\nu} \sum_{k=0}^{N-1} \left(1 - \frac{1}{16} \left(\frac{\mu}{L} \right)^{1-\nu} \right)^{N-k-1} \frac{\Delta_k^2}{\mu} \end{aligned}$$

where $R := \|x^0 - x^*\|_2$.

Proof. From Lemma 11 we obtain:

$$f(x^N) \leq c_N + E_N \quad \text{see denotation (30)}.$$

Applying Lemma 8 and then Lemma 4:

$$\begin{aligned} f(x^N) - f^* &\leq \lambda_N(\psi_0(x^*) - f^*) + E_N \\ &\stackrel{(30)}{\leq} \lambda_N \left(f(x^0) - f^* + \frac{\mu}{4} R^2 \right) \\ &+ 3 \left(\frac{\mu}{L} \right)^{1-2\nu} \sum_{k=0}^{N-1} (1-\omega)^{N-k-1} \frac{\Delta_k^2}{\mu} \\ &\stackrel{\text{Lemma 9}}{\leq} \left(1 - \frac{1}{8} \left(\frac{\mu}{2L} \right)^{1-\nu} \right)^N \left(f(x^0) - f^* + \frac{\mu}{4} R^2 \right) \\ &+ 3 \left(\frac{\mu}{L} \right)^{1-2\nu} \sum_{k=0}^{N-1} \left(1 - \frac{1}{8} \left(\frac{\mu}{2L} \right)^{1-\nu} \right)^{N-k-1} \frac{\Delta_k^2}{\mu} \\ &\leq \left(1 - \frac{1}{16} \left(\frac{\mu}{L} \right)^{1-\nu} \right)^N LR^2 \\ &+ 3 \left(\frac{\mu}{L} \right)^{1-2\nu} \sum_{k=0}^{N-1} \left(1 - \frac{1}{16} \left(\frac{\mu}{L} \right)^{1-\nu} \right)^{N-k-1} \frac{\Delta_k^2}{\mu}. \end{aligned}$$

□

So we can move to Prop. 5.

Proof of Proposition 5 (case $\mu > 0$)

Proof. Using Theorem 1 and substitute $\nu = 1 - \frac{1}{p}$, $\Delta_k = 2\sqrt{dL\delta_k}$:

$$f(x^N) - f^* \leq \left(1 - \frac{1}{16} \left(\frac{\mu}{L} \right)^{\frac{1}{p}} \right)^N LR^2 + 6d \left(\frac{\mu}{L} \right)^{2\frac{1-p}{p}} \sum_{k=0}^{N-1} \left(1 - \frac{1}{16} \left(\frac{\mu}{L} \right)^{\frac{1}{p}} \right)^{N-k-1} \delta_k.$$

We will apply Master Lemma 1 for convergence above. In designations of Master Lemma:

$$\alpha_k = 6d \left(\frac{\mu}{L} \right)^{2\frac{1-p}{p}} \left(1 - \frac{1}{16} \left(\frac{\mu}{L} \right)^{\frac{1}{p}} \right)^{N-k-1}, \quad 0 \leq k \leq N-1.$$

Number of iterations to guarantee $\mathcal{E}_0(N, \Theta) \leq \varepsilon/2$:

$$N \leq 16 \left(\frac{L}{\mu} \right)^{\frac{1}{p}} \ln \left(\frac{2LR^2}{\varepsilon} \right) + 1 \leq 17 \left(\frac{L}{\mu} \right)^{\frac{1}{p}} \ln \left(\frac{2LR^2}{\varepsilon} \right) = O \left(\left(\frac{L}{\mu} \right)^{\frac{1}{p}} \ln \left(\frac{LR^2}{\varepsilon} \right) \right).$$

Then, using Master Lemma 1 we must choose:

$$\begin{aligned} A_N &= \sum_{k=0}^{N-1} \alpha_k^{\frac{\gamma}{1+\gamma}} = (6d)^{\frac{\gamma}{1+\gamma}} \left(\frac{\mu}{L} \right)^{\frac{2\gamma(1-p)}{p(1+\gamma)}} \sum_{k=0}^{N-1} \left(1 - \frac{1}{16} \left(\frac{\mu}{L} \right)^{\frac{1}{p}} \right)^{\frac{\gamma}{1+\gamma}(N-k-1)} \\ &= (6d)^{\frac{\gamma}{1+\gamma}} \left(\frac{\mu}{L} \right)^{\frac{2\gamma(1-p)}{p(1+\gamma)}} \frac{1 - \left(1 - \frac{1}{16} \left(\frac{\mu}{L} \right)^{\frac{1}{p}} \right)^{\frac{\gamma}{1+\gamma}N}}{1 - \left(1 - \frac{1}{16} \left(\frac{\mu}{L} \right)^{\frac{1}{p}} \right)^{\frac{\gamma}{1+\gamma}}} \end{aligned}$$

Hence estimation for Wall-clock time can be provided:

$$T_{\text{total}}^{\text{IGM}} = \left(\frac{\varepsilon}{2} \right)^{-\gamma} A_N^{1+\gamma} \leq \left(\frac{\varepsilon}{12d} \right)^{-\gamma} \left(\frac{\mu}{L} \right)^{2\frac{\gamma(1-p)}{p}} \left(\frac{1 - \left(1 - \frac{1}{16} \left(\frac{\mu}{L} \right)^{\frac{1}{p}} \right)^{\frac{\gamma}{1+\gamma}N}}{1 - \left(1 - \frac{1}{16} \left(\frac{\mu}{L} \right)^{\frac{1}{p}} \right)^{\frac{\gamma}{1+\gamma}}} \right)^{1+\gamma}.$$

There are two cases.

Case 1. $\gamma \approx 0$ (sufficient small).

$$A_N = \sum_{k=0}^{N-1} \alpha_k^{\frac{\gamma}{1+\gamma}} \alpha_k \leq 1 N^{1+\gamma}.$$

$$\begin{aligned} T_{\text{total}}^{\text{IGM}} &\leq \left(\frac{\varepsilon}{12d}\right)^{-\gamma} \left(\frac{\mu}{L}\right)^{\frac{2\gamma(1-p)}{p}} N^{1+\gamma} \leq 17^{1+\gamma} \left(\frac{\varepsilon}{12d}\right)^{-\gamma} \left(\frac{L}{\mu}\right)^{2\gamma+\frac{1-\gamma}{p}} \ln^{1+\gamma} \left(\frac{2LR^2}{\varepsilon}\right) \\ &= \tilde{O} \left(\left(\frac{\varepsilon}{12d}\right)^{-\gamma} \left(\frac{L}{\mu}\right)^{2\gamma+\frac{1-\gamma}{p}} \right). \end{aligned}$$

Case 2. $\gamma \not\approx 0$ (enough big).

$$\left(\frac{1 - \left(1 - \frac{1}{16} \left(\frac{\mu}{L}\right)^{\frac{1}{p}}\right)^{\frac{\gamma}{1+\gamma}} N}{1 - \left(1 - \frac{1}{16} \left(\frac{\mu}{L}\right)^{\frac{1}{p}}\right)^{\frac{\gamma}{1+\gamma}}} \right)^{1+\gamma} \leq \left(\frac{1}{\frac{1}{16} \frac{\gamma}{1+\gamma} \left(\frac{\mu}{L}\right)^{\frac{1}{p}}} \right)^{1+\gamma} \leq \left(16 \frac{1+\gamma}{\gamma}\right)^{1+\gamma} \left(\frac{L}{\mu}\right)^{\frac{1+\gamma}{p}}.$$

Then $T_{\text{total}}^{\text{IGM}}$ can be estimated as:

$$\begin{aligned} T_{\text{total}}^{\text{IGM}} &\leq \left(\frac{\varepsilon}{12d}\right)^{-\gamma} \left(\frac{\mu}{L}\right)^{\frac{2\gamma(1-p)}{p}} \left(16 \frac{1+\gamma}{\gamma}\right)^{1+\gamma} \left(\frac{L}{\mu}\right)^{\frac{1+\gamma}{p}} \\ &= O \left((1+\gamma^{-1}) \left(\frac{\varepsilon}{12d}\right)^{-\gamma} \left(\frac{L}{\mu}\right)^{\frac{1-\gamma}{p}+2\gamma} \right). \end{aligned}$$

□

Remark 9. Same for Remark 7 one can note, that for $\gamma < 1$, the wall-clock time complexity is minimal for $p = 2$, and optimal for $p = 1$, if $\gamma \geq 1$.

Proof of Proposition 5 (convex case)

Proof. We will use regularization technique described at Vasin et al. [2023] (Remark 4.2). We introduce:

$$f_\mu(x|x^0) = f(x) + \frac{\mu}{2} \|x - x^0\|_2^2. x_\mu^* - \text{solution for problem: } f_\mu(\cdot|x^0) \rightarrow \min_{x \in \mathbb{R}^n},$$

$$f_\mu^* = f_\mu(x_\mu^*|x^0),$$

$$R_\mu = \|x_\mu^* - x^0\|_2,$$

$$\tilde{\nabla} f_\mu(x) = \tilde{\nabla} f(x) + \mu(x - x^0).$$

Note, that f_μ is μ -strongly convex, since f is convex. We will apply result of Proposition 5 to obtain $\mathcal{E}_\mu(N, \{\delta_k\}_{k \in [N]}, \Theta) \leq \frac{\varepsilon}{2}$, where \mathcal{E}_μ corresponding error bound for f_μ . We chose $\mu = \frac{\varepsilon}{R^2}$, thus:

$$T_{\text{total}}^{\text{IGM}} = \begin{cases} \tilde{O} \left(\left(\frac{\varepsilon}{24d}\right)^{-\gamma} \left(\frac{2LR^2}{\varepsilon}\right)^{\frac{1-\gamma}{p}+2\gamma} \right), & \text{if } \gamma \approx 0, \\ O \left((1+\gamma^{-1}) \left(\frac{\varepsilon}{24d}\right)^{-\gamma} \left(\frac{2LR^2}{\varepsilon}\right)^{\frac{1-\gamma}{p}+2\gamma} \right) & \text{if } \gamma \not\approx 0. \end{cases}$$

Then we can estimate $\mathcal{E}(N, \{\delta_k\}_{k \in [N]}, \Theta)$ for original function f :

$$\begin{aligned} \mathcal{E}(N, \{\delta_k\}_{k \in [N]}, \Theta) = f(x^N) - f^* &\leq f(x^N) + \frac{\mu}{2} \|x^N - x^0\|_2^2 - f^* \\ &= f_\mu(x^N|x^0) - f^* = f_\mu(x^N|x^0) - f_\mu(x^*|x^0) + \frac{\mu}{2} R^2 \\ &\leq f_\mu(x^N|x^0) - f_\mu^* + \frac{\varepsilon}{2} \leq \varepsilon. \end{aligned}$$

□

G Proof of Proposition 6

We derive the optimal wall-clock design for the adversarial-noise model directly from the bound in Sec. 4.2. Set

$$T := BN, \quad p := \frac{\beta - 1}{\beta}.$$

The wall-clock objective is $T_{\text{total}} = T\delta^{-\gamma}$.

Step 1: optimizing out the smoothing radius.

The adversarial bound contains two bias terms depending on h and δ , $\kappa_\beta L h^{\beta-1}$ and $\frac{d\delta}{h}$. For fixed δ , we balance them:

$$\kappa_\beta L h^{\beta-1} \asymp \frac{d\delta}{h}.$$

Thus

$$h^\beta = \frac{d\delta}{\kappa_\beta L}, \quad h^*(\delta) = \left(\frac{d\delta}{\kappa_\beta L} \right)^{1/\beta}.$$

With this choice,

$$\kappa_\beta L (h^*)^{\beta-1} \asymp \frac{d\delta}{h^*} \asymp a_1 \delta^p, \quad a_1 := (\kappa_\beta L)^{1/\beta} d^{(\beta-1)/\beta}.$$

Similarly,

$$\kappa_\beta^2 L (h^*)^{2(\beta-1)} \asymp \frac{d^2 \delta^2}{L (h^*)^2} \asymp a_2 \delta^{2p}, \quad a_2 := \kappa_\beta^{2/\beta} L^{\frac{2}{\beta}-1} d^{\frac{2(\beta-1)}{\beta}}.$$

Therefore, after substituting $h = h^*(\delta)$, the error bound becomes

$$\mathcal{E}(N, T, \delta) \lesssim \mathcal{E}_0(N, T) + \frac{R}{\sqrt{T}} \left(c_1 \delta^{1/(2\beta)} + c_2 \delta^{p/2} \right) + 2R a_1 \delta^p + 2N a_2 \delta^{2p},$$

where

$$\mathcal{E}_0(N, T) := \frac{LR^2}{N^2} + \frac{LR^2}{T} + \frac{Rc_0}{\sqrt{T}}, \quad c_0^2 := \kappa d \sigma_*.$$

Step 2: the δ -independent part.

The δ -independent part contains two horizons, N and $T = BN$. With respect to N ,

$$\mathcal{E}_{0,N}(N) = \frac{LR^2}{N^2}, \quad \mathcal{E}_{0,N}(N) \asymp N^{-2}.$$

Thus the N -exponent is

$$\boxed{\beta_0^{(N)} = 2.}$$

With respect to T , the large- T part is

$$\frac{LR^2}{T} + \frac{Rc_0}{\sqrt{T}}.$$

In the high-precision regime and for $c_0 > 0$, the term Rc_0/\sqrt{T} dominates LR^2/T . Hence

$$\mathcal{E}_{0,T}(T) \asymp T^{-1/2}, \quad \boxed{\beta_0^{(T)} = \frac{1}{2}.}$$

The constraint $\frac{Rc_0}{\sqrt{T}} \lesssim \varepsilon$ gives

$$T \gtrsim T_{\min} := \frac{R^2 c_0^2}{\varepsilon^2} = \frac{R^2 \kappa d \sigma_*}{\varepsilon^2}.$$

Step 3: fidelity channels.

After balancing h , the active fidelity channels are $2Ra_1\delta^p$ and $2Na_2\delta^{2p}$. For fixed N , the accuracy constraint imposes

$$\delta \lesssim \delta_D := \left(\frac{\varepsilon}{2Ra_1}\right)^{1/p}, \quad \delta \lesssim \delta_E(N) := \left(\frac{\varepsilon}{2Na_2}\right)^{1/(2p)}.$$

Since $T_{\text{total}} = T\delta^{-\gamma}$, is decreasing in δ for every $\gamma > 0$, the optimal fidelity is the largest admissible one:

$$\delta^*(N) = \min\{\delta_D, \delta_E(N)\}.$$

The transition between the two fidelity channels occurs when $\delta_D = \delta_E(N)$. Equivalently,

$$\left(\frac{\varepsilon}{2Ra_1}\right)^{1/p} = \left(\frac{\varepsilon}{2Na_2}\right)^{1/(2p)}.$$

Solving for N gives

$$N_{\text{cr}} = \frac{2R^2a_1^2}{a_2\varepsilon}.$$

Using $\frac{a_1^2}{a_2} = L$, we obtain

$$N_{\text{cr}} \asymp \frac{LR^2}{\varepsilon}.$$

Thus, in the large- N regime $N \gtrsim N_{\text{cr}}$, the accumulated quadratic channel is active:

$$\delta^*(N) = \left(\frac{\varepsilon}{2Na_2}\right)^{1/(2p)}.$$

Step 4: optimizing N .

In the large- N regime,

$$T_{\text{total}}(N, T) = T \left(\frac{2Na_2}{\varepsilon}\right)^{\gamma/(2p)}.$$

For fixed T , this is increasing in N . Therefore the optimal choice is the smallest admissible N ,

$$N^* \asymp N_{\text{cr}} \asymp \frac{LR^2}{\varepsilon}.$$

Substituting $N^* = N_{\text{cr}}$ into the active fidelity constraint gives

$$\delta^* = \left(\frac{\varepsilon}{2a_2N_{\text{cr}}}\right)^{1/(2p)} \asymp \left(\frac{\varepsilon^2}{a_2LR^2}\right)^{1/(2p)}.$$

Expanding a_2 , we obtain

$$\delta^* \asymp d^{-1}\kappa_\beta^{-1/(\beta-1)}L^{-1/(\beta-1)}R^{-\beta/(\beta-1)}\varepsilon^{\beta/(\beta-1)}.$$

The corresponding smoothing radius is

$$h^* = h^*(\delta^*) = \left(\frac{d\delta^*}{\kappa_\beta L}\right)^{1/\beta} \asymp \kappa_\beta^{-1/(\beta-1)}L^{-1/(\beta-1)}R^{-1/(\beta-1)}\varepsilon^{1/(\beta-1)}.$$

Step 5: optimizing $T = BN$.

The δ -independent term Rc_0/\sqrt{T} gives

$$T \gtrsim T_{\text{min}} = \frac{R^2c_0^2}{\varepsilon^2}.$$

Since $T_{\text{total}} = T\delta^{-\gamma}$ is increasing in T , the optimal choice is

$$T^* \asymp T_{\text{min}} = \frac{R^2\kappa d\sigma_*}{\varepsilon^2}.$$

Therefore

$$B^* = \frac{T^*}{N^*} \asymp \frac{\kappa d \sigma_*}{L \varepsilon}.$$

Step 6: optimized wall-clock cost.

The optimized wall-clock cost is $T_{\text{total}}^* = T^*(\delta^*)^{-\gamma}$. Using the expressions above,

$$T^* \asymp \frac{R^2 \kappa d \sigma_*}{\varepsilon^2},$$

and

$$(\delta^*)^{-\gamma} \asymp d^\gamma \kappa_\beta^{\gamma/(\beta-1)} L^{\gamma/(\beta-1)} R^{\gamma\beta/(\beta-1)} \varepsilon^{-\gamma\beta/(\beta-1)}.$$

Hence

$$T_{\text{total}}^* \asymp \kappa \sigma_* d^{1+\gamma} \kappa_\beta^{\gamma/(\beta-1)} L^{\gamma/(\beta-1)} R^{2+\gamma\beta/(\beta-1)} \varepsilon^{-(2+\gamma\beta/(\beta-1))}.$$

Equivalently, hiding problem-dependent constants,

$$T_{\text{total}}^* = O\left(d^{1+\gamma} \varepsilon^{-(2+\frac{\gamma\beta}{\beta-1})}\right).$$

Step 7: batching regimes.

Since

$$B^* = \frac{T^*}{N^*},$$

the batching regime is determined by comparing B^* and N^* , or equivalently comparing T^* with $(N^*)^2$. We have

$$T^* \asymp \frac{R^2 \kappa d \sigma_*}{\varepsilon^2}, \quad (N^*)^2 \asymp \frac{L^2 R^4}{\varepsilon^2}.$$

Therefore

$$B^* \leq N^* \iff T^* \leq (N^*)^2 \iff \kappa d \sigma_* \lesssim L^2 R^2.$$

Similarly,

$$B^* > N^* \iff \kappa d \sigma_* \gtrsim L^2 R^2.$$

Thus the batching transition is

$$\kappa d \sigma_* \asymp L^2 R^2.$$

H Proof of Proposition 8

Throughout this proof we use the bounded-trajectory assumption

$$\tilde{R} = \max_t \{\|z_t - x^*\|, \|z_t - y_t\|\} = O(R).$$

Thus the bias term $\tilde{R} \kappa_\beta L_\beta h^{\beta-1}$ is of order $R \kappa_\beta L_\beta h^{\beta-1}$.

Small-batch regime: $B \leq 4\kappa d$.

Set $Q := BN$. Then we get

$$E(Q, B, \delta, h) \lesssim \underbrace{\frac{\kappa^2 d^2 L R^2}{Q^2}}_{\mathcal{E}_0(Q)} + \underbrace{\frac{Q}{\kappa L h^2} \delta^2}_{\text{Tsybakov channel}} + S_{\text{sm}}(Q, B, h),$$

where the smoothing remainder is

$$S_{\text{sm}}(Q, B, h) = \frac{Q L h^2}{\kappa d} + R \kappa_\beta L_\beta h^{\beta-1} + \frac{Q}{B} \frac{(\kappa_\beta L_\beta h^{\beta-1})^2}{L}.$$

Hence $\mathcal{E}_0(Q) = \kappa^2 d^2 L R^2 Q^{-2}$, $\mathcal{E}_0(Q) \sim Q^{-2}$. For a fixed admissible h , the active wall-clock subproblem is

$$\min_{Q, \delta} Q \delta^{-\gamma} \quad \text{s.t.} \quad \frac{A}{Q^2} + C Q \delta^2 \lesssim \varepsilon,$$

with $A := \kappa^2 d^2 LR^2$, $C := \frac{1}{\kappa L h^2}$. For fixed Q , the largest feasible δ is optimal:

$$\delta^2(Q) = \frac{\varepsilon - A/Q^2}{CQ}.$$

Substituting this into $T = Q\delta^{-\gamma}$ gives

$$T(Q) = C^{\gamma/2} Q^{1+\gamma/2} \left(\varepsilon - \frac{A}{Q^2} \right)^{-\gamma/2}.$$

Let $s := \frac{A/Q^2}{\varepsilon} \in (0, 1)$. Then $Q = \left(\frac{A}{\varepsilon s}\right)^{1/2}$, and, up to s -independent factors,

$$T(s) \propto s^{-(2+\gamma)/4} (1-s)^{-\gamma/2}.$$

The first-order condition yields

$$s^* = \frac{2+\gamma}{2+3\gamma}.$$

Therefore

$$\frac{A}{(Q^*)^2} = \frac{2+\gamma}{2+3\gamma} \varepsilon, \quad CQ^*(\delta^*)^2 = \frac{2\gamma}{2+3\gamma} \varepsilon.$$

Thus

$$Q^* = \kappa d R \sqrt{L} \varepsilon^{-1/2} \left(\frac{2+3\gamma}{2+\gamma} \right)^{1/2},$$

and

$$\delta^* = h L^{1/4} (dR)^{-1/2} \varepsilon^{3/4} G(\gamma),$$

where

$$G(\gamma) := \frac{(2\gamma)^{1/2} (2+\gamma)^{1/4}}{(2+3\gamma)^{3/4}}.$$

It remains to choose h . Since

$$T^* = Q^*(\delta^*)^{-\gamma} \propto h^{-\gamma},$$

the optimal smoothing radius is the largest one allowed by $S_{\text{sm}}(Q^*, B, h) \lesssim \varepsilon$. Therefore

$$h_{\text{sm}}^*(B) = \min\{H_1, H_2, H_3(B)\},$$

where

$$H_1 \asymp \left(\frac{\varepsilon \kappa d}{Q^* L} \right)^{1/2} \asymp \varepsilon^{3/4} R^{-1/2} L^{-3/4}, \quad H_2 \asymp \left(\frac{\varepsilon}{R \kappa_\beta L_\beta} \right)^{1/(\beta-1)},$$

and

$$H_3(B) \asymp \left(\frac{\varepsilon L B}{Q^* \kappa_\beta^2 L_\beta^2} \right)^{1/(2\beta-2)} \asymp \left(\frac{B \varepsilon^{3/2} \sqrt{L}}{\kappa d R \kappa_\beta^2 L_\beta^2} \right)^{1/(2\beta-2)}.$$

Consequently,

$$T_{\text{sm}}^*(B) \asymp \kappa d^{1+\gamma/2} R^{1+\gamma/2} L^{1/2-\gamma/4} \varepsilon^{-1/2-3\gamma/4} (h_{\text{sm}}^*(B))^{-\gamma} C_\gamma,$$

where C_γ depends only on γ .

The active terms depend on N and B only through $Q = BN$. Thus batching does not improve the leading active trade-off itself. It can only affect the smoothing cap through $H_3(B)$. In the regime where H_1 or H_2 is active, one may take $B^* = 1$ and $N^* = Q^*$. If $H_3(B)$ is active, increasing B can enlarge the admissible smoothing radius, but only up to the boundary $B \leq 4\kappa d$.

Large-batch regime: $B > 4\kappa d$.

In this case, we get

$$E(N, B, \delta, h) \lesssim \underbrace{\frac{LR^2}{N^2}}_{\varepsilon_0(N)} + \underbrace{\frac{N\kappa d^2}{BLh^2} \delta^2}_{\text{Tsybakov channel}} + S_{\text{lg}}(N, B, h),$$

where

$$S_{\text{lg}}(N, B, h) = \frac{N\kappa d L h^2}{B} + R \kappa_\beta L_\beta h^{\beta-1} + \frac{N(\kappa_\beta L_\beta h^{\beta-1})^2}{L}.$$

Hence

$$\mathcal{E}_0(N) = LR^2 N^{-2}, \quad \mathcal{E}_0(N) \sim N^{-2}$$

For fixed B and admissible h , the active subproblem is

$$\min_{N, \delta} NB\delta^{-\gamma} \quad \text{s.t.} \quad \frac{A}{N^2} + C_B N\delta^2 \leq \varepsilon,$$

where $A := LR^2$, $C_B := \frac{\kappa d^2}{BLh^2}$. Repeating the one-dimensional optimization above gives

$$N^* = R\sqrt{L}\varepsilon^{-1/2} \left(\frac{2+3\gamma}{2+\gamma} \right)^{1/2},$$

and

$$\delta^*(B, h) = B^{1/2} h L^{1/4} (\kappa d^2 R)^{-1/2} \varepsilon^{3/4} G(\gamma).$$

Substituting this into $T = NB\delta^{-\gamma}$ yields

$$T_{\text{lg}}^*(B, h) \asymp B^{1-\gamma/2} \kappa^{\gamma/2} d^\gamma R^{1+\gamma/2} L^{1/2-\gamma/4} \varepsilon^{-1/2-3\gamma/4} h^{-\gamma} C_\gamma.$$

Thus the dependence on B is

$$T_{\text{lg}}^*(B, h) \propto B^{1-\gamma/2}.$$

If $0 < \gamma < 2$, increasing B is not beneficial at the active trade-off level, so the optimum is attained at the smallest admissible large batch and is covered, up to constants, by the small-batch regime. If $\gamma = 2$, the leading dependence on B is flat. If $\gamma > 2$, then $T_{\text{lg}}^*(B, h)$ decreases with B as long as the interior solution has $\delta^*(B, h) < 1$. Therefore the optimal large-batch strategy increases B until the boundary $\delta^* = 1$ is reached.

Boundary solution for $\gamma > 2$.

At the boundary $c(\delta^*) = 1$, so the active problem becomes

$$\min_{N, B} NB \quad \text{s.t.} \quad \frac{LR^2}{N^2} + \frac{N\kappa d^2}{BLh^2} \leq \varepsilon.$$

For fixed N , the smallest feasible B is

$$B(N) = \frac{N\kappa d^2}{Lh^2(\varepsilon - LR^2/N^2)}.$$

Therefore

$$T(N) = NB(N) = \frac{\kappa d^2 N^2}{Lh^2(\varepsilon - LR^2/N^2)}.$$

Minimizing in N gives $\frac{LR^2}{(N^*)^2} \asymp \varepsilon$, and hence

$$N^* \asymp R\sqrt{L}\varepsilon^{-1/2}.$$

The corresponding batch size is

$$B^* \asymp \frac{\kappa d^2 N^*}{\varepsilon L h^2} \asymp \kappa d^2 R L^{-1/2} \varepsilon^{-3/2} h^{-2}.$$

Thus

$$T^* = N^* B^* \asymp \kappa d^2 R^2 \varepsilon^{-2} h^{-2}.$$

It remains to choose h . Substituting N^* and $B^*(h)$ into $S_{\text{lg}}(N, B, h) \lesssim \varepsilon$ gives

$$h_{\text{lg}}^* = \min\{K_1, K_2, K_3\},$$

where

$$K_1 \asymp d^{1/4} L^{-1/2}, \quad K_2 \asymp \left(\frac{\varepsilon}{R\kappa_\beta L_\beta} \right)^{1/(\beta-1)}, \quad K_3 \asymp \left(\frac{\varepsilon^{3/2} \sqrt{L}}{R\kappa_\beta^2 L_\beta^2} \right)^{1/(2\beta-2)}.$$

Since $T^* \propto h^{-2}$, the optimal choice is $h = h_{\text{lg}}^*$, yielding

$$T_{\text{overbatch}}^* \asymp \kappa d^2 R^2 \varepsilon^{-2} (h_{\text{lg}}^*)^{-2}.$$

This proves the large-batch overbatching regime for $\gamma > 2$.

I Proof of Proposition 7

We first justify the batched extension used in (13). Let

$$\bar{g}_t = \frac{1}{B} \sum_{i=1}^B g_t^{(i)}$$

be the average of B conditionally independent copies of the ℓ_2 -randomized estimator. Starting from the proof of Corollary 19 in Akhavan et al. [2024], batching only changes the oracle-noise contributions: the deterministic and smoothing-bias terms remain unchanged, while the Tsybakov variance level is divided by B . Indeed, writing

$$g_t = s_t + n_t, \quad n_t = \frac{d}{2h_t} (\xi_t - \xi'_t) \zeta_t K(r_t),$$

the independent averaging gives

$$\mathbb{E} \left[\left\| \frac{1}{B} \sum_{i=1}^B n_t^{(i)} \right\|^2 \middle| x_t \right] = \frac{1}{B} \mathbb{E}[\|n_t\|^2 | x_t].$$

Thus every occurrence of the Tsybakov variance level δ^2 in the noise-dependent terms is replaced by δ^2/B . Applying the same strongly convex argument as in Akhavan et al. [2024] with this replacement gives (13).

We now solve the leading-order wall-clock problem. Put

$$a := \frac{\beta - 1}{\beta}, \quad C_0 := \frac{dL^2R^2}{\mu}, \quad C_A := \frac{L_\beta^{2/\beta}}{\mu} d^{2a}.$$

Ignoring the lower-order residual channel, the active constraint is

$$\frac{C_0}{N} + C_A \delta^{2a} (BN)^{-a} \leq \varepsilon.$$

Let

$$Q := BN, \quad \eta_N := \varepsilon - \frac{C_0}{N}, \quad S_N := \left(\frac{C_A}{\eta_N} \right)^{1/a}.$$

For fixed N and δ , feasibility requires $\eta_N > 0$, and the smallest feasible total number of oracle calls is

$$Q^*(N, \delta) = \max\{N, S_N \delta^2\}.$$

Thus, after optimizing over Q , the fixed- N objective is

$$T_N(\delta) = \max\{N, S_N \delta^2\} \delta^{-\gamma}, \quad 0 < \delta \leq 1.$$

If $0 < \gamma < 2$, then $T_N(\delta)$ is minimized at the balancing point

$$S_N (\delta^*)^2 = N.$$

Hence

$$(\delta^*)^2 = N \left(\frac{\eta_N}{C_A} \right)^{1/a}, \quad Q^*(N, \delta^*) = N, \quad B^* = \frac{Q^*}{N} = 1.$$

Substituting this δ^* into the cost gives

$$T(N) = N^{1-\gamma/2} C_A^{\gamma/(2a)} \left(\varepsilon - \frac{C_0}{N} \right)^{-\gamma/(2a)}.$$

Minimizing the last display over $N > C_0/\varepsilon$ yields

$$N^* = \frac{C_0}{\varepsilon} \frac{2\beta - 2 + \gamma}{(\beta - 1)(2 - \gamma)}.$$

Consequently,

$$\delta^* \asymp d^{-1/2} LR \mu^{\frac{1}{2(\beta-1)}} L_\beta^{-\frac{1}{\beta-1}} \varepsilon^{\frac{1}{2(\beta-1)}} C_\beta(\gamma),$$

where

$$C_\beta(\gamma) = \left(\frac{\gamma\beta}{2\beta - 2 + \gamma} \right)^{\frac{\beta}{2(\beta-1)}} \left(\frac{2\beta - 2 + \gamma}{(\beta - 1)(2 - \gamma)} \right)^{1/2}.$$

Therefore

$$T_{\text{total}}^* \asymp d^{1+\gamma/2} L^{2-\gamma} R^{2-\gamma} L_\beta^{\frac{\gamma}{\beta-1}} \mu^{-1-\frac{\gamma}{2(\beta-1)}} \varepsilon^{-1-\frac{\gamma}{2(\beta-1)}} C_\beta(\gamma).$$

If $\gamma \geq 2$, then the fixed- N objective is minimized, up to leading order, at the largest admissible fidelity level $\delta^* = 1$. Indeed, on the region $S_N \delta^2 \leq N$, one has

$$T_N(\delta) = N\delta^{-\gamma},$$

which decreases with δ . On the region $S_N \delta^2 \geq N$, one has

$$T_N(\delta) = S_N \delta^{2-\gamma},$$

which is decreasing for $\gamma > 2$ and constant for $\gamma = 2$. Hence $\delta^* = 1$ is leading-order optimal for all $\gamma \geq 2$.

Substituting $\delta = 1$ into $Q^*(N, \delta)$, we obtain

$$Q^*(N, 1) = \max \left\{ N, \left(\frac{C_A}{\varepsilon - C_0/N} \right)^{1/a} \right\}.$$

Thus the remaining one-dimensional problem is

$$\min_{N > C_0/\varepsilon} \max \left\{ N, \left(\frac{C_A}{\varepsilon - C_0/N} \right)^{1/a} \right\}.$$

The first term is increasing in N , while the second term is decreasing in N . Therefore the continuous leading-order optimum is attained at the balancing point

$$N = \left(\frac{C_A}{\varepsilon - C_0/N} \right)^{1/a}.$$

Equivalently,

$$\varepsilon N - C_0 = C_A N^{1-a}.$$

Since $1 - a = 1/\beta$, the high-precision solution satisfies

$$N^* \asymp C_A^{1/a} \varepsilon^{-1/a}.$$

At the balancing point, $Q^* = N^*$, and hence the sequential leading-order optimizer can be chosen with

$$B^* = \frac{Q^*}{N^*} = 1.$$

Therefore

$$T_{\text{total}}^* = Q^* \asymp C_A^{1/a} \varepsilon^{-1/a}.$$

Substituting

$$C_A = \frac{L_\beta^{2/\beta}}{\mu} d^{2a}, \quad \frac{1}{a} = \frac{\beta}{\beta - 1},$$

gives

$$N^* \asymp T_{\text{total}}^* \asymp d^2 L_\beta^{2/(\beta-1)} \mu^{-\beta/(\beta-1)} \varepsilon^{-\beta/(\beta-1)}, \quad B^* = 1.$$

It remains to verify that the residual channel is lower-order. Let A_{main} and A_{res} denote the main noise channel and the residual channel in (13). Then

$$\frac{A_{\text{res}}}{A_{\text{main}}} = L^2 L_\beta^{-4/\beta} d^{4/\beta-1} \delta^{-2(\beta-2)/\beta} B^{(\beta-2)/\beta} N^{-2/\beta}.$$

For $0 < \gamma < 2$, we have

$$B^* = 1, \quad N^* \asymp \varepsilon^{-1}, \quad \delta^* \asymp \varepsilon^{1/(2(\beta-1))},$$

and hence

$$\frac{A_{\text{res}}}{A_{\text{main}}} \asymp \varepsilon^{1/(\beta-1)} \rightarrow 0.$$

For $\gamma \geq 2$, the sequential leading-order optimizer has

$$\delta^* = 1, \quad B^* = 1, \quad N^* \asymp \varepsilon^{-\beta/(\beta-1)}.$$

Therefore

$$\frac{A_{\text{res}}}{A_{\text{main}}} \asymp \varepsilon^{2/(\beta-1)} \rightarrow 0.$$

Thus the residual channel is lower-order in the high-precision regime.

Finally, although the sequential leading-order optimizer can be chosen with $B^* = 1$, for $\gamma \geq 2$ the same total-work order can be redistributed across batches. Taking $\delta = 1$, any choice satisfying

$$N \gtrsim \frac{C_0}{\varepsilon}, \quad Q = BN \gtrsim C_A^{1/a} \varepsilon^{-1/a}$$

achieves the same leading accuracy. Hence one may reduce the sequential depth to $N \asymp C_0/\varepsilon$ by increasing

$$B \asymp \frac{C_A^{1/a} \varepsilon^{-1/a}}{C_0/\varepsilon},$$

without changing the leading total oracle work.

I.1 Details for regularization and comparison

Let f be convex and assume that an optimal solution x^* exists with

$$\|x_0 - x^*\| \leq R.$$

For $\mu > 0$, define

$$f_\mu(x) := f(x) + \frac{\mu}{2} \|x - x_0\|^2.$$

Then f_μ is μ -strongly convex. Let x_μ^* be its minimizer. Since

$$f_\mu(x_\mu^*) \leq f_\mu(x^*),$$

we have

$$f_\mu(x_\mu^*) - f^* \leq \frac{\mu}{2} \|x^* - x_0\|^2 \leq \frac{\mu R^2}{2}.$$

Therefore, if

$$f_\mu(\hat{x}) - f_\mu(x_\mu^*) \leq \frac{\varepsilon}{2},$$

then

$$f(\hat{x}) - f^* \leq f_\mu(\hat{x}) - f^* \leq \frac{\varepsilon}{2} + \frac{\mu R^2}{2}.$$

Choosing

$$\mu = \frac{\varepsilon}{R^2}$$

gives $f(\hat{x}) - f^* \leq \varepsilon$. Thus it is enough to solve the regularized problem to accuracy $O(\varepsilon)$ with

$$\mu \asymp \frac{\varepsilon}{R^2}.$$

We now substitute this value of μ into the strongly convex Tsybakov baseline used by REGULARIZED ZO-SGD. For $0 < \gamma < 2$,

$$T_{\text{sc}} \asymp d^{1+\gamma/2} L^{2-\gamma} R^{2-\gamma} L_\beta^{\gamma/(\beta-1)} \mu^{-1-\frac{\gamma}{2(\beta-1)}} \varepsilon^{-1-\frac{\gamma}{2(\beta-1)}}.$$

Since

$$\mu^{-1-\frac{\gamma}{2(\beta-1)}} \asymp R^{2+\gamma/(\beta-1)} \varepsilon^{-1-\frac{\gamma}{2(\beta-1)}},$$

we get

$$T_{\text{reg}} \asymp d^{1+\gamma/2} L^{2-\gamma} L_\beta^{\gamma/(\beta-1)} R^{4-\gamma+\gamma/(\beta-1)} \varepsilon^{-2-\gamma/(\beta-1)}.$$

Hence the ε -exponent is

$$p_{\text{reg}} = 2 + \frac{\gamma}{\beta-1}.$$

For $\gamma \geq 2$,

$$T_{\text{sc}} \asymp d^2 L_\beta^{2/(\beta-1)} \mu^{-\beta/(\beta-1)} \varepsilon^{-\beta/(\beta-1)}.$$

Substituting $\mu \asymp \varepsilon/R^2$ yields

$$T_{\text{reg}} \asymp d^2 L_\beta^{2/(\beta-1)} R^{2\beta/(\beta-1)} \varepsilon^{-2\beta/(\beta-1)} = d^2 L_\beta^{2/(\beta-1)} R^{2\beta/(\beta-1)} \varepsilon^{-2-\frac{2}{\beta-1}}.$$

We now compare this with ACCELERATED ZO-SGD. In the small-batch regime,

$$T_{\text{acc}} \asymp \kappa d^{1+\gamma/2} R^{1+\gamma/2} L^{1/2-\gamma/4} \varepsilon^{-1/2-3\gamma/4} (h_{\text{sm}}^*(B))^{-\gamma}.$$

Here

$$h_{\text{sm}}^*(B) = \min\{H_1, H_2, H_3(B)\},$$

where

$$H_1 \asymp \varepsilon^{3/4}, \quad H_2 \asymp \varepsilon^{1/(\beta-1)},$$

and

$$H_3(B) \asymp \left(\frac{B\varepsilon^{3/2}}{d} \right)^{1/(2\beta-2)}.$$

Since the bound is decreasing in $h_{\text{sm}}^*(B)$, we take the largest admissible batch size in the small-batch regime:

$$B \asymp 4\kappa d.$$

Then

$$H_3(B) \asymp \varepsilon^{3/(4(\beta-1))}$$

up to κ -dependent constants. Since

$$\frac{3}{4(\beta-1)} < \frac{1}{\beta-1},$$

we have $H_2 \lesssim H_3(B)$ for sufficiently small ε . Therefore $H_3(B)$ is not active for the leading ε -exponent, and

$$h_{\text{sm}}^*(B) \asymp \varepsilon^s, \quad s := \max\left\{\frac{3}{4}, \frac{1}{\beta-1}\right\}.$$

Consequently,

$$T_{\text{acc}} \asymp d^{1+\gamma/2} \varepsilon^{-(\frac{1}{2}+\frac{3\gamma}{4}+\gamma s)}.$$

Thus

$$p_{\text{acc}} = \frac{1}{2} + \frac{3\gamma}{4} + \gamma s.$$

If $\beta \leq 7/3$, then $s = 1/(\beta-1)$. Hence

$$p_{\text{acc}} = \frac{1}{2} + \frac{3\gamma}{4} + \frac{\gamma}{\beta-1},$$

and

$$p_{\text{reg}} - p_{\text{acc}} = \frac{3}{4}(2-\gamma) > 0.$$

Thus $p_{\text{acc}} < p_{\text{reg}}$ for all $0 < \gamma < 2$.

If $\beta > 7/3$, then $s = 3/4$, so

$$p_{\text{acc}} = \frac{1}{2} + \frac{3\gamma}{2}.$$

The accelerated method is better when

$$\frac{1}{2} + \frac{3\gamma}{2} < 2 + \frac{\gamma}{\beta-1}.$$

Solving this inequality gives

$$\gamma < \gamma_{\text{crit}}(\beta) := \frac{3(\beta-1)}{3\beta-5}.$$

For $\beta > 7/3$, one has

$$1 < \gamma_{\text{crit}}(\beta) < 2.$$

Therefore, for $\beta > 7/3$, ACCELERATED ZO-SGD has the smaller ε -exponent when $\gamma < \gamma_{\text{crit}}(\beta)$, while REGULARIZED ZO-SGD has the smaller ε -exponent when $\gamma_{\text{crit}}(\beta) < \gamma < 2$.

Finally, in the regime $\gamma \geq 2$, ACCELERATED ZO-SGD gives

$$T_{\text{acc}} \asymp d^2 \varepsilon^{-2} (h_{\text{lg}}^*)^{-2}.$$

Using

$$h_{\text{lg}}^* \asymp \varepsilon^{1/(\beta-1)}$$

for the leading (d, ε) -scaling, we get

$$T_{\text{acc}} \asymp d^2 \varepsilon^{-2 - \frac{2}{\beta-1}}.$$

This matches the leading (d, ε) -scaling of REGULARIZED ZO-SGD:

$$T_{\text{reg}} \asymp T_{\text{acc}} \asymp d^2 \varepsilon^{-2 - \frac{2}{\beta-1}}.$$

The difference is in sequential depth: ACCELERATED ZO-SGD uses

$$N_{\text{acc}} \asymp R\sqrt{L} \varepsilon^{-1/2},$$

whereas REGULARIZED ZO-SGD has deterministic sequential scale

$$N_{\text{reg}} \asymp dL^2 R^4 \varepsilon^{-2}.$$